



THE HONG KONG
POLYTECHNIC UNIVERSITY

香港理工大學

Pao Yue-kong Library

包玉剛圖書館

Copyright Undertaking

This thesis is protected by copyright, with all rights reserved.

By reading and using the thesis, the reader understands and agrees to the following terms:

1. The reader will abide by the rules and legal ordinances governing copyright regarding the use of the thesis.
2. The reader will use the thesis for the purpose of research or private study only and not for distribution or further reproduction or any other purpose.
3. The reader agrees to indemnify and hold the University harmless from and against any loss, damage, cost, liability or expenses arising from copyright infringement or unauthorized usage.

IMPORTANT

If you have reasons to believe that any materials in this thesis are deemed not suitable to be distributed in this form, or a copyright owner having difficulty with the material being included in our database, please contact lbsys@polyu.edu.hk providing details. The Library will look into your claim and consider taking remedial action upon receipt of the written requests.

Pao Yue-kong Library, The Hong Kong Polytechnic University, Hung Hom, Kowloon, Hong Kong

<http://www.lib.polyu.edu.hk>

**THE STUDY OF WINDOW DESIGN TO ENHANCE NATURAL
VENTILATION IN RESIDENTIAL BUILDINGS IN HONG
KONG**

LIU TIANQI

PhD

The Hong Kong Polytechnic University

2020

**The Hong Kong Polytechnic University
Department of Building Services Engineering**

**THE STUDY OF WINDOW DESIGN TO ENHANCE NATURAL
VENTILATION IN RESIDENTIAL BUILDINGS IN HONG
KONG**

LIU TIANQI

**A thesis submitted in partial fulfilment of the requirements for the degree of
Doctor of Philosophy**

June 2020

CERTIFICATE OF ORIGINALITY

I hereby declare that this thesis is my own work and that, to the best of my knowledge and belief, it reproduces no materials previously published or written, nor material that has been accepted for the award of any other degree or diploma, except where due acknowledgement has been made in the text.

_____ (Signed)

Tianqi Liu (Name of Student)

ABSTRACT

Abstract of thesis entitled: The study of window design to enhance natural ventilation
in residential buildings in Hong Kong

Submitted by: Tianqi Liu

For the degree of: Doctor of Philosophy

at The Hong Kong Polytechnic University in August, 2020

Due to the rapid economic development and urbanisation in the past two decades in Hong Kong, energy consumption in high-rise residential buildings has risen sharply. Energy statistics in Hong Kong show that from 2007 to 2017, the percentage of electricity consumption for air-conditioning (AC) in the residential sector increased from 33% to 38%. The significant increase in cooling energy use is due to the impact of climate change and the higher thermal comfort and indoor air quality requirements.

Natural ventilation uses available wind to reduce cooling load, dilute indoor air pollutants and provide thermal comfort in buildings. In favourable climates, residential units with natural ventilation can save 10%–30% of the cooling energy use. Thus, natural ventilation is an effective means to reduce energy consumption for air-conditioning. Wider use of natural ventilation in high-rise residential buildings is, therefore, receiving considerable and increasing attention.

Windows are typically provided in residential buildings. Occupants are expected to adjust its opening degree for natural ventilation. However, the continuous increase in energy consumption for air-conditioning in residential sector in Hong Kong indicates that Hong Kong people have

not made efficient use of natural ventilation to reduce cooling energy use. Natural ventilation performance of a residential unit is determined by the interactive effects of window type, window opening degree, relative positions of window groups, window orientation and local wind conditions. While window orientation and local wind conditions are often subject to site constraints, other window design options are within the control of building designers. On this basis, it is necessary to investigate the influence of window designs in residential buildings to encourage wider and more efficient use of natural ventilation for reducing cooling energy use and providing thermal comfort. Such information will be useful to users, building designers and policymakers as well as researchers in search of improvement in natural ventilation in Hong Kong and elsewhere in the world.

Taking all the considerations given above, this thesis presents a study of the influence of window designs on natural ventilation performance in residential buildings in Hong Kong. In this study, carefully-design and novel methodologies were adopted to achieve the intended research objectives, which include walk-through surveys, site measurements, controlled experiments, computational fluid dynamics simulations, energy simulations, market surveys and statistical analyses. In the statistical analyses, novel approaches including the Central Composite Design method, the Squeeze theorem, the response surface regression method and the artificial neural network were used.

Natural ventilation performance of three window types that are commonly used in residential buildings in Hong Kong was evaluated. Their common use were identified by walk-through surveys. The evaluation took into account the interactive influences of four possible window orientations, two relative positions of window groups (cross and single-sided ventilation modes) and nine representative coincident wind data sets. The wind data sets were developed based on

a decade's hourly meteorological data in Hong Kong. The results lead to the conclusion that amongst all window types, side hung window is most effective, followed in descending order are top hung window and sliding window. As for the relative positions of window groups, it was found that if window groups can only be located on the same side of a residential unit (single-sided ventilation mode), side hung windows and south-facing top hung windows are preferred.

According to walk-through surveys on window opening habits of Hong Kong residents, it was found that there are limited and inefficient use of natural ventilation in residential buildings in Hong Kong. To encourage wider use of natural ventilation, the optimum window opening degree was investigated. The results show that the optimum window opening degree for Hong Kong, taking into account the seasonal wind conditions and all possible design options, should be in the range of 0.6 to 0.9.

Considering that most residential buildings in Hong Kong are permanently limited to locate the window groups on the same side of a wall to become single-sided ventilation, the use of transom window (TW) of different designs to enhance ventilation was thus investigated. Site measurements were conducted at two carefully selected units to determine the influential design characteristics. The results show that indoor air change rate is most sensitive to the presence of TW and the rate is affected the most by the position of TW to the window, followed by wind speed, size of TW, orientation of TW, and wind direction. It was found that depending on the TW's physical characteristics, the improvement in air change per hour (ACH) because of its incorporation ranges from 117 % to 190%, and the average is 153.5%.

Based on the improvement in ACH created by TW of the best and the worst designs, whether enhanced ventilation can achieve thermal comfort and further reduce energy usage for cooling

are questions that are yet to be answered convincingly. For this purpose, cooling energy usage of a simple air-conditioning system and a hybrid system (using enhanced ventilation created by TW supplemented with air-conditioning) for achieving the same thermal comfort in high-rise residential buildings in Hong Kong were compared. The results found that depending on the TW design, average improvement in ACH ranges from 117 % to 190%, and the associated cooling energy saving from hybrid system ranges from 22.2% to 22.7%. These results confirm the effective use of TW in reducing cooling energy use and providing thermal comfort in high-rise residential buildings in Hong Kong.

From the above, the academic contributions of this thesis on the study of window designs in enhancing ventilation in residential buildings in Hong Kong are in four aspects. They include the identification of the most effective window type, the optimum window opening degree, the TW designs to rectify poor ventilation associated with single-sided ventilation that cannot be avoided in most residential buildings in Hong Kong and elsewhere in the world, and the cooling energy savings for the use of TW. It can be seen that the objectives are original. The methodologies adopted are novel. The results are validated and verified and the findings are expected to be useful to the users, building designers and policymakers in Hong Kong as well as researchers for better utilization of natural ventilation to cut cooling energy use and to those living in countries with similar climatic conditions to Hong Kong.

PUBLICATIONS ARISING FROM THE THESIS

Journal papers:

Liu, T., & Lee, W. L. (2019). Using response surface regression method to evaluate the influence of window types on ventilation performance of Hong Kong residential buildings. *Building and Environment*, 154, 167–181.

Liu, T., & Lee, W. L. (2019). Influence of window opening degree on natural ventilation performance of residential buildings in Hong Kong. *Science and Technology for the Built Environment*, 512(1–2), 1–14.

Liu, T., & Lee, W. L. (2020). Evaluating the influence of transom window designs on natural ventilation in high-rise residential buildings in Hong Kong. *Sustainable Cities and Society*, 62(1), 102406.

Liu, T., & Lee, W.L. (2020). Evaluating the effectiveness of transom window in reducing cooling energy use in high-rise residential buildings in Hong Kong. *Building engineering*. (Under Rev. (n.d.)).

Conference papers:

Liu, T., & Lee, W. L. (2018). Influence of window opening degree on natural ventilation performance of residential buildings in Hong Kong. In Hong Kong-4th Asia Conference of International Building Performance Simulation Association (ASim2018), Hong Kong, China.

ACKNOWLEDGEMENTS

This thesis presents the results of three years of hard work. It would have never been completed without the help and support from many people.

First, I must show my sincere gratitude to my supervisor, Dr. Lee Wai Ling, who guided me in the right direction and continuous support during my Ph.D. She gave me abundant time and trust me in self-thinking and exploration and offered tireless supports and valuable suggestions. Multiple works of mine were initiated by her inspiring ideas and would not be a success without her acute thinking, rigorous logic, and professional guidance. Besides, she acted as a role model to me not only academically but also in life. There are so many things I want to say, but no words can express my gratitude to her.

I am also grateful to my co-supervisor, Dr. Chau Chi Kwan for his irreplaceable help and guidance on my research work. Thanks to my friends, Dr. Chan Sin Yi, Guo Yi Chen, Ma Xin Tong and Wang Xin, for accompanying and encouraging me through this long journey. I would like to thank especially Dr. Yuen Ka Chun, for providing me generous assistance and valuable advice during my first involvement in measurements. I am so lucky to meet you all and I wish you a bright and wonderful future and wish our friendship be forever.

I greatly appreciate my family, dad, mom, and my sisters. Your unconditional supports and understanding make me brave and fearless of the difficulties ahead. Your endless and selfless love motivates me to be myself. No matter where I am, I deeply love you forever.

My heartfelt appreciation goes to Mr. Ou. Thanks to the cares and loves from you and your lovely families. I had a great time with you in the past three years and I am sure this will be continued in the future.

CONTENTS

CERTIFICATE OF ORIGINALITY	3
ABSTRACT.....	4
PUBLICATIONS ARISING FROM THE THESIS.....	8
ACKNOWLEDGEMENTS.....	9
CONTENTS.....	11
LIST OF FIGURES	15
LIST OF TABLES.....	17
LIST OF ABBREVIATIONS.....	18
CHAPTER 1 INTRODUCTION	23
1.1 Background.....	23
1.2 Utilizing natural ventilation in residential buildings	23
1.3 Research gaps, objectives and significance	24
1.3.1 Research gaps and significance	24
1.3.2 Organization of this thesis	28
CHAPTER 2 LITERATURE REVIEW	30
2.1 Wind conditions.....	30
2.2 Window type.....	31
2.3 Window opening degree	33
2.4 Transom window designs	34
2.4.1 The Influence of Transom Window Designs on natural ventilation performance..	35
2.4.2 The effectiveness of transom window in reducing cooling energy use	36
2.5 Summary.....	37

CHAPTER 3	METHODOLOGY	38
3.1	Site measurements	38
3.2	CFD simulations	39
3.2.1	k-epsilon standard equations	41
3.2.2	k-epsilon RNG equations	42
3.3	Energy simulations.....	42
3.4	Representative wind conditions	43
3.5	Representative residential estate and unit	46
3.6	Summary	47
CHAPTER 4	INFLUENCE OF WINDOW TYPE.....	48
4.1	Walk-through survey	48
4.2	Site Measurements	49
4.3	Simulation validations	54
4.4	CFD simulations	57
4.4.1	The hypothetical unit	57
4.4.2	Further simulations	58
4.5	Response surface regression analysis	60
4.6	Results and Analysis	62
4.6.1	The RSR model.....	62
4.6.2	Model Verification.....	64
4.6.3	Influence of independent variables	65
4.6.4	Influence of interactive variables.....	71
4.7	Summary.....	75
CHAPTER 5	INFLUENCE OF WINDOW OPENING DEGREE	76
5.1	Walk-through surveys.....	76

5.2	Site measurements	77
5.3	CFD simulations	79
5.4	Identification of the optimum DEG	80
5.5	Results and Analysis	81
5.5.1	The resultant model.....	81
5.5.2	Model Verification.....	83
5.5.3	Influence of DEG	84
5.5.4	The optimum DEG.....	86
5.6	Summary.....	88
CHAPTER 6 INFLUENCE OF TRANSOM WINDOW DESIGN		90
6.1	Site measurements	90
6.2	Identifying a representative residential unit.....	97
6.3	CFD simulations and validations	99
6.3.1	Simulation validations	100
6.3.2	Representative building level.....	103
6.4	ANN model development	106
6.5	Results and discussion	108
6.5.1	ANN model.....	108
6.5.2	Influence of different design parameters	112
6.5.3	Impact on ACH.....	119
6.6	Summary.....	120
CHAPTER 7 THE EFFECTIVENESS OF TRANSOM WINDOW IN REDUCING COOLING ENERGY USE.....		122
7.1	CFD simulations and validations	122
7.1.1	The representative residential unit.....	122

7.1.2	Physical characteristics of TW.....	123
7.1.3	Local wind environments.....	124
7.1.4	Validations and simulations.....	124
7.1.5	Site verifications	124
7.2	Energy simulations.....	125
7.2.1	Market survey	125
7.2.2	The AC and hybrid systems.....	127
7.2.3	Operating parameters	129
7.3	Results and discussions.....	130
7.3.1	Ventilation rates	130
7.3.2	Site verifications	132
7.3.3	Cooling energy saving	133
7.4	Summary.....	135
CHAPTER 8 CONCLUSIONS AND RECOMMENDATION FOR FUTURE RESEARCH		
	136
8.1	Conclusions.....	136
8.1.1	Identification of the preferred windows types	136
8.1.2	Determination of the most optimum window opening degree.....	137
8.1.3	Prediction of natural ventilation enhancement by the incorporation of transom window	138
8.1.4	Evaluation of cooling energy saving by the incorporation of TW.....	139
8.2	Limitations of the study	140
8.3	Recommendations for Future Research	141
REFERENCE.....		142

LIST OF FIGURES

Figure 3.1 Illustration of the determination of range of variable.....	44
Figure 4.1 Site layout of the studied building block.....	50
Figure 4.2 Layout of the studied building block (top) and the studied unit (bottom)	51
Figure 4.3 Measurement positions in the studied unit	51
Figure 4.4 Wind conditions during measurements	52
Figure 4.5 Decay curves of the two window types.....	53
Figure 4.6 Computational domain region and boundary conditions.....	55
Figure 4.7 Comparison of simulated and measured results	56
Figure 4.8 Floor layout of the hypothetical unit (west-facing windows)	58
Figure 4.9 Comparison of simulated and predicted ACHs.....	64
Figure 4.10 Average ACH with wind speed.....	66
Figure 4.11 Ventilation performance of CV and SV	67
Figure 4.12 Indoor airflow distribution of west facing SH window.....	67
Figure 4.13 Pressure distribution of west facing SH, TH and SLD windows	70
Figure 4.14 ACH by window orientation	71
Figure 4.15 Influence of wind speed by window types	72
Figure 4.16 Influence of ORN by window types.....	72
Figure 4.17 Influence of VNT by window types	72
Figure 5.1 Window opening habit	77
Figure 5.2 Decay curves for different window opening degrees	78
Figure 5.3 Comparison of simulated and measured results	78
Figure 5.4 Influence of individual variables (excluding DEG) on ACH.....	81
Figure 5.5 Comparison of simulated and predicted ACHs.....	84

Figure 5.6 ACH for different DEGs	85
Figure 5.7 Discharge coefficient for different DEGs.....	86
Figure 6.1 Site layout of the studied building block.....	91
Figure 6.2 Layout of the two identical studied units	91
Figure 6.3 Site measurement photos.....	94
Figure 6.4 SF ₆ concentration decay curves by design parameters.....	96
Figure 6.5 Site plan of Tseung Kwan O (TKO) and the studied building block X	97
Figure 6.6 Floor layout of Harmony one type estate	98
Figure 6.7 Layout of unit D1 with floor dimensions and window details.	99
Figure 6.8 CFD settings and testing positions for comparison.....	102
Figure 6.9 Locations of pressure coefficients on the building façade	104
Figure 6.10 Artificial neuron network structure.	106
Figure 6.11 ANN models establishment process	107
Figure 6.12 Influence of different design parameters on ACH	108
Figure 6.13 r and MSE of models with different neuron numbers	110
Figure 6.14 Comparison between the actual and predicted ACHs	110
Figure 6.15 RIF by design parameters	112
Figure 6.16 Illustration of flow path under two different positions of TW.	113
Figure 6.17 Flow development, velocity gradient and pressure gradient for two WINs.....	114
Figure 6.18 Average ACH with wind speed.....	117
Figure 6.19 Opening area of TW on average ACH	117
Figure 6.20 Amplification factors K by orientations.	119
Figure 7.1 Physical characteristics of TW	124
Figure 7.2 Control logic of the two systems	129
Figure 7.3 Comparison of the measured and simulated results	133

LIST OF TABLES

Table 2-1 Window types.....	31
Table 3-1 Representative coincident wind conditions	45
Table 4-1 Summary of window types.....	49
Table 4-2 Accuracy of major instruments	52
Table 4-3 Independent variables and coded value in RSR model	63
Table 4-4 Summary of standardized coefficients (B).....	63
Table 4-5 Q^* and ΔP of three window types.....	68
Table 4-6 Summary of VIF.....	70
Table 4-7 ACH_{max} for different apertures design.....	74
Table 5-1 Independent variables and coded value in the resultant model	82
Table 5-2 Standardized coefficients.....	83
Table 5-3 DEG for all scenarios	87
Table 6-1 Range of varied parameters of TW	92
Table 6-2 Major instruments and their accuracy	94
Table 6-3 Comparison of three refined meshes	102
Table 6-4 Pearson correlation coefficients by building level	105
Table 6-5 ACHs for TW with different designs	120
Table 7-1 Construction details	123
Table 7-2 Adjusted performance data of RACs.....	126
Table 7-3 Daily patterns of occupancy, lighting, small power and RAC	130
Table 7-4 Weighted average monthly \overline{ACH} (h) by different TW designs	132
Table 7-5 Cooling energy use by months	134

LIST OF ABBREVIATIONS

Nomenclature

Symbols	Description
A	Area (m ²)
ACR	Air change rate (kg/s)
ACH	Air change per hour (/h)
b	Coefficient of the regression model
BH	Bottom hung
CCD	Central composite design
COP	Coefficient of performance
C	Concentration (ppm)
Cd	Discharge coefficient
Cp	Pressure coefficient
CP	Number of centre point (s)
CFD	Computational fluid dynamic
CTR	Centre
CV	Cross ventilation
D	Distance between the window and the opposite wall (m)
DIR	Wind direction (degree)
DR	Door
DB	Dry bulb
DEG	Window opening degree
e	Set
E	East
f	Frequency
F	Floor
G	Number of variables
HT	Height (m)
I	Turbulent intensity (%)
j	Normalized capacity
J	Capacity (kW)
k	Turbulence kinetic energy (m ² /s ²)

K	Amplification factor
lt	Length scales of turbulence (m)
LG	Length (m)
LFT	Left
m	Transformed
MSE	Mean square error
N	North
NB	Number of the data sets
NR	Number of neurons
NV	Normalized vector
O	Occurrence
ORN	Orientation
p	Normalized power
P	Pressure (Pa)
pw	Normalized power
PW	Power (kW)
ΔP	Pressure differential (Pa)
PRESS	Predicted residual error sum of squares
Q	Airflow rate (m ³ /s)
Q*	Effectiveness of window openings
r	Pearson correlation coefficient
R	Average correlation coefficient
R ²	Coefficient of determination
RH	Relative humidity
RAC	Room air-conditioner
RGT	Right
RIF	Relative impact factor
RSR	Response surface regression
S	South
SH	Side hung
SV	Single-sided ventilation
SS	Sum of the squared residual

SLD	Sliding
SPD	Wind speed (m/s)
t	Time
T	Temperature
TH	Top hung
TS	Thermal sensation
TW	Transom window
TKO	Tseung Kwan O
TYP	Window type
u	Velocity component
U	Average wind speed (m/s)
v	Velocity component
vi	Velocity vector
V	Volume (m ³)
V _{eff}	Effective volume (m ³)
VNT	Ventilation mode
VIF	Variance inflation factor
w	Humidity ratio
W	West
w/	With
w/o	Without
WD	Width
WIN	Window
x	x position
X	Design variables
\bar{X}	Centre point value
y	y position
z	z position

Greek Symbol

α	Power law exponent
ρ	Air density (kg/m ³)

μ	Viscosity (Pa·s)
ε	Turbulence energy dissipation rate (m ² /s ³)
λ	Ratio

Subscript

Adjusted	Adjusted
ACHVD	Achieved
bd	Building
c	Particular wind condition
cod	Coded
d	Underlying
dir	Direction
e	Effective
g	Option
h	Hidden
H	Height
i	Indoor
ip	Input
j	j th
k	k th
L	Lower
m	Variable m
mt	Month
max	Maximum
min	Minimum
M	Measured
MC	Maximum cooling
max	Maximum
n	Number of measurements
o	Outdoor
O	Outside
op	Output
OPT	Optimum

p	Planning
Predicted	Predicted
q	Number of wind conditions
U	Upper
r	Particular DEG
R	Rated
ref	Reference
S	Simulated
st	Street
spd	Speed
T	Target
Total	Total sum of squared residual
U	Upper
V	Input
w	Wall
x	Level x
y	Level y
1	Initial state
2	End state

Superscript

s	Emphatic weight index
t	De-emphatic weight index

CHAPTER 1 INTRODUCTION

1.1 Background

Hong Kong is located in the sub-tropical region with an extremely hot and humid climate for nearly half the year. As such, air-conditioning is essential for enhancing the indoor environment. According to energy statistics in Hong Kong, the percentage of electricity consumption for air-conditioning (AC) in the residential sector increased from 33% to 38% in the past decade (2007-2017) [1]. The significant increase in consumption was due to the ever-growing demands for better thermal comfort and higher natural ventilation requirements, especially during the hot and humid summer months [2]–[4]. This indicates that it is necessary to use strategies to reduce cooling energy consumption.

1.2 Utilizing natural ventilation in residential buildings

Natural ventilation is a gift from nature. It is a process of supplying ambient air to displace indoor air to provide a healthy and comfortable environment in buildings. Unlike mechanical ventilation such as using fan or AC, natural ventilation is driven by natural forces without demanding any extra energy in the process. Thus, utilizing natural ventilation is a preferred option for reducing cooling energy use especially in the moderate seasons in Hong Kong [5].

Unlike commercial buildings being sealed with large glass windows and require high level of indoor environmental quality, residential buildings are more flexible to be designed for utilizing natural ventilation. Better utilization of natural ventilation has been receiving considerable and increasing attentions for years [6]. With careful building design and in favourable climates, using

natural ventilation in residential units can save 10% to 30% of total energy consumption for air-conditioning [7].

1.3 Research gaps, objectives and significance

1.3.1 Research gaps and significance

The availability of natural ventilation in residential buildings is determined by a combination of external and internal factors [8].

External factors include the urban form (e.g., density and site coverage), the building typology (e.g., building form and dimensions), and micro-climatic conditions, which are often subject to constraints or beyond the control of building designers and architects. Thus, in this study, the urban form and building typology are carefully defined to represent typical characteristics of residential buildings in Hong Kong. While for micro-climatic conditions, as natural ventilation is mainly wind-driven, the availability of natural ventilation is affected the most by the wind speed and wind direction [9], [10]. Given wind speed and wind direction are highly unstable and changeable, in the study of window designs, careful considerations have been given to these two parameters.

Internal factors include the floor layout, apertures, and orientation, which can be altered by building designers and architects the way they deem appropriate [11]. Among these factors, previous research has already indicated that aperture design plays a significant role in natural ventilation performance [8]. Building aperture means any designed opening in a building including any door, window, and skylight. In aperture design, window, which can be provided

in a wall or door in residential buildings, is considered the most important because it can be used by the occupants to adjust the ventilation rate. In general, windows on a wall are called “window”, while windows in a door are called “transom window”.

Although many researchers dedicated to window design investigations, there are limited literature in the public domain for building designers and policy makers in search of performance improvement in natural ventilation and building energy use. Therefore, the objectives of the study are to answer the following four questions:

1. What is the most preferred window type for Hong Kong residential units to enable natural ventilation utilization?
2. What is the optimum window opening degree taking into account seasonal wind conditions of Hong Kong?
3. Can transom window enhance natural ventilation in high-rise residential buildings given single-sided ventilation cannot be avoided for most of the residential units in Hong Kong? What are the impacts of different TW designs on ventilation?
4. Can enhanced ventilation created by transom window reduce cooling energy usage and provide the desired thermal comfort?

To address the above questions, this study consists four major parts of work as follows.

Part 1 focuses on evaluating the influence of window types on natural ventilation performance. Many research works have already been done in identifying the window types that can enhance ventilation performance in residential buildings. However, little has taken window sash and interactive effects into consideration. As there is no clear definition for different types of

windows, to begin with, the different window types were classified according to the way the sash and the frame are held together. A walk-through survey was then conducted to evaluate the most used window types in Hong Kong and the residents' window opening habits. The interactive effects of different design factors on ventilation performance were examined. They include window type, wind conditions, relative positions of window groups (cross and single-sided ventilation modes), window orientations, and floor layout. Nine sets of representative wind datasets were used to represent the wind conditions. A hypothetical residential unit was used to represent typical floor layout of residential units in Hong Kong. Statistical analyses were employed to quantify the influence of different factors. Based on an optimisation process, the most preferred window type for Hong Kong residential units was determined.

Based on the walk-through survey results, the residents' window opening habits were identified. Part 2 is to evaluate the optimum opening degree to encourage wider and more efficient use of natural ventilation. The evaluation was based on three most used window types, operating under nine sets of representative wind datasets in Hong Kong, four possible window orientations, and two ventilation modes. The hypothetical residential unit was again adopted for the evaluation. Regression analysis was employed to quantify their influence on natural ventilation and to extrapolate the optimum window opening degree for different internal designs and wind conditions.

Transom window (TW) has been confirmed effective in enhancing ventilation in residential units. However, the investigations are either on their presence or relative positions on a single house basis. There has been no consideration of other physical characteristics of TWs and the high-rise characteristics of residential buildings. Adding that in the design of openings, the openings' physical characteristics on ventilation is often investigated, there should be no exception for TWs.

Part 3 of this study aims to evaluate the impacts of different physical characteristics of TW in enhancing natural ventilation in high-rise residential buildings in Hong Kong. Site measurements were conducted to select the influential design characteristics of TW and to assess the uncertainty of simulations. A residential unit in a public housing estate was identified to represent typical public housing unit in Hong Kong. The local wind environments were determined by statistical analyses. The effectiveness of TW and the impact of different designs in enhancing natural ventilation were evaluated.

Despite TW has been demonstrated to be effective in enhancing natural ventilation in high-rise residential buildings in Hong Kong, virtually no work has been done to demonstrate its effectiveness in reducing cooling energy consumption and providing the desired thermal comfort. For this purpose, Part 4 of this study is to compare the cooling energy usage of a simple air-conditioning (AC) system with that of a hybrid system (using enhanced ventilation created by TW supplemented with air-conditioning) for achieving the same thermal comfort in a representative residential unit identified in Part 3 and other characteristics identified in Parts 1 and 2. The hour-by-hour air temperatures and the cooling energy use of the hybrid and the only AC systems were predicted. The simulated air velocities and temperatures were used for thermal acceptability analysis. The results confirm the effective use of TW in reducing cooling energy use and providing thermal comfort in high-rise residential buildings in Hong Kong.

The results of this study are expected to be useful to the users, building designers and policymakers in Hong Kong as well as researchers for better utilization of natural ventilation to cut cooling energy use and to those living in countries with similar climatic conditions to Hong Kong.

1.3.2 Organization of this thesis

This thesis is organized in 8 Chapters.

Chapter 1 introduces the research background, gaps, and significance, as well as the outline of this thesis.

Chapter 2 reviews relevant literatures and research works in wind conditions, window types, window opening degrees and transom window designs.

Chapter 3 explains the research methodology adopted in this study, including site measurement methods, simulation methods, statistical analysis methods, and the identification of the representative studied units.

Chapter 4 focuses on the evaluation of different window types on natural ventilation performance. The evaluation was conducted based on three commonly used window types, two ventilation modes, four window orientations and nine coincident wind datasets.

Chapter 5 presents the study of optimum window opening degree on natural ventilation performance. The optimum window opening degree was determined by how the window type, ventilation mode, window orientation and wind conditions were integrated.

Chapter 6 examines the impacts of different physical characteristics of TW in enhancing natural ventilation in high-rise residential buildings in Hong Kong including its presence, position on the door, aspect ratio, opening area, position relative to window and orientation.

Chapter 7 investigates the effectiveness of transom window in reducing cooling energy use. The cooling energy use of the hybrid and the only AC systems were compared.

Chapter 8 provides the conclusions of this study and recommendations for future work.

CHAPTER 2 LITERATURE REVIEW

To identify the research gaps in previous studies, relevant works in four aspects were reviewed. They are wind conditions, window type, window opening degree, and transom window designs. Research gaps are highlighted in each section.

2.1 Wind conditions

In previous studies, representative wind conditions (wind speed and wind direction) are often determined based on prevailing wind conditions [12]–[14] or annual-mean wind conditions [15]–[17]. When based on the prevailing wind conditions, the highest frequency of occurrence of wind speed and wind direction in an annual meteorological database derived from rose diagram are used [13]. While when based on the annual-mean wind conditions, the annual mean wind speed along with several main prevailing wind directions are used [15]–[17]. As such, representative wind speed and wind direction are separately determined to ignore their coincident characteristics.

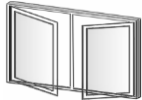


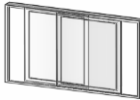
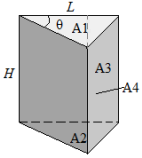
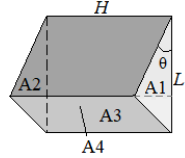
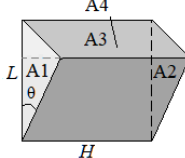
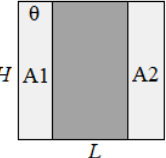
Recently, the use of coincident wind data sets has been investigated in meteorology and wind energy studies. M. Bilgili et al. [18] used the artificial neural networks method to predict the local wind conditions and compare them with a reference meteorological database. The results indicate that wind speed and wind direction often occur simultaneously to confirm that coincident wind data set provides a better and more reliable meteorological data for meteorological research. Fu et al. [19] investigated the wind-resistance of high-rise buildings. The investigation found that when evaluating the probability of occurrence of wind, the distribution functions for wind

speed and direction could reflect their dependent occurrence. To fill the research gap, there is a need to develop representative wind data sets based on coincident wind speed and wind direction to represent typical wind conditions for Hong Kong.

2.2 Window type

On window design, the impact of window type is one of the most investigated aspects. However, by far, there is no clear definition for different window types and the classification varies from region to region. One common classification is by the window shapes to have a round circle window, arched window and bay window, etc. [20]–[22]. As far as natural ventilation is concerned, windows are more often determined by way of sash and frame are held together [23]. There are four major window types, side hung (SH), top hung (TH), bottom hung (BH) and sliding (SLD). Their geometry and opening areas are given in Table 2-1.

Table 2-1 Window types

Window types				
Classification	Side hung	Top hung	Bottom hung	Sliding window
Abbreviation	SH	TH	BH	SLD
Geometry				
Opening area (=ΣAx)*	$A=L^2 \cdot \sin(\theta) + L \cdot H \cdot \sin(\theta) \cos(\theta) + (L - L \cos(\theta)) \cdot H$			$A=1/2 L \cdot H \cdot \theta$

Note: * θ is the window opening range, which is the opening angle for SH, TH and BH windows, and is the sliding length for SLD window

Previous research works have focused on evaluating the preferred window type on natural ventilation. Yang et al. [24] conducted wind tunnel tests and simulations to confirm that

ventilation performance of BH window increases with the opening angle. Heiselberg [25] measured discharge coefficients of SH and BH windows by laboratory experiments and found that they did not vary much. It was also concluded that for both single-sided and cross ventilation, SH window is preferred in summer and BH window is preferred in winter. Roetzel et al. [26] compared different window types for different climatic conditions and concluded that for non-heating seasons, SH window opening to inside can serve as a reducer to increase the incoming airflow speed and thus is preferred over SLD windows and TH windows opening to outside. Gao and Lee conducted a series of measurements and simulation studies to evaluate the influence of ventilation modes [27], window types [12] and external obstructions [28] on natural ventilation performance of high-rise residential buildings in Hong Kong. The results indicated that ventilation performance is most affected by window type and concluded that SH window is most preferred for subtropical climate. Miramontes et al. [29] conducted a similar study for low-rise residential buildings in Colima of Mexico. It was concluded that louvre window is preferred over SH and BH windows for tropical climate.

It is noted from the above that many works have already been done on the preferred window type to enhance natural ventilation in residential buildings. However, the window performance has been investigated either independently, without considering the interactive effects of the relative positions of window groups and window orientations [13-17], or the studies have been based on very limited wind data sets [14-19]. The wind data sets (wind speed and wind direction) assumed were often independently selected based on the highest cumulative frequency of occurrence or mean values of an annual meteorological database. However, the coincident wind speed and wind direction, which are always provided for good quality meteorological data [18], have never been considered in previous works.

Because of the lack of relevant research, there is a need to address the interactive effects of the ventilation modes, window orientations, and coincident wind conditions in the evaluation of the influence of window types on natural ventilation performance of residential units in Hong Kong. A mathematical model is also necessary to enable quick estimation of ventilation performance and to facilitate quantification of influences of different design variables.

2.3 Window opening degree

Window opening degree (DEG) is defined as the ratio of the opening range to the maximum openable range. Opening range refers to the opening angle (maximum openable angle is assumed 90°) for hinged windows like top hung, side hung and bottom hung windows, and refers to the sliding length for sliding windows. While for DEG, despite it is often used by residential users to adjust the window opening area, its influence on natural ventilation performance is rarely used as a studied parameter. Instead, window opening area is often used in previous research works.

Heiselberg et al. [25] conducted a series of laboratory experiments on the performance of SH and BH windows and confirmed the influence of window opening area on ventilation performance. Others are mainly focused on evaluating its influence on the discharge coefficient, which indirectly affects ventilation performance and the residents' window opening habits. Regarding influence on the discharge coefficient, Hult et al. [30] performed CFD simulations to confirm that it increases with window opening area. Heiselberg et al. [31] found that the discharge coefficient is affected not only by window opening area but also by the geometry of window openings, and airflow conditions. Yang et al. [24] conducted wind tunnel tests and CFD simulations to identify that loss coefficients exhibit an inverse square relationship with discharge coefficients. It was found that a large increase in ventilation performance can be achieved by the

partial opening of windows. In relation to window opening habits, Schweiker et al. [32] employed a stochastic analysis to confirm that it is determined by the environmental conditions and the residents' lifestyle. Fritsch et al. [33] measured the window opening areas of four office premises to develop a stochastic model. It was concluded from the developed model that habit is determined by the outdoor temperature and the occupation period. A similar result was found by Herkel et al. [34].

There is no doubt that many works have already been done on window design and window opening area but they are always separately investigated. Besides, little literature has considered window opening degree (DEG) as a studied parameter. No investigations to date have been done on identifying the interactive influence of DEG with full considerations of the window design options, wind conditions and users' habits for efficient natural ventilation. To address this gap, there is a need to identify the window opening habits of Hong Kong residents and the optimum DEG for efficient natural ventilation to reduce cooling energy use.

2.4 Transom window designs

Many research works have evaluated the influence of relative positions of window groups on natural ventilation. In the evaluations, the relative positions of the window groups are often classified into two ventilation modes: single-sided ventilation, where window groups are located in the same side of the wall [35], and cross ventilation, where window groups are on the perpendicular or parallel walls [36]. Evola and Popov [34] evaluated the influence of relative positions of windows and confirmed that cross ventilation is preferred. J. Perén et al. [35] conducted CFD simulations to evaluate the influence of the vertical position of window outlets and found that there is no significant influence. Gao and Lee conducted a series of site

measurements and simulations to investigate the influence of relative window positions [31] for high-rise residential buildings in Hong Kong. It was concluded that cross ventilation is most preferred for the Hong Kong environment.

Besides, much of the research on natural ventilation has already concluded that cross ventilation is most preferred [37]–[39]. However, for high-density high-rise environments like in Hong Kong [40], high-rise residential towers are often designed with four identical wings linked by a cross piece to form X-shaped towers. On each wing, there are two to four residential units arranged in a back-to-back manner to optimise the spatial efficiency. As a result, the residential units in Hong Kong are permanently limited to single-sided ventilation [41].

Transom window (TW), a glass panel mounted on the top of a doorframe, was first introduced in the 14th century for increasing natural light and decoration [42]. At that time, TWs were often sealed for privacy, preventing insects and for protection from severe weather [43]. With poor ventilation associated with single-sided ventilation has become a concern, TWs have later evolved to become openable to facilitate effective ventilation in residential units [44]–[49].

2.4.1 The Influence of Transom Window Designs on natural ventilation performance

Previous research works have focused on evaluating if TW is effective in enhancing natural ventilation and the influence of the relative positions on its effectiveness. Howard-Reed et al. [44] conducted a series of site measurements to confirm that even occasional opening of TW can enhance the indoor air change rate. Chen et al. [50] employed CFD simulations to compare air change rate under cross ventilation created by floor opening with that facilitated by TW. It was found that the adoption of TW can achieve better performance. Chiang et al. [45] used numerical

simulation to examine the distribution of air contaminants and the temperature field in a kitchen in Taiwan. It was found that a properly located TW can effectively improve indoor air quality. N. Chao et al. [46] conducted a similar study for a bedroom in Taiwan. It was concluded that depending on its position relative to windows, TW can effectively dilute the indoor CO₂ concentration and maintain indoor thermal comfort. Recently, Aflaki et al. [49] performed site measurements and CFD simulations to evaluate the effectiveness of using TW to create cross ventilation in a residential unit in Malaysia. It was found that TW can increase the air change rate by 27% under favourable wind conditions.

It is evident from the above that the effectiveness of TW in enhancing natural ventilation has been confirmed and is significant. However, the TW performance has been investigated either on its presence or relative positions in a single house. There has been no consideration of other physical characteristics of TWs and in the context of characteristics of high-rise residential buildings.

2.4.2 The effectiveness of transom window in reducing cooling energy use

Whether enhanced ventilation created by TW can achieve thermal comfort and further reduce energy usage for cooling are questions that are yet to be answered convincingly [44]–[46], [49]. However, many research have already found that for subtropical climates, natural ventilation can only be used during a limited period of time in a year and in favourable climates [51], [52].

To fill this research gap, it is required to investigate the effectiveness of TW in reducing cooling energy usage and providing thermal comfort in high-rise residential buildings in Hong Kong. However, based on results of previous studies, instead of relying purely on enhanced ventilation

facilitated by TW to replace air-conditioning system (AC system) to achieve thermal comfort, the use of enhanced ventilation supplemented with air-conditioning (hybrid system) should be investigated.

2.5 Summary

The research gaps were identified in this Chapter which includes:

1. To identify the influence of window types on natural ventilation performance of residential units in Hong Kong, taking into account the interactive effects of ventilation modes, window orientations, and coincident wind conditions.
2. To identify the window opening habits of Hong Kong residents and the optimum DEG for efficient natural ventilation.
3. To investigate the impacts of different physical characteristics of TWs in enhancing natural ventilation in the context of characteristics of high-rise residential buildings.
4. To investigate the effectiveness of TW, integrated with other aperture designs in reducing cooling energy usage and providing thermal comfort in high-rise residential buildings in Hong Kong.

CHAPTER 3 METHODOLOGY

This chapter presents the methodology adopted for investigating the influence of window designs on natural ventilation. The investigation methods, as outlined below, include site measurements, CFD simulations, and energy simulations. To set internal and external conditions for CFD and energy simulations, methods to derive the representative wind conditions and the representative residential estate and unit are also discussed. Other methods adopted for specific studies such as walk-through surveys and market surveys are discussed in the relevant chapters.

3.1 Site measurements

Site measurement has been recognized as the most reliable way to provide accurate results and is the most authoritative reference to modify the simulation modelling [53]. In natural ventilation studies, measurements are often taken in existing buildings or actual sites [54], [55] and the temperature and velocity are recorded [12], [56]. However, site measurements have limitations due to the constraints on instrumentation for measurements (i.e. instruments for measurements, labours, site constrained), unsteady external wind conditions, and the essential uncertainty of the experiments. Besides, it is difficult to determine the natural ventilation performance in an urban environment due to the complex and compact surrounding obstructions so site measurements are often employed to support simulation studies.

In this study, different sets of site measurements were conducted at different sites. They were done for providing data for validation of CFD settings, for identifying influential parameters for further studies and for verifications of simulation results.

Tracer gas decay method is the most widely used method to assess ventilation rate through openings. By this method, a proper amount of tracer gas is injected into the internal space and readable tracer gas sensors are used for recording the concentration at the sampling points during the monitoring period to evaluate natural ventilation performance.

SF₆ was chosen as the tracer gas in this study because it is easy to measure at low concentration. It is non-toxic and more importantly, it is not a natural component of air [57]. Thus, it is by far the most commonly used tracer gas in ventilation studies [58]. Details for the site measurements are introduced in Chapters 4 to 7.

Air change per hour (ACH, /h) was used to quantify natural ventilation performance.

3.2 CFD simulations

Computational fluid dynamic (CFD) simulation method was used to simulate the outdoor and indoor airflow of the buildings so as to enable the prediction of the achievable ventilation rate and indoor air velocity for different window designs. FLUENT 13.0 was employed for the CFD simulations [59].

By numerically solving a set of partial differential equations in the computational field, it can provide a high-efficient, accurate prediction of the fluid flow characteristics, including the air velocity, pressure distribution, etc. The CFD simulation method fills the limitations of the site measurement method in reducing the cost for measurements, allowing quick assessment of different designs, providing visualized and comprehensive numerical information, and enabling the simulation of airflow under different physical conditions.

The Reynolds-Averaged Navier-Stokes (RANS) turbulence modelling approach is used in this study for solving the numerical solutions of the airflow. The RANS was selected for its less computing time comparing with other modelling methods (i.e. large eddy simulation method or the direct numerical simulation method) since it solves the time-averaged flow parameters and is the most widely used in natural ventilation studies [60]. The governing equations are given below:

Continuity equation:

$$\frac{\partial u_i}{\partial x_i} = 0 \quad (3.1)$$

Momentum equation:

$$\frac{\partial}{\partial x_j} (\rho u_i u_j) = -\frac{\partial P}{\partial x_i} + \frac{\partial}{\partial x_j} \left[\mu \left(\frac{\partial u_i}{\partial x_j} + \frac{\partial u_j}{\partial x_i} - \overline{\rho u_i' u_j'} \right) \right] \quad (3.2)$$

Where u_i and u_i' are the mean and fluctuating airflow velocity component in the direction of x_i ;

P is the mean pressure; ρ is the density of the air; $\overline{\rho u_i' u_j'}$ is the Reynolds stress.

The objective of the RANS' turbulent models is to solve the Reynolds stress that accounting for the fluctuations of turbulence in fluid momentum by two principle approaches; the eddy-viscosity model and the Reynolds-stress model [61]. As far as window design study is concerned, two

turbulence models based on the RANS approach are introduced below. The default settings of the models were used for further investigations.

3.2.1 k-epsilon standard equations

The k-epsilon (k- ε) standard equations have been widely and successfully used in indoor airflow simulation for its reasonable accuracy [62], [63] and less computing time [60]. The three-dimensional of k- ε standard transport equations are given by:

$$\frac{\partial(\rho k u_i)}{\partial x_i} = \frac{\partial}{\partial x_j} \left[\left(\mu + \frac{\mu_t}{\sigma_k} \right) \frac{\partial k}{\partial x_j} \right] + P_k - \rho \varepsilon \quad (3.3)$$

$$\frac{\partial(\rho \varepsilon u_i)}{\partial x_i} = \frac{\partial}{\partial x_j} \left[\left(\mu + \frac{\mu_t}{\sigma_\varepsilon} \right) \frac{\partial \varepsilon}{\partial x_j} \right] + C_{1\varepsilon} \frac{\varepsilon}{k} P_k - C_{2\varepsilon} \rho \frac{\varepsilon^2}{k} \quad (3.4)$$

Where k is the turbulent kinetic energy; ε is the dissipation rate; P_k is the production of the turbulent kinetic energy and is determined as:

$$P_k = -\overline{\rho u_i \dot{u}_j} \frac{\partial u_j}{\partial x_i} \quad (3.5)$$

The turbulent viscosity μ_t is calculated in terms of k and ε by:

$$\mu_t = \rho C_\mu \frac{k^2}{\varepsilon} \quad (3.6)$$

The five modelling variables $C_{1\varepsilon}$, $C_{2\varepsilon}$, C_μ , σ_k and σ_ε keep default model constant with the value of 1.44, 1.92, 0.09, 1.0 and 1.3 respectively.

3.2.2 k-epsilon RNG equations

The Re-Normalization Group (RNG) has been extensively used for indoor airflow simulations [61]. Comparing with the standard k- ϵ , the modification of ϵ equation make it accounts for the small scales of the fluid motions with the form as:

$$\frac{\partial(\rho\epsilon u_i)}{\partial x_i} = \frac{\partial}{\partial x_j} \left[\left(\mu + \frac{\mu_t}{\sigma_\epsilon} \right) \frac{\partial \epsilon}{\partial x_j} \right] + C_{1\epsilon} \frac{\epsilon}{k} P_k - C_{2\epsilon}^* \rho \frac{\epsilon^2}{k} \quad (3.7)$$

Where

$$C_{2\epsilon}^* = C_{2\epsilon} + \frac{C_\mu \eta^3 (1 - \eta/\eta_0)}{1 + \beta \eta^3} \quad (3.8)$$

$$\eta = Sk/\epsilon, \quad S = (2S_{ij}S_{ij})^{1/2} \quad (3.9)$$

$$S_{ij} = \frac{1}{2} \left(\frac{\partial u_i}{\partial x_j} + \frac{\partial u_j}{\partial x_i} \right) \quad (3.10)$$

Where u_j is the mean and fluctuating airflow velocity component in the direction of x_j ; Values for $C_{1\epsilon}$, $C_{2\epsilon}$, C_μ , σ_k and σ_ϵ are 1.42, 1.68, 0.0845, 0.7194 and 0.7194 respectively; $\eta=4.38$ and $\beta=0.015$.

3.3 Energy simulations

Energy simulations were used to evaluate cooling energy reduction derived by the utilization of natural ventilation for different window designs.

Performance evaluation was accomplished by the use of the building energy simulation programme “EnergyPlus” [64]. EnergyPlus has been successfully used in similar studies [65], [66] and its simulation accuracy have been verified against other programs for building thermal behaviour evaluation [67]. It is a component-based system simulation program. It allows the addition of an extra component to model natural ventilation. In it, a building’s thermal response to outdoor climate conditions (e.g. outdoor temperature, humidity, solar gain), internal heat gains (e.g. equipment, human occupancy) [68], [69], airflow rate through buildings and the corresponding heat removal by convection [70] and cooling equipment can be accurately predicted. The result generated by EnergyPlus after the simulation run is comprehensive. It allows users to extract the required data, which include temperature, moisture content, mass flow rate in selected nodes, and hour-by-hour cooling energy usage.

In this study, based on the achievable ventilation rate and indoor air velocity for different window designs predicted by CFD simulations, together with the energy usage and temperature predicted by energy simulations, thermal acceptability and cooling energy usage for different window designs can be determined.

3.4 Representative wind conditions

Representative coincident wind conditions are required for CFD simulations. They were developed by reference to the hourly meteorological data of Hong Kong in the last ten years (2004 to 2013). Based on the meteorological records, the first step is to define for the maximum (X_{\max}), average (\bar{X}) and minimum (X_{\min}) values each studied parameter (X). Given natural ventilation is mainly wind-driven and there is only small difference in temperature between outdoor and indoor happen in the moderate seasons in Hong Kong where natural ventilation is

often used [71], [72], thus the studied parameters include only the wind speed (X_{spd}) and wind direction (X_{dir}). But as there are bound to be extreme wind conditions that are rare and anomalous, the Central Composite Design (CCD) method and the Squeeze Theorem, as recommended by other studies [73], were employed to remove the extreme values and to determine the representative wind conditions.

For determining the required values for X_{spd} and X_{dir} , it is necessary to determine the minimum required number of data sets (NB) that can provide not only high precision in further analysis but also reduce simulation time. NB can be estimated by Equation (3.11) which is 9 in this study [74].

$$NB = 2^G + 2G + CP \tag{3.11}$$

Where G is the number of variables ($=2$); and CP is the centre point value which is normally set as 1 [75], [76].

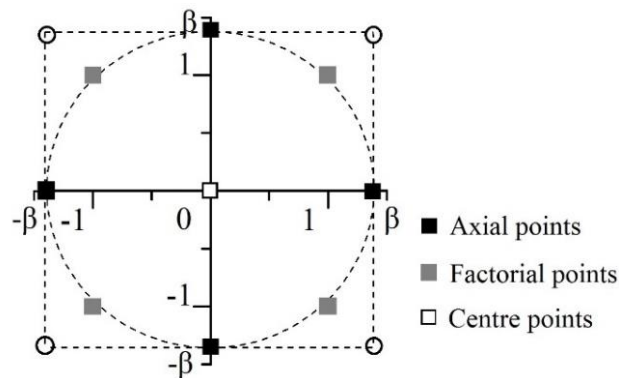


Figure 3.1 Illustration of the determination of range of variable

Besides the centre point, CCD method involves factorial points and axial points (Figure 3.1).

In Figure 3.1, the axial points are X_{\max} and X_{\min} which are lying on the circumference of the circle and \bar{X} is the centre point value. They were normalised to $+\beta$ and $-\beta$, where β equals $\sqrt{2}$. The Squeeze Theorem [77] was then applied to remove the extreme values in intervals of 0.1 m/s for X_{spd} and 30 degrees for X_{dir} and to keep the centre point unchanged for determining X_{\max} and X_{\min} . The interval (=0.1 m/s) for wind speed was determined based on the same decimal point as the meteorological data, while that of the wind direction (=30 degrees) was by common practice [78]–[80].

Table 3-1 Representative coincident wind conditions

Run <i>i</i>	X_{cod}		X_{n}	
	X_{spd}	X_{dir}	X_{spd} (m/s)	$X_{\text{dir}}^{1,2}$ (Degree, °)
1	-1	-1	1	30
2	1	-1	4.8	30
3	-1	1	1	150
4	1	1	4.8	150
5	$-\beta$	0	0.21	90
6	β	0	5.59	90
7	0	$-\beta$	2.9	5.15
8	0	β	2.9	174.85
9	0	0	2.9	90

Note: ¹ North is 0°; ² 50% of the wind direction (181° to 360°) belonging to sky vault positions at the back of the window surface were considered by modelling the window at four possible orientations (North, East, South and West).

Upon the removal of the extreme values and the determination of X_{\max} and X_{\min} , the representative coincident wind conditions (X_{n}), coded as $-\beta$, ± 1 , 0, $+\beta$ (X_{cod}) in Figure 3.1, can be determined by Equation (3.12). Results are shown in Table 3-1.

$$X_{\text{cod}} = \frac{2(X_{\text{n}} - \bar{X})}{X_{\text{max}} - X_{\text{min}}} \quad (3.12)$$

3.5 Representative residential estate and unit

Hong Kong is famous for its rapidly developed economy, urbanization and high population density [81]. Population estimates show that the population density in Hong Kong is 6830 persons per square kilometre [82], ranking in the 8th most densely populated city in the world [83].

The high population, other than natural increase, is attributed to the cumulative influx of immigrants from Mainland China, resulting in a growth of population from 6.49 million in 1997 to 7.39 million in 2017. Adding to that is the sharp reduction of the average household size from 3.3 to 2.8 in the past decade years, leading to a sustained high demand for residential housings [84], [85]. In 2017, the number of domestic households was 2.54 million. It is almost impossible to review the floor layout of all residential units in Hong Kong to study the window design on natural ventilation enhancement. Thus, residential estates must be carefully selected to represent typical characteristics of residential units in Hong Kong for the intended studies.

There are two types of domestic housing in Hong Kong, which are private housing and public housing accounting for 53.8% and 45.4% (0.7% for temporary housing) households respectively.

Private housing, which is developed by private developer, plays an important role in the housing needs of the society. Private housing is usually characterised by its flexible design (i.e. the variety of window types; window dimensions; flexible ventilation modes). It is developed to satisfy the needs of the property market and end-users. The building designers are thus given more freedom in the window designs. Therefore, for the evaluation of the optimum window type and window opening degree, a hypothetical unit, which was formulated to represent typical characteristics of

private housing, was used as a studied unit. The hypothetical unit has been employed for several other ventilation studies in Hong Kong [86], [87].

Public housing, affordable rental housing for middle and low-income residents, has been provided by the Hong Kong Government since 1954. The Hong Kong Housing Authority, committed to design public housing, has everlastingly updated its design concept and construction process to satisfy social, economic and market demands [88]. To optimise cost effectiveness and spatial efficiency, the public housing blocks in Hong Kong are of standardised and compact designs. The compact design characteristics made the public housing permanently limited to single-sided ventilation. Therefore, the evaluation of using transom window to facilitate ventilation enhancement is based on a representative residential unit selected from a typical public housing estate in Hong Kong.

Details of the hypothetical unit and the representative residential unit are presented in Chapters 4 and 6.

3.6 Summary

The theoretical backgrounds, reasons and key features of the methods used across the four major parts of work of this thesis were introduced which include site measurements, CFD simulations, energy simulations, representative wind conditions and representative residential estate and unit. Details of each method in achieving the intended objectives of this study are introduced in individual chapters.

CHAPTER 4 INFLUENCE OF WINDOW TYPE

This Chapter presents the investigations of the influence of window type on enhancing natural ventilation in a residential building in Hong Kong. The investigations have considered the interactive effects of window types, other aperture designs and local wind conditions. To achieve the intended objectives, walk-through surveys, site measurements, simulation validations, CFD simulations and response surface regression analysis were conducted. The response surface regression analysis was employed to formulate a prediction model to quickly examine the ventilation performance and to facilitate quantification of influences of different design options. The nine representative wind data sets formulated by the Central Composite Design method and the Squeeze Theorem (introduced in Chapter 3) were used for CFD simulations. Further, a multi-criteria optimisation method was used to identify the most preferred window type for Hong Kong residential units.

4.1 Walk-through survey

Walk-through surveys were conducted in the evening in October 2017 to ascertain the most used window types and windows opening habits in residential buildings in Hong Kong. Façade images of 31 constituent residential estates of Centa-City Index (CCI)¹ amounting to 9965 windows were taken. The 31 residential estates were chosen because the constituent estates in CCI are of sufficient representation in Hong Kong. This time period was chosen for having the highest occupancy in most residential units [89] and the most moderate weather condition [90] .

¹ The Centa-City Index (CCI) is a monthly index based on all transactions records as registered with the Land Registry in Hong Kong to reflect property price movements in the previous 1-2 months.

The results of the walk-through survey for different window types are summarized in Table 4-1.

While results of window opening habits are reported in Chapter 5.

It can be seen that among different window types, SH window is the most used (63.9%), followed by TH window (35.85%) and SLD window (0.26%).

Table 4-1 Summary of window types

Type	Number of windows			Total	Percent (%)
	NT	KLN	HK		
TH	562	2711	299	3572	35.9
SH	1114	4410	843	6367	63.9
SLD	6	12	8	26	0.2
Total	1682	7133	1150	9965	100

Remarks: NT= New Territories; KLN = Kowloon; HK= Hong Kong Island

4.2 Site Measurements

Site measurements were conducted at a carefully selected site to provide data for validation of the CFD settings. The unit on the third floor was selected because: 1) the building block where the unit is located is situated at an isolated site with few external obstructions to enable a focused study of the influence of window types under varying wind conditions (Figure 4.1); 2) it consists of two different types of windows (SH and TH) of the same area to enable direct comparison of performance of two types of windows; and 3) the studied area dimensionally matches the hypothetical unit to be used for further studies (bedroom dimensions) (Figure 4.3).

As mentioned in Chapter 3, the tracer gas decay method was adopted for measuring ACH [91]. Before each set of ACH measurement, all furniture and doors were properly sealed to avoid unintentional infiltration. Windows in the room were fully opened for 10 minutes to ensure

indoor and outdoor temperatures were the same to remove the buoyancy-effect. The windows were then closed and a proper amount of SF₆ (measurable but not exceeding the maximum precision of B&K 1302 (=130 ppm)) was injected into the space to achieve an initial concentration of 100 ppm. Since SF₆ is heavier than air, a mechanical device was used to ensure SF₆ concentration of the entire studied area was in equilibrium.

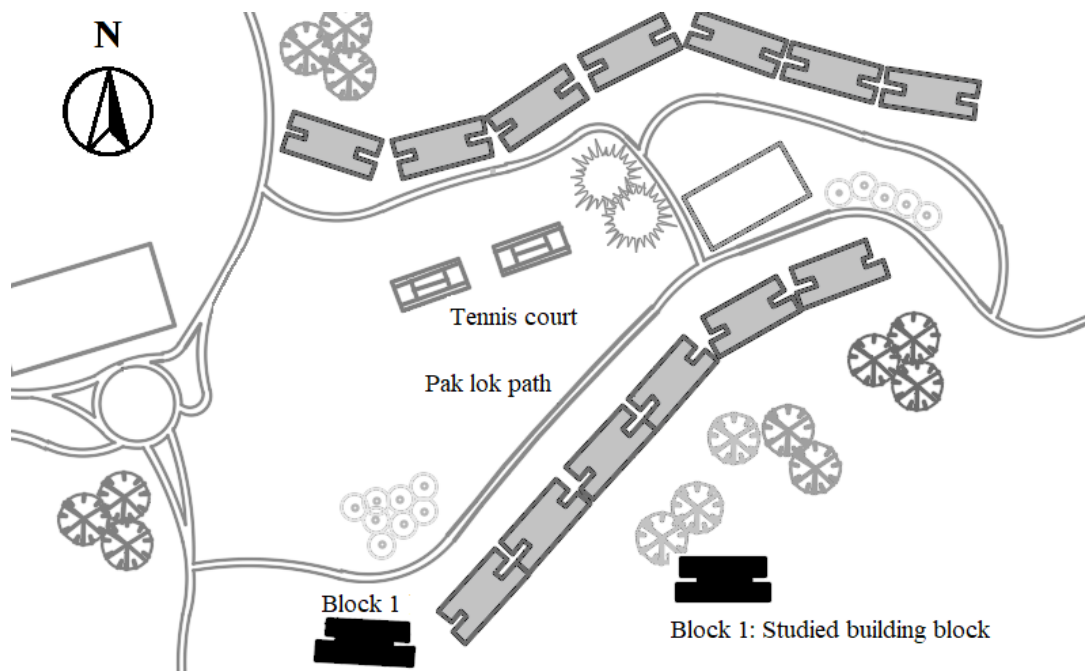


Figure 4.1 Site layout of the studied building block

Upon achieving equilibrium, the studied TH windows (W1 and W2 in Figure 4.3) and SH windows (W3 and W4 in Figure 4.3) were fully opened simultaneously. Tracer gas concentrations near the four studied windows were then measured at 40-second intervals. Figure 4.3 shows the four measurement positions (P1 to P4). They were set 500 mm from the middle of the opened windows as recommended by a previous study on airflow through windows to avoid interactions of two adjacent window openings [44]. Bruel & Kjaer multi-gas analyser type 1302 was employed for the SF₆ concentration measurements.

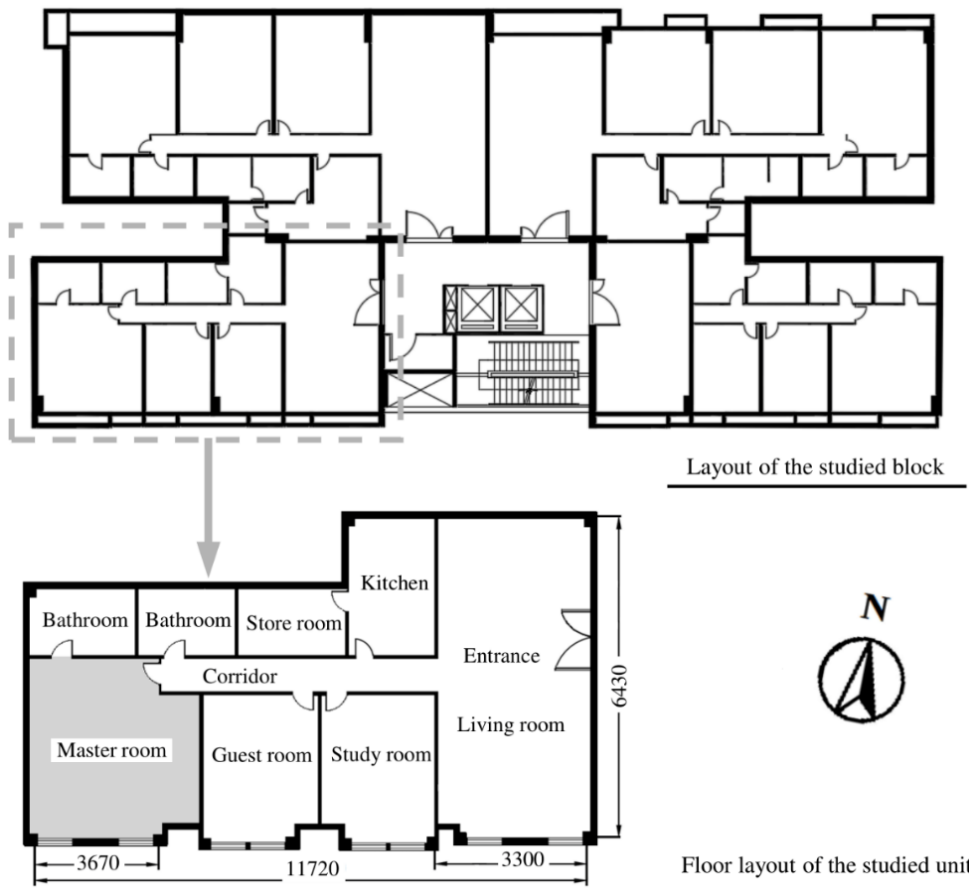


Figure 4.2 Layout of the studied building block (top) and the studied unit (bottom)

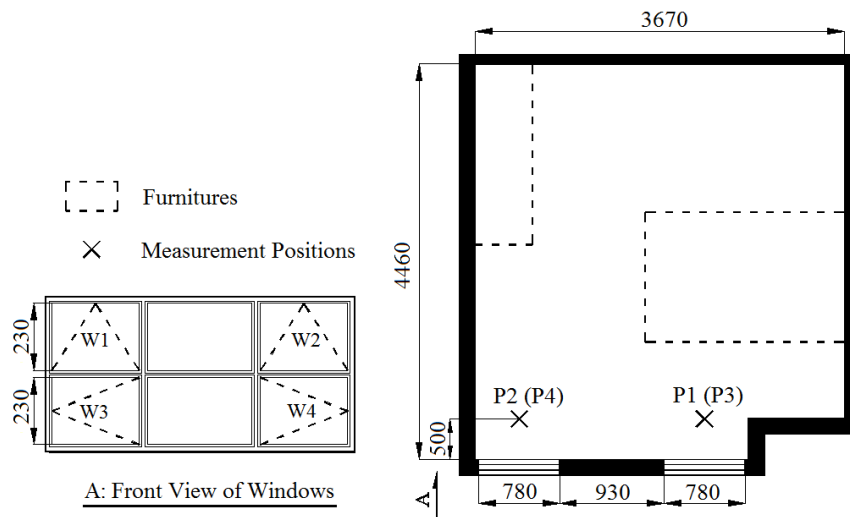


Figure 4.3 Measurement positions in the studied unit

Outdoor meteorological conditions on the two measurement dates were monitored in accordance with American Society for Testing and Materials (ASTM) standards [91]. The portable meteorological station was set up at an unobstructed location 10 meters from the studied unit to

measure the prevailing wind conditions. The station consists of an ultrasonic anemometer HD 2003 for outdoor wind direction and velocity monitoring; and temperature sensor for outdoor air temperature measurement. Wind conditions during measurements are shown in Figure 4.4. The mean wind speed and wind direction, which are 1.3 m/s and 30° (North East direction), were used as boundary conditions for simulation validation.

All sensors were calibrated before site measurements. Readings were recorded at a one-second interval. Accuracy of the measuring instruments is summarised in Table 4-2.

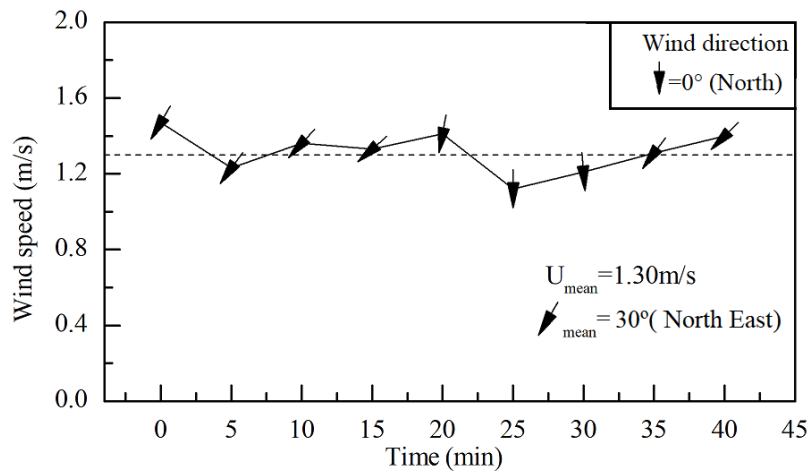


Figure 4.4 Wind conditions during measurements

Table 4-2 Accuracy of major instruments

Measured parameter	Instrument	Accuracy
Tracer gas concentration	Bruel& Kjær 1302	±2.5%
Outdoor wind speed and temperature	HD 2003 anemometer	Both ±1%
Indoor temperature	Temperature Logger	±3.5 °C

Figure 4.5 compares the decay in SF₆ concentration for the two window types under fully opened condition. The decay process was classified into three phases, as shown in the figure. Phase one was the injection process where SF₆ concentration was charged to 130 ppm level. Phase two was

the mixing process where the SF₆ concentration (ppm) at all measurement positions became the same. Phase three was the decay process where the four windows were opened, and the SF₆ concentration at the four measurement positions decreased gradually.

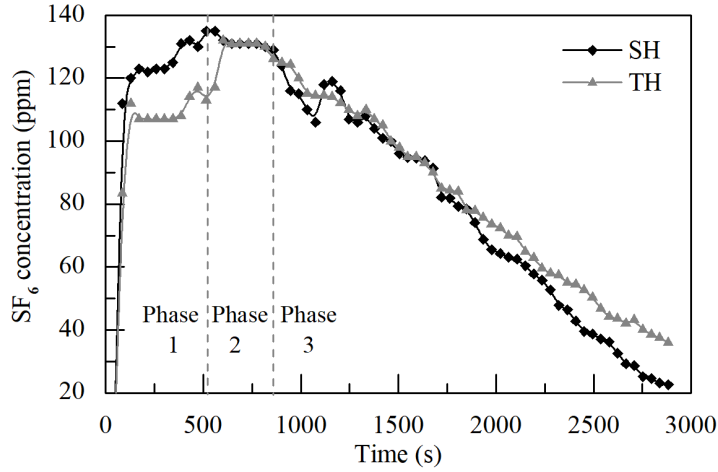


Figure 4.5 Decay curves of the two window types

On mass balance, as SF₆ was in equilibrium in the space, the mass balance equation could therefore be expressed as:

$$V_e \times \frac{dC_i(t)}{dt} = -C_i \times Q_e + C_o \times Q_e \quad (4.1)$$

Where V_e is the effective room volume (m³); C_i is the indoor SF₆ concentration (ppm); C_o is the outdoor SF₆ concentration which is zero (ppm); Q_e is the effective volume flow rate (m³/s) and t is time (s).

By integration of Equation (4.1), and based on the initial concentration of SF₆ for $C(t_1)$ and t_1 , Q_e can be rewritten as:

$$Q_e = V_e \frac{\ln \frac{C(t_1)}{C(t_2)}}{(t_2 - t_1)} \quad (4.2)$$

Where $C(t_2)$ is the concentration of SF₆ at the end (ppm); and t_2 is the end time (t).

The air-change per hour (ACH) is then defined as:

$$ACH = \frac{Q_e \times 3600}{V_e} \quad (4.3)$$

As the four windows were opened together, there were minor disturbances in air flow from individual windows but judging from the decay slope, it can be concluded that SH windows performed slightly better than TH windows. The calculated air-change rate based on the decay process can be used for simulation validations.

4.3 Simulation validations

In the simulations, the outdoor meteorological data recorded during site measurements were used as the boundary condition (Figure 4.6). A three-dimensional model of the building block where the studied unit is located was established and the mesh was generated by Integrated Computer Engineering and Manufacturing (ICEM) Software, which is a grid generation software under ANSYS workbench.

Domain height and width, based on a previous study with similar terrain characteristics, were set as 5 times the width (5WD) and 3 times the height (3HT) of the studied building block [12],

while the domain length was determined by trial simulations. Trial simulations were done by increasing the domain length in multiples of the length (LG) of the building block, from 1LG to 15LG. It was found that simulation results differed only by 2.5% between 5LG and 15LG. Considering the need to maintain a balance between computing time and accuracy of results, the domain region was finally set as $5LG \times 5WD \times 3HT$, which corresponds to $154m \times 71.85m \times 90.75m$.

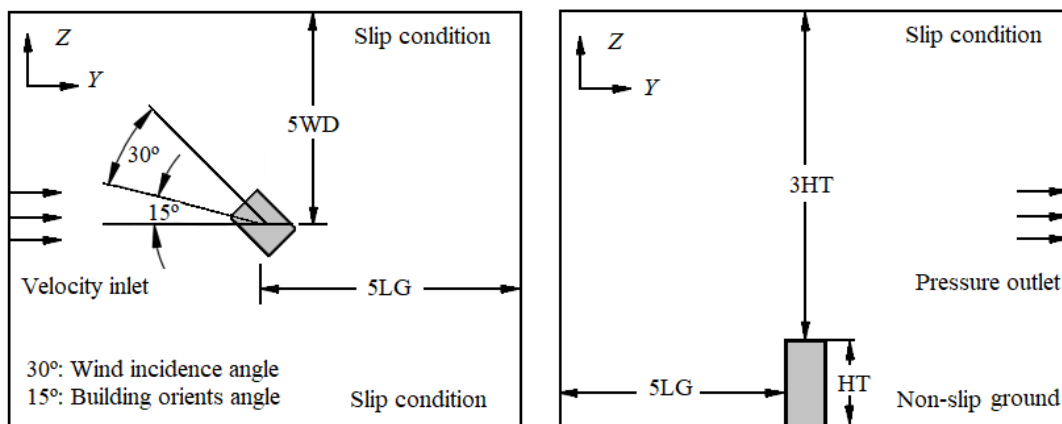


Figure 4.6 Computational domain region and boundary conditions.

In this study, no external obstructions were included in the computational region. This is considered an adequate simplification because there are no major obstructions around the studied building block as mentioned earlier. Thus enables a focused study on comparing the performance of TH and SH windows.

Grid generation was started with the smallest control volume 0.005m from the crucial walls; and a stretching factor of 1.3 was adopted to expand the grid size. Grid refinement to the walls, grounds and places with large gradients were performed by the unstructured hexahedral mesh and the prism methods to become 320,676 volumes. To enable grid independence test, a finer grid of 960,647 volumes, determined by a mesh generation software ICEM [92], [93], was used.

Simulation results based on the two grid volumes showed that there were negligible differences in air distribution and ACH, confirming that the grid independence test was satisfactory.

The renormalisation group model, k-epsilon RNG turbulence model, was used to simulate steady-state ventilation performance. The SIMPLE (Semi-Implicit Method for Pressure-Linked Equations) algorithm was used to couple pressure and velocity.

A wind power law (Equation 4.4) [94] was used to adjust the site measurement results to obtain the incoming air velocity profile.

$$\frac{U_z}{U_{ref}} = \left(\frac{HT}{HT_{ref}} \right)^\alpha \quad (4.4)$$

Where HT_{ref} is the reference height where the meteorological station was located (=10m); U_{ref} is the mean velocity at the reference height during measurement; and α is the power-law exponent having the same terrain characteristics as used in a previous study (i.e. open terrain, grassland with few well-scattered obstructions) is taken as 0.2 [95].

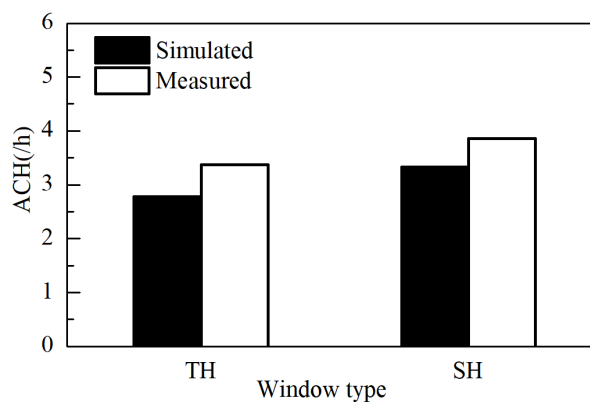


Figure 4.7 Comparison of simulated and measured results

Figure 4.7 shows the comparison between simulated and measured results, illustrating that the differences between ACH in simulation and real measurements, both for SH and TH windows, are in the range of 17%. Given the range of differences is within acceptable limits [5], and the consistency in the two sets of data, validations were regarded as acceptable. It is therefore reasonable to adopt the k-epsilon RNG turbulence model and the associated parameter settings for further CFD investigations.

4.4 CFD simulations

After validating the CFD simulation settings, and identifying the representative coincident wind conditions, further CFD simulations were done to investigate the performance of different windows types based on a hypothetical residential unit with different window positions.

4.4.1 The hypothetical unit

Hong Kong is a small place. However, the number of domestic households was 2.54 million in 2017. It is almost impossible to review the floor layout of all residential units in Hong Kong to study the influence of window type on ventilation performance. The hypothetical unit formulated to represent characteristics of typical residential units in Hong Kong was thus employed for the study. It was formulated based on an extensive survey of floor areas, floor layouts, window dimensions and construction details of residential buildings in Hong Kong. Considering that it would be rather complex to deal with wide combinations of surrounding buildings, the hypothetical unit was assumed located on the ground floor at an isolated site. This, according to a previous study, does not affect the investigation of the influence of interior design parameters on the ventilation performance [28]. The floor layout of the hypothetical unit with different

window positions to represent single-sided ventilation (Figure 4.8 (a)) and cross ventilation (Figure 4.8 (b)) are given. The three types of windows are of dimensions 780mm×600m (WD×HT) and are amounted on the same position of the wall.

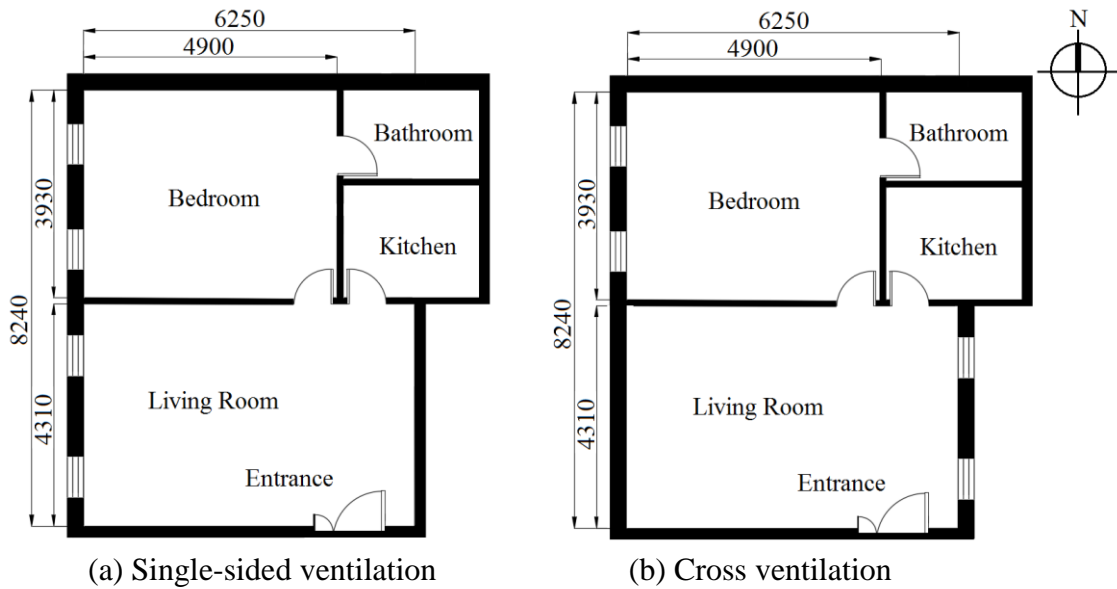


Figure 4.8 Floor layout of the hypothetical unit (west-facing windows)

Single-sided and cross ventilations were considered because they correspondingly represent the least and the most preferred ventilation modes [27], [96] to facilitate evaluation of the interactive effects of window types, ventilation modes and window orientations on ventilation performance of residential units.

4.4.2 Further simulations

Based on four possible window orientations, three window types, two ventilation modes and the nine representative wind conditions (Table 3-1), a total of 216 ($4 \times 3 \times 2 \times 9 = 216$) cases were generated for CFD simulations. FLUENT 13.0 [59] was used for simulating the air change rate (ACR) through each window (total 4 windows) in the hypothetical unit.

ACR can be determined by the decay method and by integrating the velocity vector across window openings. Considering that solving the concentration equations in the decay method is time-consuming, previous studies have confirmed the satisfactory use of the integration method for single-sided ventilation that is convective dominant [16], [97]. In this study, regardless of the ventilation mode, the studied windows were assumed fully opened to the outside to receive incoming air to result in a convective dominant ventilation [39]. Thus integration method was used in calculating ACR.

ACR is defined as:

$$Q = \int \vec{v} \times d\vec{A} = \frac{1}{2} \sum_j \sum_{i=1}^n |v_i \times n_i| \times A_i \quad (4.5)$$

Where v_i is the velocity vector; n_i is the velocity vector normal to the windows; A_i is the cell i face area of the window; n_i is the total number of cells at the window and j is window j of the building. According to the mass conservation law, incoming and outgoing airflow rates should be the same and thus a factor 1/2 is used in Equation (4.5) (assuming the difference between incoming and outgoing flow is less than 0.002kg/s [98]).

FLUENT surface integration was used to calculate ACR. Thus the creation of surface is important not only for integral outcomes, but also for visualising the flow field around openings. Given there were 280 cases (216 studied cases as mentioned above plus 64 testing cases (completely different from the studied cases) for verification of the resultant RSR model (explained in Section 4.6.2) to run; 1120 outputs (4 windows in each case) to generate; and to

analyse 3360 window cell areas A_i (Equation (4.5)), co-simulation tools were used to execute simulation runs and to organise the vast volume of output data. Journal script [99] was employed to automatically vary input and boundary conditions to generate simulation cases and to organise the output data. Python [100] was employed for algorithm analysis to commit simulation runs and to check consistency of the incoming and outgoing airflows to confirm suitability of Equations (4.3) and (4.5) for calculation of ACHs.

In further simulations, only the wind effect was considered. This approximation is acceptable because the windows were amounted at the same level and the separation between floors were air-tight to diminish the buoyancy effect, making the wind-effect dominant [35], [101], [102].

4.5 Response surface regression analysis

The response surface regression (RSR) was employed to develop the mathematical model to facilitate investigation of the interactive effects of different parameters on ventilation performance of residential units. RSR has been proved to be one of the most efficient and highly accurate metamodeling approach, which has been widely used in other research areas, in particular chemistry and biochemistry for the optimisation of experimental processes [73], [74]. It has also been proved to have high accuracy in studying interactive relationships [75], [76].

Based on the 216 sets of CFD simulation results, a computer software Design-Expert [103], [104] was used to generate the RSR model. The RSR model is used to relate ACH with the studied variables, as shown in Equation (4.6) [105]:

$$ACH = b_0 + \sum_{j=1}^5 b_{1j} x_j + \sum_{j=1}^5 b_{jj} x_j^2 + \sum_j \sum_{k>j} b_{jk} x_j x_k + \sum_j \sum_{k>j} \sum_{l>k} b_{jkl} x_j x_k x_l \quad (4.6)$$

Where ACH is the response value; x_i is the i^{th} response variable ($i = j, k, l$); b_j represents the i^{th} coefficient ($i = 0$ to 1 for linear; jj to jkl for interactive).

A family of regression models was generated by Design-Expert. Among them, an acceptable model was selected based on the sequential model sum of square (SMSS) test. They include checking the degree of order, the variance inflation factor (VIF), the coefficient of determination (R^2), the adjusted R^2 , the predicted R^2 , the p-value, and the signs of the coefficients. A third order model, according to previous research works, is considered the maximum for a regression model with acceptable level of accuracy [73], [106]. The VIF value was used to remove variables with high multi-collinearity. Although there are no straight requirements of an acceptable R^2 value, a model is generally considered good if R^2 is more than 0.5 [107] and the difference between the adjusted R^2 and the predicted R^2 is less than 0.2 [108].

The predicted R^2 ($R_{Predicted}^2$) is calculated by using the predicted residual sums determined by removing one case from the 216 simulation cases as shown in Equation (4.7):

$$R_{Predicted}^2 = 1 - \frac{PRESS}{SS_{Total}} \quad (4.7)$$

Where $PRESS$ is the predicted residual error sum of squares, SS_{Total} is the total sum of the squared residual.

The p-value is used to determine the significance of a variable, and an acceptable value is typically equal to or less than 0.05 [109]. The signs of the coefficients are used to judge if the model is reasonable.

The verification of the resultant model was done based on testing data sets.

4.6 Results and Analysis

4.6.1 The RSR model

After performing the 216 CFD simulation runs and calculation of ACH (by Equations (4.3) and (4.5)), Design-Expert was used to build the RSR model and the model that passed the SMSS test is shown in Equation (4.8).

$$\begin{aligned}
 ACH = & -0.96 + 4.38 SPD + 0.009 DIR + 0.29 VENT_{CV} + \left\{ \begin{array}{l} 0.61 ORN_N \\ 0.12 ORN_E + \left\{ \begin{array}{l} 0.40 TYP_{SH} \\ 0.03 TYP_{TH} \end{array} \right\} \\ 0.90 ORN_S \end{array} \right\} \\
 & 1.81 SPD \times VENT_{CV} + \left\{ \begin{array}{l} 1.33 SPD \times TYP_{SH} \\ 0.42 SPD \times TYP_{SH} \end{array} \right\} + \left\{ \begin{array}{l} 0.12 VENT_{CV} \times TYP_{SH} \\ 0.05 VENT_{CV} \times TYP_{TH} \end{array} \right\} \\
 & \left\{ \begin{array}{l} 0.41 ORN_N \times TYP_{SH} \\ 0.24 ORN_E \times TYP_{SH} \\ 0.42 ORN_S \times TYP_{SH} \end{array} \right\} + \left\{ \begin{array}{l} 0.02 ORN_N \times TYP_{TH} \\ 0.10 ORN_E \times TYP_{TH} \\ 0.47 ORN_S \times TYP_{TH} \end{array} \right\} + \left\{ \begin{array}{l} 0.37 SPD \times VENT_{CV} \times TYP_{SH} \\ 0.35 SPD \times VENT_{CV} \times TYP_{TH} \end{array} \right\} \quad (4.8)
 \end{aligned}$$

The abbreviation for the quantitative and qualitative variables are summarized in Table 4-3.

It is worth mentioning that the resultant model consists of a mix of quantitative and qualitative variables. To deal with the qualitative variables (VNT, ORN and TYP), the dummy variable

method was adopted to assign the value 0 or 1 to indicate the absence or presence of a particular condition except the base group against which the comparisons are made. In this case, the less preferred conditions identified in the review of the calculated ACH were chosen as the base group, i.e. single-sided ventilation (SV), west facing window (ORN_W), and sliding window (TYP_{SLD}). Accordingly, for ORN, only north (N), south (S) and east (E) were coded, and likewise for VNT and TYP, only cross ventilation, SH window and TH window were coded.

Table 4-3 Independent variables and coded value in RSR model

Abbreviation		Description	Unit / Code
SPD		Wind speed	m/s
DIR		Wind direction	Degree
VNT	CV	Ventilation mode - Cross ventilation	No = 0 / Yes = 1
	SV	Ventilation mode - Single-sided ventilation	Base
ORN	N	Orientation - North	No = 0 / Yes = 1
	E	Orientation - East	No = 0 / Yes = 1
	S	Orientation - South	No = 0 / Yes = 1
	W	Orientation - West	Base
TYP	SH	Window type - Side hung	No = 0 / Yes = 1
	TH	Window type - Top hung	No = 0 / Yes = 1
	SLD	Window type - Sliding	Base

Table 4-4 Summary of standardized coefficients (B)

Independent variable		Interactive variables (Product Term)							
		1	SPD	VNT _{CV}	ORN			VNT _{CV} · TYP	
					ORN _N	ORN _E	ORN _S	TYP _{SH}	TYP _{TH}
SPD		8.32	—	—	—	—	—	0.70	0.67
DIR		0.05	—	—	—	—	—	—	—
VNT	CV	4.96	3.44	—	—	—	—	—	—
	SV (Base)	—	—	—	—	—	—	—	—
ORN	ORN _N	0.61	—	—	—	—	—	—	—
	ORN _E	0.12	—	—	—	—	—	—	—
	ORN _S	0.90	—	—	—	—	—	—	—

	ORN _w (Base)	—	—	—	—	—	—	—	—
TYP	TYP _{SH}	3.88	2.52	1.19	0.41	0.24	0.42	—	—
	TYP _{TH}	1.62	0.80	0.83	0.06	0.10	0.47	—	—
	TYP _{SLD} (Base)	—	—	—	—	—	—	—	—

The R^2 , adjusted R^2 and predicted R^2 of the resultant model are 0.86, 0.85 and 0.83, respectively, and confirm goodness-of-fit of the resultant model. The standardised coefficients (B) were used to quantify the influences of the independent and interactive variables. Results are summarised in Table 4-4.

It can be seen that positive coefficients have been generated for all independent variables. This is considered reasonable because the less desired options were set as the base group. The influence of the independent and interactive parameters are discussed in subsequent sections.

4.6.2 Model Verification

To examine the accuracy of the RSR model, a verification based on external validation is presented in this section [110].

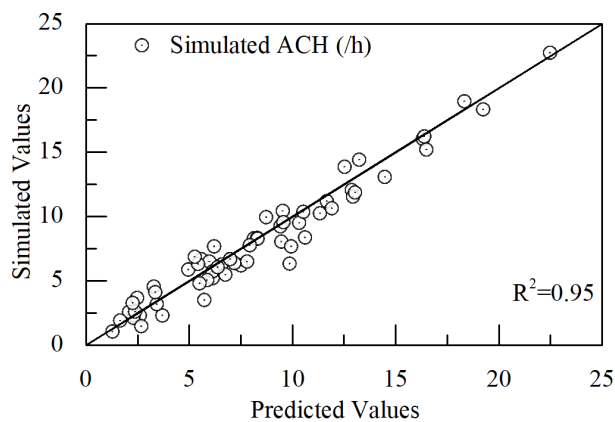


Figure 4.9 Comparison of simulated and predicted ACHs

External validation was performed using 64 testing data sets which are additional cases generated from the range of data from which the model was derived. Use of these 64 additional cases is to fulfil the 30% rule [111] (i.e. the use of 30% of the studied cases ($216 \times 0.3 = 64$ cases) as testing data sets).

ACH of the 64 cases was predicted by simulation and the RSR model (Equation 4.8). Results are compared in Figure 4.9, showing that the R^2 is 0.95 and confirms that the RSR model can be used for further analyses.

4.6.3 Influence of independent variables

4.6.3.1 Wind conditions

It is no surprise (Table 4-4) that ACH is most sensitive to change of SPD ($B = 8.32$) because ACH is mainly wind-driven [112]. However, it is noted that DIR has been removed from Equation (4.8) and it shows the smallest influence ($B = 0.05$) on ACH.

The removal and the small influence of DIR can be explained by the variance inflation factor (VIF). VIF for variable m (VIF_m) is given below:

$$VIF_m = \frac{1}{1 - R_m^2} \quad (4.9)$$

Where R_m^2 is the R^2 of the RSR model on the exclusion of m , which is 0.96 for the exclusion of *DIR*.

Based on Equation (4.9), VIF_{DIR} is calculated as 15.8 which is much greater than the generally acceptable value of 10 and this confirms a serious multi-collinearity with other variables [113], [114]. The serious multi-collinearity can be explained by the angular-linear relationship between SPD and DIR [115], [116]. This angular-linear relationship happens because DIR is periodic (0° to 360°) while that SPD is random and highly variable (0 to $+\infty$). The joint probabilities of distribution [19], which is a normal distribution [117], is often used for describing their relationship.

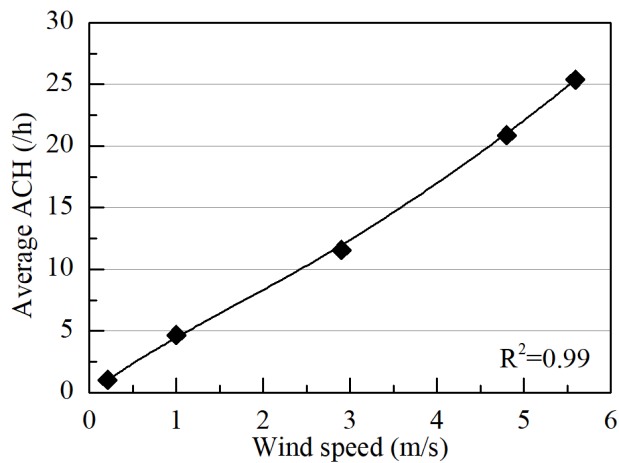


Figure 4.10 Average ACH with wind speed

Figure 4.10 shows the relationship between ACH and SPD, illustrating that ACH increases with SPD and the two exhibit a nearly linear relationship. The linear relationship can be explained by the two analytical models presented earlier (Equation (4.3) and (4.5)).

4.6.3.2 Ventilation modes

Changing the ventilation mode from SV to CV is the second most influential variable on ACH ($B=4.96$).

To explain, Figure 4.11 shows the ventilation performance of CV and SV modes, represented by two parameters, x/D and U/U_{ref} . Where x is the horizontal distance from the centre of the window (m); D is the horizontal distance between the centre of the window and the opposite wall (m); U is the average wind speed at distance x (m/s); and U_{ref} is the external wind speed at reference height (m/s).

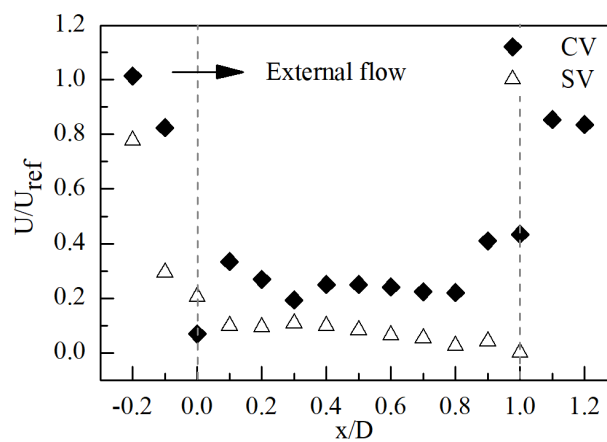


Figure 4.11 Ventilation performance of CV and SV

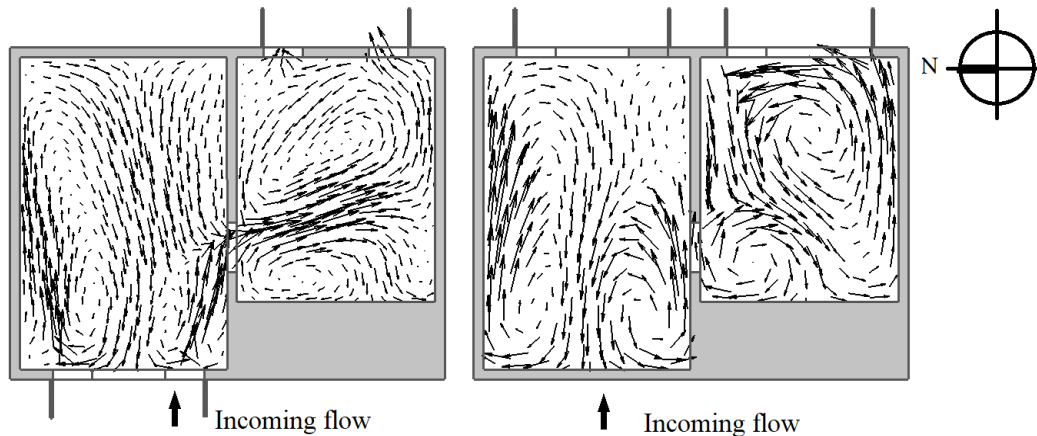


Figure 4.12 Indoor airflow distribution of west facing SH window

It can be seen that U/U_{ref} for CV at all x/D values are consistently higher than that of SV. Furthermore, U/U_{ref} of CV exhibits a U-shape while SV has a decaying trend. Figure 4.12 depicts a more intensive and well mixed airflow distribution of the CV than SV modes for a west facing

SH window. These can be explained by the fact that window sets of CV serve separately as air inlets and outlets while those of SV serve simultaneously as air inlets and outlets.

4.6.3.3 Window types

Changing window types from SLD to SH and TH is the third most influential variable on ACH (B=2.75). To explain, the effectiveness of window openings in admitting incoming air into internal space (Q^*) can be calculated by Equation (4.10) [118], [119]. Results are summarised in Table 4-5.

$$Q^* = \frac{Q}{U_H \cdot A} \quad (4.10)$$

Where $U_H \cdot A$ is the ideal air flow rate through a window opening (m^3/s); Q is the air flow rate through a window opening calculated by Equation (4.5), taking both friction and contraction losses into account (m^3/s); A is the window opening area (m^2).

Table 4-5 Q^* and ΔP of three window types

Window type	Dimensionless flow rate	Pressure differential ΔP
	Q^*	(pa)
SH	0.26	3.80
TH	0.23	3.54
SLD	0.11	2.33

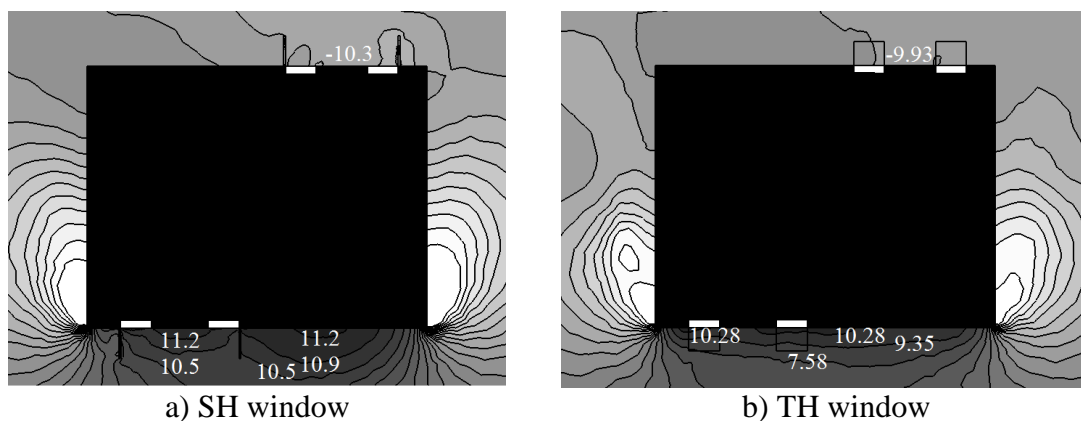
It can be seen in Table 4-5 that SH window has the highest Q^* (=0.26), followed by TH (=0.23) and SLD (=0.11). Given U_H is the same for all window types, the higher Q^* for SH and TH windows can be explained by Equation (4.11) [31].

$$Q = C_d A \sqrt{\frac{2\Delta P}{\rho}} \quad (4.11)$$

Where C_d is the discharge coefficient; ΔP is the pressure differential across the air inlets and outlets (Pa), and ρ is the air density (kg/m^3).

It can be seen in Equation (4.11) that Q is determined by C_d and ΔP . However, previous studies have already concluded that C_d does not vary much by window types [25], [120]. Thus, the better performance of SH and TH windows can be explained by the difference in ΔP , summarised also in Table 4-5.

The higher ΔP for SH and TH windows is attributed to the effect of window sash on airflow through a window opening. Figure 4.13 depicts cross-sections showing the increase in ΔP between incoming and outgoing air entrained by window sashes for a west facing window. It can be seen that SH window returns the highest ΔP ($=11.2 - (-10.3)$ pa), followed by TH ($=10.28 - (-9.93)$ pa), and the lowest is SLD. ΔP ($=10.02 - (-5.48)$ pa) because there is no window sash for SLD window.



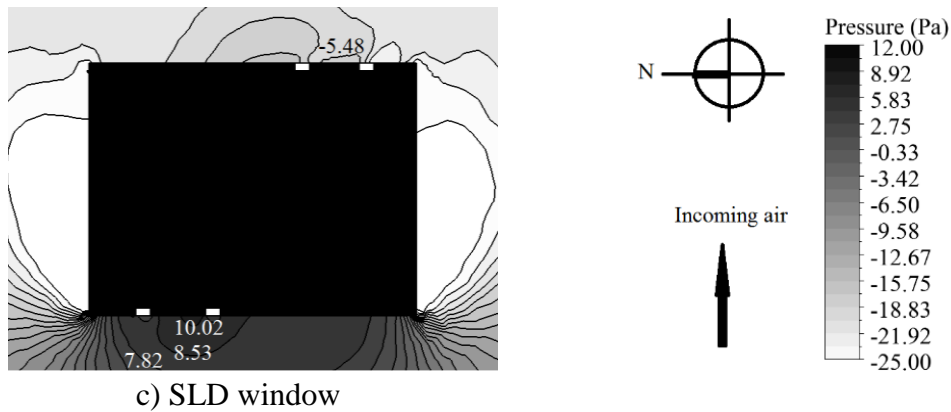


Figure 4.13 Pressure distribution of west facing SH, TH and SLD windows

4.6.3.4 Window orientations

The influence of window orientation is smaller than that of other variables ($B= 0.41$). This again can be explained by the VIF.

VIF of the independent variables were calculated by Equation (4.9) and are summarized in Table 4-6. It can be seen that VIF_{ORN} is the highest ($= 3.45$). The relatively high VIF points to collinearity with other variables. To investigate, additional RSR models were generated by removal of one of the studied variables each time to see the influence on VIF_{ORN} . It was found that by the removal of SPD, VIF_{ORN} dropped to 1.35 to confirm that ORN had high collinearity with the most influencing variable, SPD. The results explain the small influence of ORN on ACH.

Table 4-6 Summary of VIF

Variable	R^2	VIF
SPD	0.26	1.35
CON	0.55	2.22
TYP	0.60	2.50
ORN	0.71	3.45

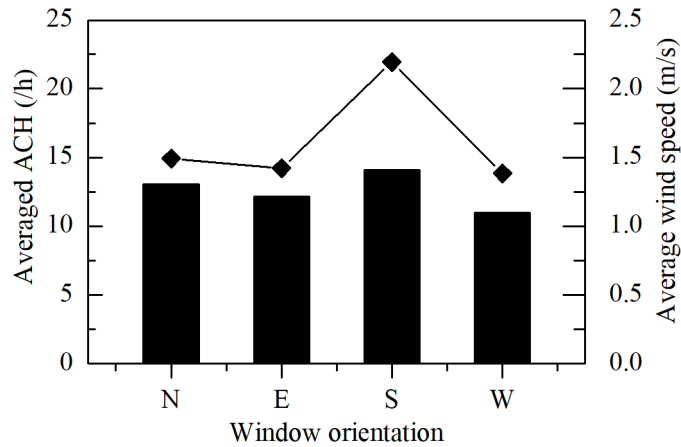


Figure 4.14 ACH by window orientation

Figure 4.14 shows the change of ACH by ORN. It can be seen that south facing window is most preferred, followed in descending order by north, east and west facing windows. To explain, the hourly meteorological data of Hong Kong for the last ten years were used to compute the average wind speed for the four orientations. Results are also compared in the figure, showing that they share the same pattern of variation and confirm the collinearity between ORN and SPD.

4.6.4 Influence of interactive variables

It can be seen that there are product terms in the RSR model (Equation (4.8)), implying that there are interactive effects on ACH by TYP, SPD, VNT and ORN. Given the focus of this study is to evaluate the influence of TYP on ACH, its interactive influences with other variables are discussed.

From the signs of coefficients in Equation (4.8) and the B values in Table 4-4, it is noted that improvement in ACH can be obtained when TYP is varied together with SPD or/and VNT, or with ORN.

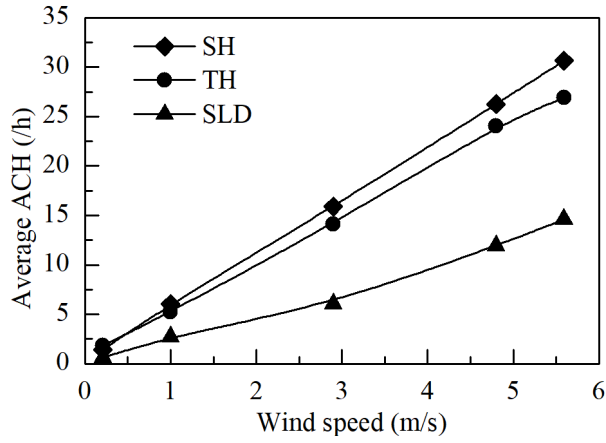


Figure 4.15 Influence of wind speed by window types

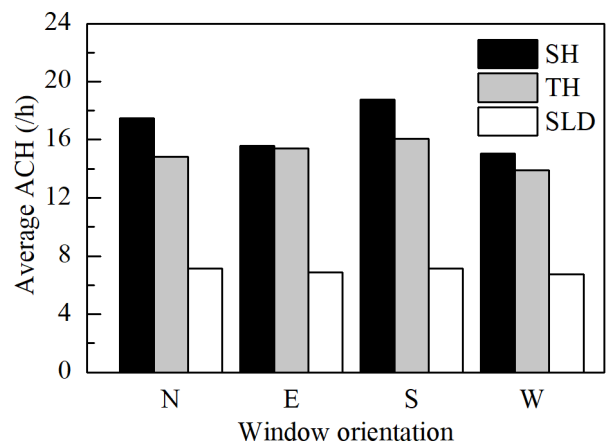


Figure 4.16 Influence of ORN by window types

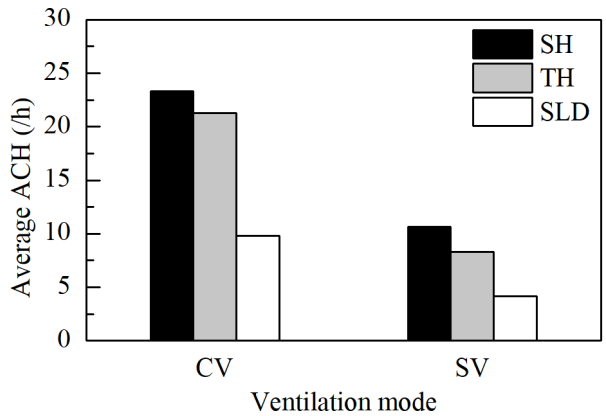


Figure 4.17 Influence of VNT by window types

To better explain the above, the influence of SPD, ORN and VNT on ACH by TYP (SH, TH and SLD) are shown in Figures 4.15, 4.16 and 4.17 respectively. It can be seen in the figures that

amongst the three window types, SH window always performs the best, followed in descending order by TH window and SLD window.

Given the interactive effect of TYP with SPD, VNT and ORN on ACH, to enable the selection of a suitable window type for the maximum ACH to save cooling energy, the desirability function method [121] was employed for a multi-criteria optimisation.

A multi-criteria optimisation using the desirability function method can be mathematically defined by Equation (4.12) [122].

$$\left. \begin{aligned}
 &ACH_{ACHVD} < ACH_L, & d = 0 \\
 &ACH_L \leq ACH_{ACHVD} \leq ACH_T, & d = \left(\frac{ACH_{ACHVD} - ACH_L}{ACH_T - ACH_L} \right)^s \\
 &ACH_T \leq ACH_{ACHVD} \leq ACH_U, & d = \left(\frac{ACH_{ACHVD} - ACH_U}{ACH_T - ACH_U} \right)^t \\
 &ACH_{ACHVD} > ACH_U, & d = 0
 \end{aligned} \right\} \quad (4.12)$$

Where ACH_{ACHVD} is the achieved ACH; d is the desirable range from 0 to 1, indicating the level of achievement of the desired design; subscripts L , T and U are the lower, target and upper limit of the achieved ACH; and s and t are the weight index to emphasize or de-emphasize the importance of a desirability level (they are both given value of 1 for having the same importance).

Based on the 216 CFD simulation results and Equation (4.12), Design-Expert was again employed for the optimisation process. The optimisation was done based on the average wind speed of Hong Kong by orientations in cooling seasons (where air-conditioners are usually

needed) from April to October [51] of the last ten years. The maximum achievable ACH (ACH_{max}) for different apertures designs are summarised in Table 4-7.

It can be seen in Table 4-7 that SH window returns the highest ACH_{max} for all aperture designs, followed in descending order are TH and SLD windows. The ACH_{max} for SH and TH windows are 124% and 97% higher than the SLD window. By taking the median, being the typical value of a data set, as an acceptable ACH_{max} , it is noted that SLD window cannot fulfil the requirements for all apertures designs. If the use of single-sided ventilation mode cannot be avoided (this is typical for Hong Kong residential units design [123], [124]), the use of SH windows (excluding west facing windows) and south facing TH windows is acceptable. The use of west facing windows should always be avoided.

Table 4-7 ACH_{max} for different apertures design

VNT	ORN	SPD	ACH_{max} (/h)		
		(m/s)	SH	TH	SLD
CV	N	1.9	16.32	13.88	7.52
	E	2.11	17.37	15.34	7.49
	S	1.97	17.23	15.52	7.21
	W	1.49	9.43	8.98	5.03
SV	N	1.9	8.42	6.62	3.80
	E	2.11	8.52	7.16	3.32
	S	1.97	8.98	7.95	3.48
	W	1.49	3.28	3.50	2.21
Mean	All	1.87	11.19 (+124%)	9.87 (+97%)	5.01
Median			7.74		

Given simulation inputs were validated, the resultant model was verified, and the influence of the independent and interactive variables were well-explained, it can be concluded that SH window is always preferred for achieving better ventilation performance in Hong Kong environment, followed (in descending order) by TH and SLD window.

4.7 Summary

The influence of window types on natural ventilation performance of residential units in Hong Kong, taking into account the interactive effects of the ventilation modes, window orientations, and coincident wind conditions, was investigated. The investigation was based on site measurements, market surveys, computational fluid dynamics (CFD) simulations and statistical analyses. In the walk-through surveys, it was identified that side hung, top hung and sliding windows were three most used window types in Hong Kong. A mathematical model for quantifying the interactive influences of different window designs on ventilation performance was developed by the response surface regression analysis. Based on the mathematical model, it was found that ventilation performance (quantified by air change per hour (ACH)) was most sensitive to change of wind conditions, followed in descending order, by ventilation mode, window type and window orientation. Regarding interactive effects, it was found that there is a positive effect on ACH when window type is changed together with wind speed and or ventilation mode, or only the window orientation is changed. On selection of window type to reduce consumption of energy for cooling, the multi-criteria optimisation results indicated that side hung (SH) window is most preferred, followed in descending order by top hung (TH) and sliding (SLD) windows. The maximum achievable ACH by SH and TH windows is 124% and 97% higher than the SLD window.

CHAPTER 5 INFLUENCE OF WINDOW OPENING DEGREE

The walk-through surveys introduced in Chapter 4 indicate that Hong Kong households have very limited and inefficient use of natural ventilation. To encourage wider and more efficient use of natural ventilation, it is necessary to identify the optimum window opening degree (DEG) for the reference of users and building designers. For this purpose, this Chapter presents the evaluations and results. The evaluations involved walk-through surveys, site measurements, CFD simulations and statistical analyses. Regression analysis was employed to generate the results including a model to enable quick estimation of ventilation performance and extrapolation of the optimum window opening degree for different design variables under seasonal wind conditions.

5.1 Walk-through surveys

Based on the façade images of the 9965 windows collected in the walk-through surveys, window opening ranges were calculated. Inverse perspective transform and bilinear interpolation method [125], [126] were employed to retouch the warp façade images [127], [128]. The pin-hole relationship was then used to determine the pixel coordinates of the windows [129]. The pixel-based images were further scaled up to their actual dimensions. Based on the scaled-up images, the least-squares method [130] and the trigonometric relationship [131] were used to compute the opening range for the windows and thus the DEGs.

Figure 5.1 summarizes the results. Amongst the 9965 windows, only 38.9% of the windows were opened and against which, 60% were with an opening degree less than 0.3 (Figure 5.1). The results show the limited and inefficient use of natural ventilation in residential buildings in Hong

Kong and point to the need to identify the optimum DEG for the reference of users and building designers.

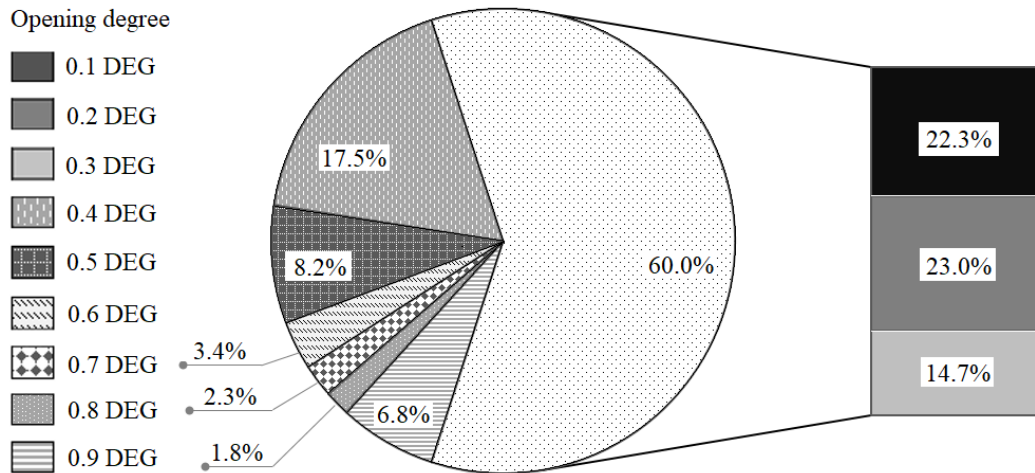


Figure 5.1 Window opening habit

5.2 Site measurements

Site measurements described in Chapter 4 were again employed for evaluations of ventilation performance under different DEGs and for simulation validations.

Before the actual site measurements, trial measurements on fully opened windows (DEG =1) were conducted. The measured ACH values, at the same outdoor meteorological conditions, were found comparable with that of the study outlined in Chapter 4 [132] to confirm the reliability and repeatability of the site measurements. The windows were then closed and a proper amount of SF₆ was injected into the space to reach a concentration level of around 100ppm. Upon SF₆ concentration of the entire studied area was in equilibrium, the studied SH and TH windows were adjusted simultaneously to the same pre-determined DEGs (0.3 to 0.6) using a 60 cm diameter full-scale protractor.

Figure 5.2 compares the decay in SF₆ concentration for different window opening degrees. It can be seen from the decay slopes that, regardless of the window type, ventilation performance improves with DEG for the site measurement conditions.

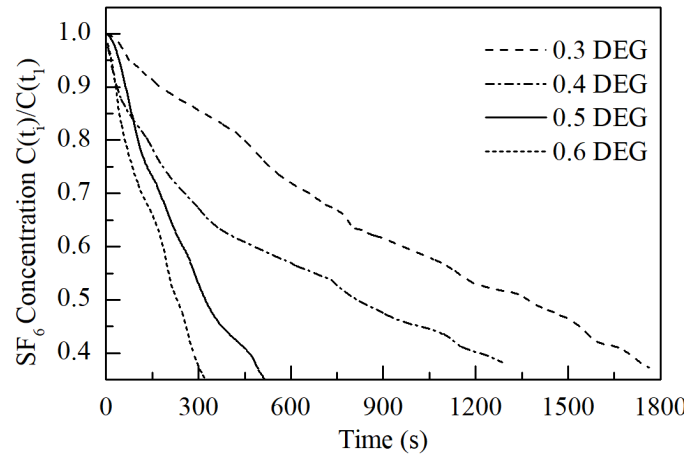


Figure 5.2 Decay curves for different window opening degrees

The measured ACH of the two window types for different DEGs, determined based on the mass balance of SF₆ in Equations (4.3) and (4.5), were used for simulation validations and for parameters settings for further CFD simulations.

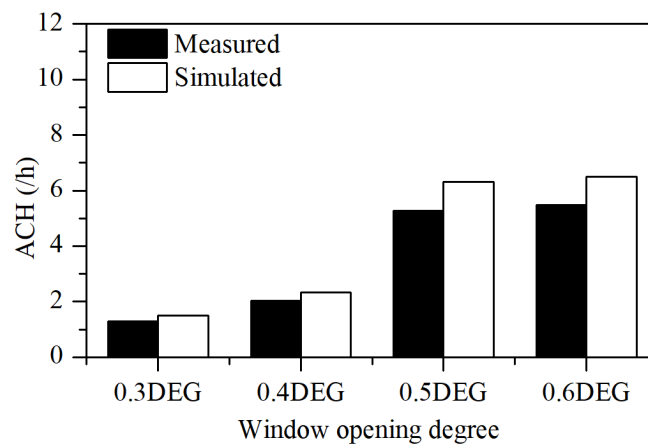


Figure 5.3 Comparison of simulated and measured results

The standard k-epsilon ($k-\epsilon$) turbulent model was used to simulate the steady state natural ventilation. The SIMPLE (Semi-Implicit Method for Pressure-Linked Equations) was used to couple pressure and velocity. Momentum equation was discretized by the second-order upwind scheme while turbulent equations were by the first-order upwind scheme. The convergence criteria were set as 10^{-3} for all variables and a mass balance difference less than 0.002kg at openings [98].

The measured and simulated results were compared as given in Figure 5.3 and their difference was within 20%, which is within the generally acceptable range[5] to confirm successful validation.

5.3 CFD simulations

Nine representative wind data sets, derived from the hourly meteorological data of Hong Kong in the last ten years (2004-2013) (Table 3-1 in Chapter 3) were again used for CFD simulations.

Further CFD simulations were conducted to investigate the interactive influences of DEG with full considerations of the window design options, wind conditions and users' habits. Three most used window types (SH, TH, and SLD), and the DEGs from 0.1 to 0.9 were considered. The studied hypothetical residential unit, the window dimensions of 780mm×600mm (WD×HT) and the validated input settings, as outlined in Chapter 4, were again adopted.

Single-sided and cross ventilations were assumed for the hypothetical residential unit because they correspondingly represent the least and the most preferred ventilation modes. Thus for each

layout, there were two ventilation modes, four possible orientations, three window types, nine representative wind conditions, and nine DEGs to become 1944 cases (= 2×4×3×9×9).

5.4 Identification of the optimum DEG

To identify the relative influence of the studied variables, regression analyses were employed to develop mathematical models to relate them with ACH, as shown in Equation (5.1).

$$ACH = b_0 + \sum_{j=1}^5 b_{1j} x_j + \sum_{j=1}^5 b_{jj} x_j^2 + \sum_j \sum_{k>j} b_{jk} x_j x_k + \sum_j \sum_{k>j} \sum_{l>k} b_{jkl} x_j x_k x_l \quad (5.1)$$

Where *ACH* is the dependent variable; x_j, x_k, x_l, x_m, x_n are the studied variables; b_j represents the i^{th} coefficient ($i = 0$ to 1 for linear; $i = jj$ to jkl for interactive).

A family of regression models were generated by SPSS [133]. Amongst them, an acceptable model was selected based on the sequential model sum of square (SMSS) test [134]. They include checking the degree of order; the variance inflation factor (VIF), the coefficient of determination (R^2), the adjusted R^2 , the predicted R^2 , and the p-value. The signs of the coefficients were also checked.

The verification of the resultant model was done based on testing data sets.

Based on the resultant model, the standardized coefficient (B) values were used to confirm the significant influence of DEG on ACH.

The resultant model was also used to identify optimum DEG (DEG_{OPT}). This is done by partial derivatives of the resultant model with respect to DEG as shown in Equation (5.2).

$$\left. \frac{\partial g(ACH)}{\partial DEG} \right|_{g(ACH)=DEG_{OPT}} = 0 \quad (5.2)$$

Where $g(ACH)$ is the resultant mathematical model (Equation (5.1)); DEG_{OPT} is the optimum DEG for all design options; and DEG is ranging from 0.1 to 0.9 with 0.1 increment.

5.5 Results and Analysis

5.5.1 The resultant model

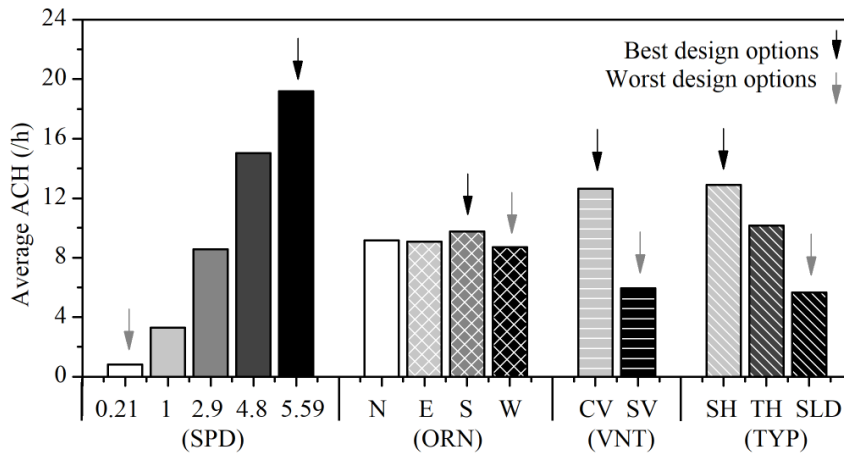


Figure 5.4 Influence of individual variables (excluding DEG) on ACH

In the model, qualitative variables including window types (TYP), ventilation mode (VNT), orientation (ORN), and wind direction (DIR) were again coded by the dummy variable method. To enable the determination of the base group, the average ACH obtained from 1944 simulation cases were compared in Figure 5.4. It is noted that for each group of studied variables, there are the best and the worst design options, as highlighted in Figure 5.4. The worst design options were

chosen as the base group (i.e. ORN_W , VNT_{SV} , TYP_{SLD}). They were therefore excluded in the model.

Based on the acceptable values for SMSS test [135], the resultant model, with p-value of all the included variables greater than 0.01 and the coefficient of determination (R^2), adjusted R^2 and predicted R^2 close to 1 (0.72, 0.70 and 0.66) to confirm passing the test, is shown in Equation (5.3).

$$\begin{aligned}
 ACH = & -11.27 + 3.28 \times SPD + 0.001 \times DIR \\
 & + 3.21 \times VNT_{CV} + 2.70 \times DEG \\
 & + \begin{cases} 0.61 \times ORN_N \\ 1.15 \times ORN_S \\ 0.45 \times ORN_E \end{cases} + \begin{cases} 6.84 \times TYP_{SH} \\ 4.75 \times TYP_{TH} \end{cases} \\
 & + \begin{cases} 5.16 \times DEG \cdot TYP_{SH} \\ 4.69 \times DEG \cdot TYP_{TH} \end{cases} + 7.61 \times VNT_{CV} \cdot DEG
 \end{aligned} \tag{5.3}$$

The abbreviation for the quantitative and qualitative variables are summarized in Table 5-1.

It can be seen that positive coefficients have been generated for all the variables (independent and product terms). This is judged to be reasonable because the worst design options were set as the base group. The standardized regression coefficient B was used to quantify the influence of the studied variables on ACH. They are summarized in Table 5-2.

Table 5-1 Independent variables and coded value in the resultant model

Abbreviation		Description	Unit / Code
SPD		Wind speed	m/s
DIR		Wind direction	Degree
DEG		Window opening degree	0 to 1
VNT	CV	Ventilation mode - Cross ventilation	No = 0 / Yes = 1
	SV	Ventilation mode - Single-sided ventilation	Base

ORN	N	Orientation - North	No = 0 / Yes = 1
	E	Orientation - East	No = 0 / Yes = 1
	S	Orientation - South	No = 0 / Yes = 1
	W	Orientation - West	Base
TYP	SH	Window type - Side hung	No = 0 / Yes = 1
	TH	Window type - Top hung	No = 0 / Yes = 1
	SLD	Window type - Sliding	Base

Table 5-2 Standardized coefficients

Variable	Standardized coefficient		Sig. Rank
	B	Average	
SPD	0.57	—	1
DIR	0.02	—	6
VNT _{CV}	0.16	0.08	3
VNT _{SV} (Baseline)	—		
ORN _N	0.03	0.03	5
ORN _E	0.02		
ORN _S	0.05		
ORN _W (Baseline)	—		
TYP _{SH}	0.31	0.18	2
TYP _{TH}	0.22		
TYP _{SLD} (Baseline)	—		
DEG	0.07	—	4
VNT×DEG	0.23	—	1
TYP _{SH} ×DEG	0.14	0.13	2
TYP _{TH} ×DEG	0.13		

Amongst the independent variables, SPD (B=0.58) introduced the highest influence on ACH, followed in descending order are TYP (B=0.18), VNT (B=0.08), DEG (B=0.07), and DIR (B=0.02). For interactive effect, it is noted that DEG contributes to the only two product terms, VNT×DEG and TYP×DEG, to confirm the significant influence of DEG on ACH.

5.5.2 Model Verification

To verify the accuracy of the resultant model, external validation was performed [136].

To perform the external validation, 583 additional cases were generated from the range of data from which the model was derived as testing cases. The number of testing cases was again determined based on the 30% rule as described in Section 4.6.2, with a total number of 583 cases ($30\% \times 1944$ studied cases) which are completely different from the studied cases as testing data sets.

ACH of the 583 cases was simulated by CFD simulations and compared with the results predicted by the resultant model (Equation (5.4)). Results are presented in Figure 5.5 and the R^2 is 0.60. Considering there are over 500 cases, the resultant R^2 confirms that the resultant model can be used for further analysis [137].

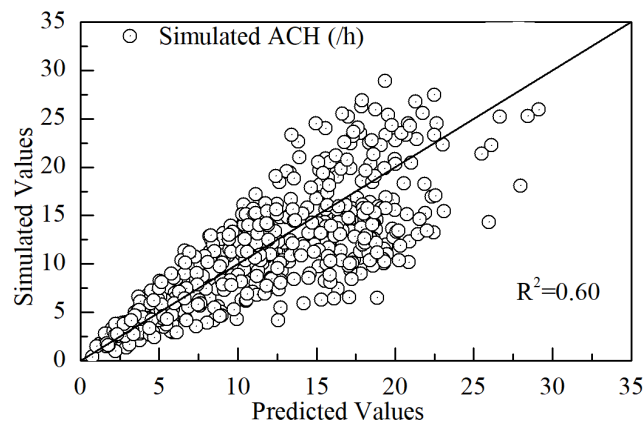


Figure 5.5 Comparison of simulated and predicted ACHs

5.5.3 Influence of DEG

Figure 5.6 relates the average ACHs and DEGs for all design options (1944 simulation cases). It can be seen that they exhibit a polynomial relationship ($R^2 = 0.994$) to show ACH increases with

DEG. To explain, it is noted that from Equation (4.11) that Q, represented by ACH, is mainly affected by Cd.

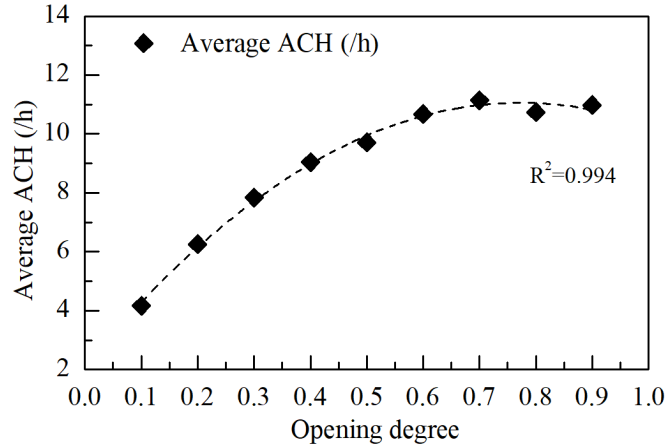


Figure 5.6 ACH for different DEGs

But as C_d is affected by combinations of different factors [138]–[140], it is almost impossible to quantify the influence of C_d by DEG for all design options. Reference was therefore made to previous studies to focus only on cases with east-facing windows whereby the incoming air is perpendicular to the window opening. C_d for single-sided and cross ventilation mode can be calculated by Equation (5.4) [141], [142].

$$C_d = \begin{cases} C_{d1}A + C_{d2}A & ; \text{ for SV Mode} \\ \frac{1}{\sqrt{\left(\frac{1}{C_{d1}A}\right)^2 + \left(\frac{1}{C_{d2}A}\right)^2}} & ; \text{ for CV Mode} \end{cases} \quad (5.4)$$

Based on the calculated C_d values, the average discharge coefficients (C_d) for the selected cases were computed and related to DEGs as shown in Figure 5.7. It can be seen that they exhibit also a polynomial relationship.

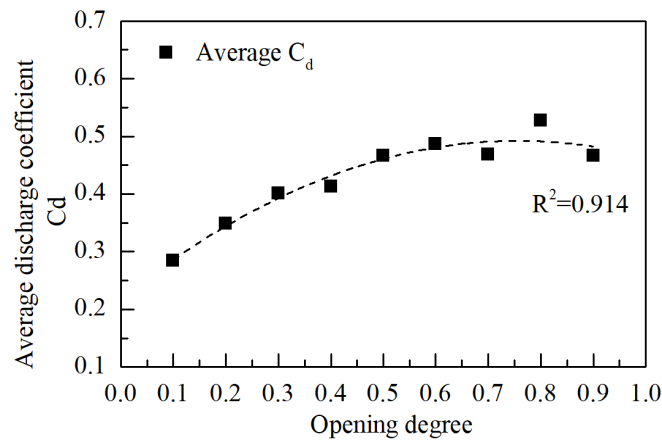


Figure 5.7 Discharge coefficient for different DEGs

Combining Figure (5.6) and (5.7) implies that Q and C_d exhibit a linear relationship which is in agreement with Equation (4.11) [143] to explain the polynomial relationship between ACH and DEG.

5.5.4 The optimum DEG

Given ACH increases with DEG, the optimum DEG (DEG_{OPT}) for all design options can be quantified by partial derivatives of the resultant model (Equation (5.3)) with respect to DEG as shown in Equation (5.2).

It was found that for all design options, DEG_{OPT} occurs at 0.7 and a maximum ACH (ACH_{max}) of 11.1 can be obtained.

To determine the DEG_{OPT} for the worst and the best design option groups, the corresponding simulated results were extracted for regression analysis. Regression models with polynomial relationships were again obtained for the two groups of design options ($R^2_{Worst} = 0.947$; R^2_{Best}

=0.963). Partial derivatives of the regressed models with respect to DEG were again conducted. The DEG_{OPT}, together with the corresponding design variables, are summarized in Table 5-3. It can be seen that to achieve ACH_{max}, the DEG_{OPT} are 0.9 and 0.7 respectively.

Table 5-3 DEG for all scenarios

	TYP	VNT	ORN	SPD (m/s)	DEG_{OPT}	ACH_{max}(/h)	
Worst design options	SLD	SV	W	0.21	0.9	0.2	
Best design options	SH	CV	S	5.59	0.7	36.8	
Season	Spring	--	--	--	2.59	0.8	13.1
	Summer	--	--	--	1.43	0.9	8.0
	Fall	--	--	--	2.04	0.8	5.7
	Winter	--	--	--	1.85	0.6	10.1
All design options	--	--	--	--	0.7	11.1	

Besides the design options, the seasonal condition also affect DEG_{OPT}. Seasonal condition is represented by the relative frequency of occurrence (*f*) of a particular wind condition by seasons, where spring starts from March for three months, and thereafter for summer, fall and winter, each lasts for a three-month period. *f* is determined by Equation (5.5). The results are summarized in Table 5-3.

$$f = \frac{O_c}{\sum_{i=1}^q O_c} \quad (5.5)$$

Where *f* is the relative frequency of occurrence of a particular wind condition by season; *O_c* is the frequency of occurrence of a particular wind condition *c* (from the representative wind data sets); and *q* is the number of representative wind conditions (=9).

Based on the seasonal f , an analysis of ACH and DEG was conducted. The average ACH (\overline{ACH}) for different DEGs were determined based on Equation (5.6).

$$\overline{ACH}_{(j,k,l,c),r} = \frac{\sum f(\overline{ACH})_{(j,k,l,c),r}}{\sum f} \quad (5.6)$$

Where $\overline{ACH}_{(j,k,l,c),r}$ is the average ACH for a particular DEG ($r = 0.1$ to 0.9) operating under combination of 4 independent variables (j, k, l, c).

Regression analysis on the relationship between ACH and DEG by seasons was again conducted. Partial derivatives were again employed to determine DEG_{OPT} ($R^2_{Spring} = 0.937$; $R^2_{Summer} = 0.908$; $R^2_{Fall} = 0.909$; $R^2_{Winter} = 0.947$) for ACH_{max} . The results, together with the case for all design options, best design options, and worst design options, are summarized in Table 5-3.

Given simulation inputs were validated, the resultant model was verified, and the influence of the DEG on ACH was well-explained, it can be concluded that based on Table 5-3 that for achieving better ventilation performance in Hong Kong environment, the window opening degree should be in the range of 0.6 to 0.9.

5.6 Summary

The optimum window opening degree for residential buildings in Hong Kong was investigated by walk-through surveys, site measurements, CFD simulations and statistical analyses. The walk-through surveys on window opening conditions of 9965 windows in Hong Kong indicated

that Hong Kong households had very limited and inefficient use of natural ventilation. Site measurements were conducted at a carefully selected unit for simulation validations. CFD simulations were done based on the hypothetical residential unit designed with 3 most used window types, 9 window opening degrees, 9 representative wind data sets, 2 ventilation modes and 4 orientations to become 1944 studied cases. A mathematical model to enable quick estimation of ACH for different design variables was developed by regression analysis. The model's adequacy and prediction accuracy were verified. Based on the mathematical model, it was found that ACH was very much influenced by the window opening degree. To identify the optimum window opening degree, the simulated ACH by window opening degree for all design options, the worst design options, the best design options, and by seasons were evaluated. It was found that the optimum window opening degree should be in the range of 0.6 to 0.9 to maximize the use of natural ventilation in residential buildings in Hong Kong. The results, together with the mathematical model relating annual ACH with different design variables, provide very useful information for building users as well as researchers for better use of natural ventilation to cut cooling energy use. It is also useful for building designers in designing windows with opening restrictors.

CHAPTER 6 INFLUENCE OF TRANSOM WINDOW DESIGN

Previous studies have already confirmed that transom window (TW) is useful for ensuring adequate ventilation in residential units. However, the impact of different physical characteristics of TW on ventilation, particularly in the context of characteristics of high-rise residential buildings have never been investigated in extant literature. To fill this gap, the effectiveness of TW of different designs in enhancing natural ventilation is evaluated on the basis of a high-rise residential development in Hong Kong. Site measurements were conducted at two carefully selected units to determine the influential design characteristics. Statistical analyses were employed to identify a representative residential unit and local wind environments. Further CFD validations and simulations were done to predict the ACH achievable by different TW designs. Based on the simulation results, a rigorous sensitivity analysis using artificial neural network was performed. Accordingly, the improvement in natural ventilation by the incorporation of TW of different designs was determined.

6.1 Site measurements

Site measurements were conducted to identify the influential physical characteristics of TW for further studies and for site verifications to be discussed in Chapter 7.

Table 6-1 shows the range of values for physical characteristics. As the site measurements adopt the controlled-experiment method, only one input of each design parameter is varied for each set of controlled experiment to determine the total number of experimental cases. There are also parameters that cannot be varied due to site constraints, which include the position of TW relative

to window and the TW orientation (shaded in Table 6-1). As such, their influence has not been investigated in the site measurements.

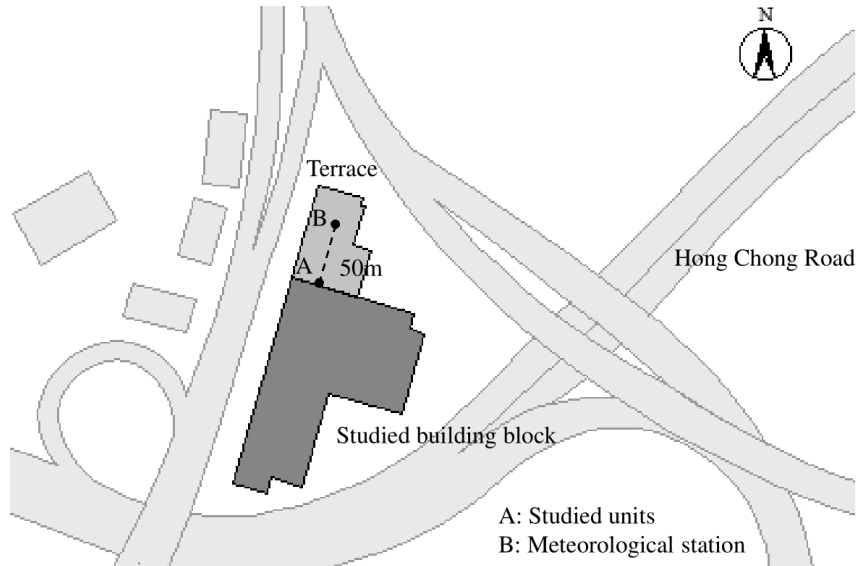


Figure 6.1 Site layout of the studied building block

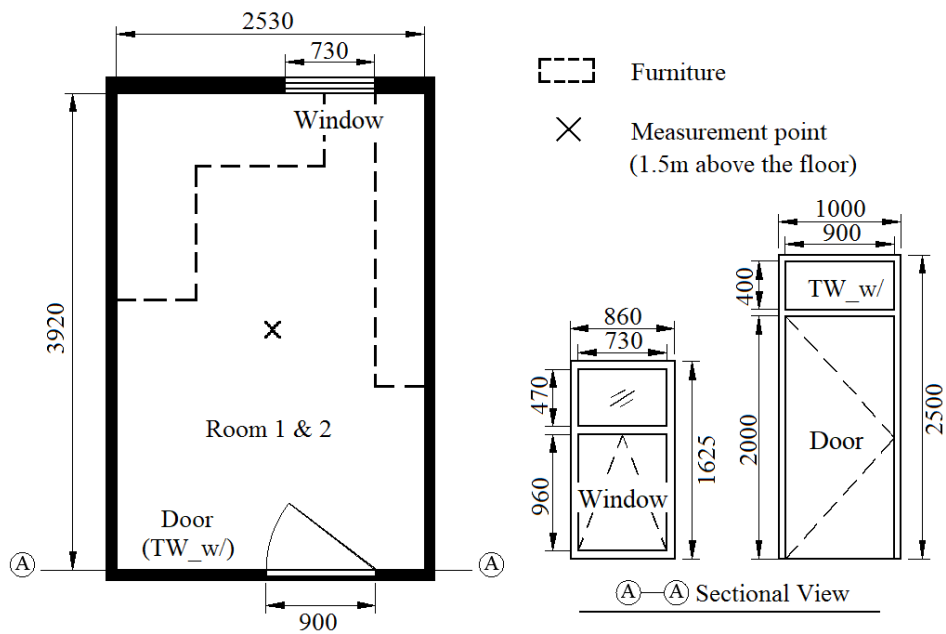


Figure 6.2 Layout of the two identical studied units

Table 6-1 Range of varied parameters of TW

Design parameter		Input variables		No. of experimental cases	No. of simulation cases	Dimensions WD×HT(m)	Remarks
Description	Abbreviation	Description	Abbreviation				
Presence of TW	TW	With and Without	TW_w and TW_w/o	1	2	0.9 ×0.4 and 0	
Position on the door	DR	Left, Centre and Right	DR_LFT, DR_CTR and DR_RGT	2	N/A	0.3 × 0.4 (all cases)	Same height; Same area
Aspect ratio (the ratio of WD and HT)	AR	4 (maximum) and 1 (minimum)	AR_4 and AR_1	1	N/A	0.8×0.2 and 0.4×0.4	Same area
Free opening area – no grille (m ²)	A	25%, 33%, 50%, 66%, 75% and 100%	A_0.25, A_0.33, A_0.5, A_0.66, A_0.75 and A_1	5	6	0.225×0.4, 0.3×0.4, 0.45×0.4, 0.6×0.4, 0.675×0.4 and 0.9×0.4	Same height
Position relative to window	WIN	Left and Right	WIN_LFT and WIN_RGT	N/A	2	0.9×0.4	Same area
Orientation	ORN	East, South, West and North	ORN_E, ORN_S, ORN_W and ORN_N	N/A	4	0.9×0.4	Same orientation as window; Same area

For determining dimensions of the TW, reference is made to building regulations of Hong Kong which require that the main entrance door to a residential unit should be of standard width of 900 mm and a minimum height of 2000 mm [144], [145]. Considering that the typical headroom of residential units in Hong Kong is 2500 mm [146], the maximum opening area of the TW ($A_{_1}$) is therefore 900 mm (WD) \times 400 mm (HT) (excluding TW and door frames). The possible opening area of the TW ($A_{_0.25}$ to $A_{_1}$) is determined based on a survey of different kinds of openings in TWs available in the market.

Site measurements were conducted at two carefully selected units located in Kowloon Hong Kong from 27 to 30 November 2018. The two units were selected because: 1) they are located in an isolated site which is barely obstructed; 2) the very few ambient obstructions are at a spherical distance greater than 50 meters from the studied units; 3) the two units are adjacent to each other; and 4) the two units are identical in dimensions, architectural layout and furniture layout. To facilitate the site measurements, entrance doors were replaced with tailor-made doors provided with TW. The opening area is adjustable from 900 mm (WD) \times 400 mm (HT) to fully closed position. The site layout and the layout of the studied units, together with their dimensions are given in Figure 6.1 and Figure 6.2 respectively. Top-hung windows are used in the two rooms.

Site measurement photos are shown in Figure 6.3. Figure 6.3 (a) shows the tailor-made plywood door with TW. Figure 6.3 (b) shows that the furniture in the two rooms is properly covered to avoid unintentional infiltration. Figure 6.3 (c) shows the portable meteorological station set up in the corridor for measuring indoor meteorological conditions. Figure 6.3 (d) shows the portable meteorological station for measuring outdoor meteorological conditions at similar level as the studied units.



(a) TW (WD×HT=0.8m×0.2m)



(b) Sealed furniture



(c) Corridor wind speed and temperature



(d) Outdoor meteorological station

Figure 6.3 Site measurement photos

Table 6-2 Major instruments and their accuracy

Measured parameter	Instrument	Accuracy	Measurement Intervals
Tracer gas concentration	Bruel& Kjær 1302	±2.5%	40 seconds
Outdoor wind speed and temperature	HOBO outdoor data logger	±4%	1 second
Corridor wind speed and temperature	HOBO indoor data logger	±0.25m/s and ±1%	1 second
Indoor temperature	Temperature logger	±0.35°C	1 second

Sulfur hexafluoride (SF_6) was used as the tracer gas to measure the ventilation rate in the room. Before the start of the experiment, all windows in the rooms were fully opened for nearly 10 minutes to remove interference of the buoyancy effect. With the window closed, an appropriate amount of SF_6 (around 130 ppm) was injected into the room until the concentration was at equilibrium. Mechanical devices were used in both units to ensure the heavy density SF_6 was spread evenly in the entire measuring area. Upon equilibrium, the experiments were started by

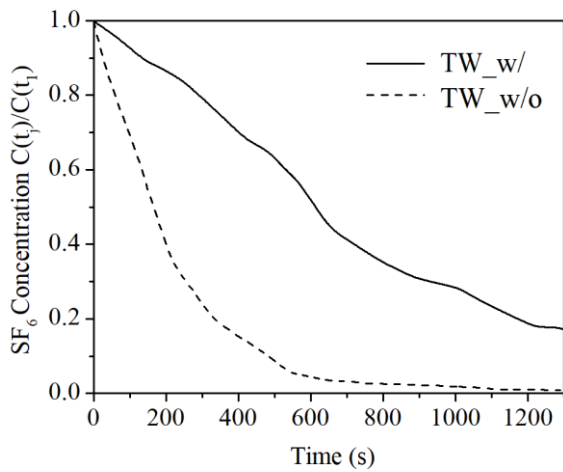
simultaneously opening the window and TW in the two rooms. Walkie-talkie devices were used to synchronise the experimental procedures. The windows were opened to an optimum opening angle of 60 degrees by a 60 cm diameter full-scale protractor [147]. The TWs were opened to different opening areas as summarised in Table 6-1.

During the experiments, SF₆ concentrations measured at the center of the studied rooms are shown in Figure 6.3; these were measured at 40-second intervals. The measurement position is based on previous studies on ventilation performance measurements [27], [91], [148]. Indoor and outdoor meteorological conditions were monitored during the measurements. The indoor meteorological station was set up at the corridor at 2m level to avoid interference. The outdoor meteorological station was set up at an unobstructed location 50m in front of the studied units as illustrated in Figure 6.1. All sensors were calibrated before site measurements. Accuracy of measuring instruments and the recording interval times are summarised in Table 6-2.

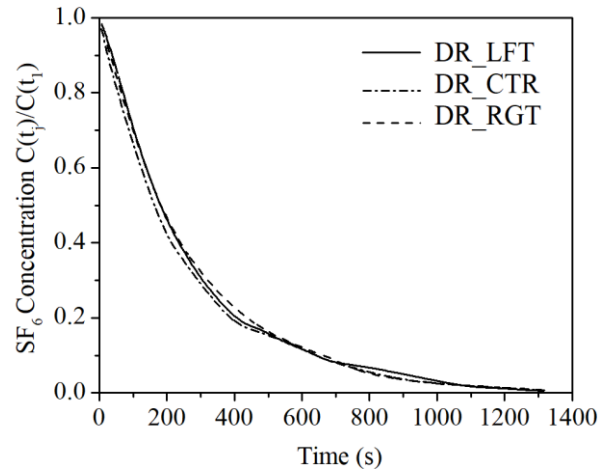
Figures 6.4 (a) to (d) present SF₆ concentration decay curves by design parameters for different experimental cases. To enable direct comparison of different input variables, the measured SF₆ concentration (C) values were normalised to range from 0 to 1, and log-transformed into the same decay slope by Equation (6.1) to determine K for calibrating the results of the corresponding experimental cases.

$$\ln(C(t_j)/C(t_1))_{e_1} \cdot K = \ln(C(t_j)/C(t_1))_{e_2} \quad (6.1)$$

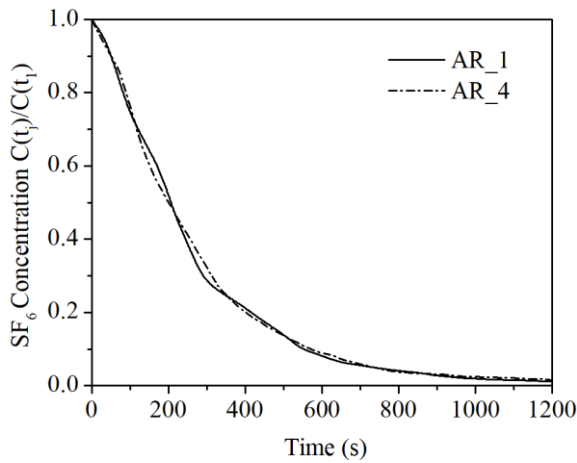
Where t_j is the time j ; t_1 is the initial time; e_1 is the controlled-experiment in set 1 experiments; e_2 is the controlled-experiment in set 2 experiments; K is the amplification factor.



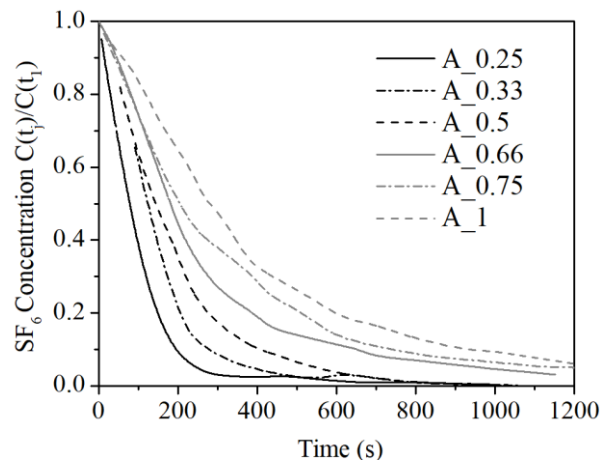
(a) Comparison between TW_w/ and TW_w/o on the door



(b) Comparison of different positions on the door



(c) Comparison of different aspect ratios



(d) Comparison of different opening areas

Figure 6.4 SF₆ concentration decay curves by design parameters

Under the same initial SF₆ concentration, for different experimental cases, i.e. $(C(t_j) / C(t_1)) = 1$, where t_j is the time j ; t_1 is the initial time), a steeper decay curve indicates a more significant influence on the natural ventilation performance. It can be seen that across different design parameters, the presence of TW and the opening area of TW (A) exhibit more significant influence on the natural ventilation, while different input variables such as the position of TW on the door (DR) and the aspect ratio (AR) exhibit very little influence. Thus the former two design parameters (TW; and A) should be included for further investigations while the latter

two design parameters (DR and AR) can be excluded in further investigations. The influence of DR is little because of the fixed position of the door in the studied unit which implies a very small change in TW position. While influence of AR is little because of the constant friction loss between AR_4 and AR_1[149].

6.2 Identifying a representative residential unit

A public housing estate in Tseung Kwan O (TKO) was chosen for the study. It was chosen because 44.6% of the population resides in public housing estates in Hong Kong [150]. Among different types of public housing estates, the harmony one type adopted in TKO is the most newly developed and widely used [151], [152]. Harmony one type usually comprises several high-rise blocks, with standard floor layout and units of different sizes [153]. Each housing block is of 40 storeys with 20 units on each floor, thus having up to 800 households.

TKO (Figure 6.5) consists of 16 blocks. Block X (highlighted in Figure 6.5) is significantly surrounded by other blocks and has the most unfavourable wind environment in terms of availability of natural ventilation. It was therefore selected for the study.

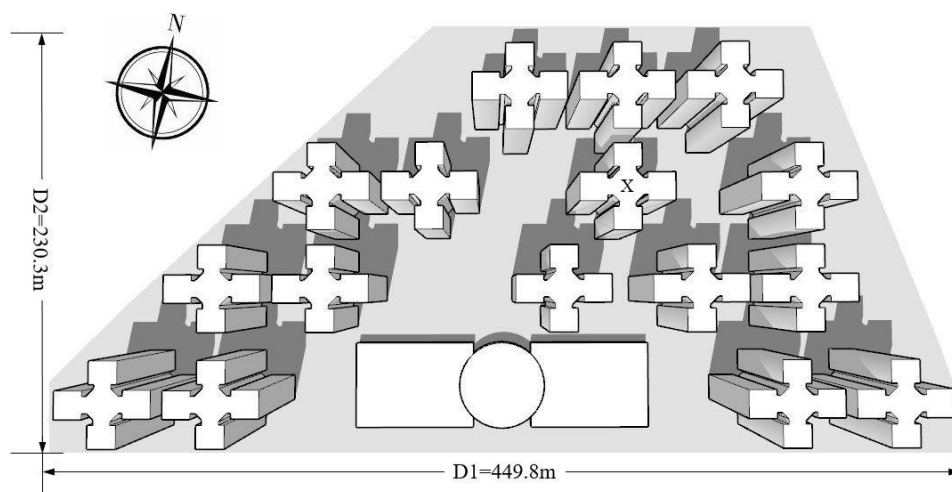


Figure 6.5 Site plan of Tseung Kwan O (TKO) and the studied building block X

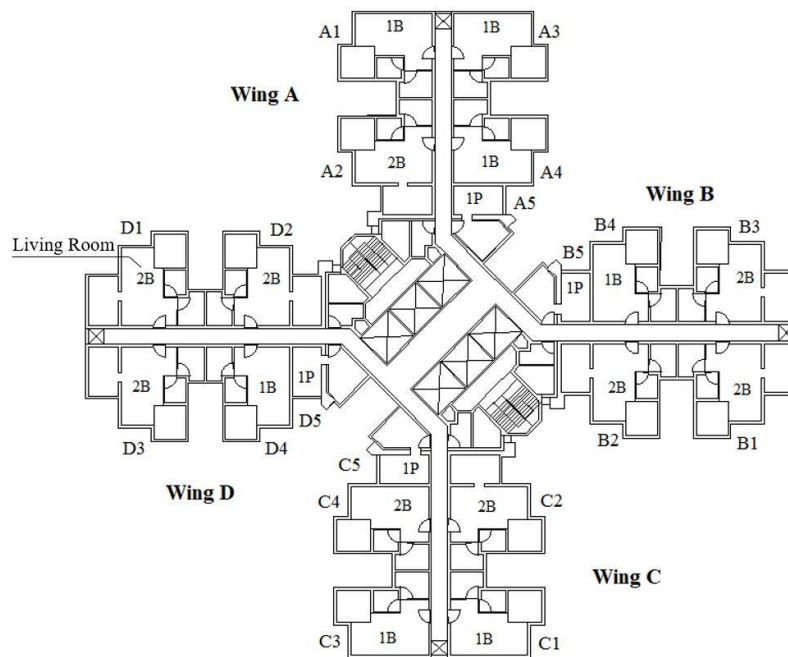


Figure 6.6 Floor layout of Harmony one type estate

The floor layout of harmony one type estate is shown in Figure 6.6. Each block consists of four wings (named as A–D) and each wing comprises five units on each floor. On each floor, there are three types of units. They are one-bedroom (1B), two-bedrooms (2B) and single studio (1P) units.

Among these three types of units, 2B units have the largest floor area, and in the studied building block, wing D is located at the most sheltered corner. Therefore, unit D1, a 2B unit, was selected for the study because it has the smallest window to floor area ratio and possesses the worst wind environment.

Considering that TW should be on the outer door to facilitate cross ventilation, the living room therefore becomes the only viable space for its incorporation. In the living room, the TW position is determined by the door position relative to the window (WIN), which can be on the

left or right (WIN_LFT and WIN_RGT). These two scenarios are further investigated (Table 6-1).

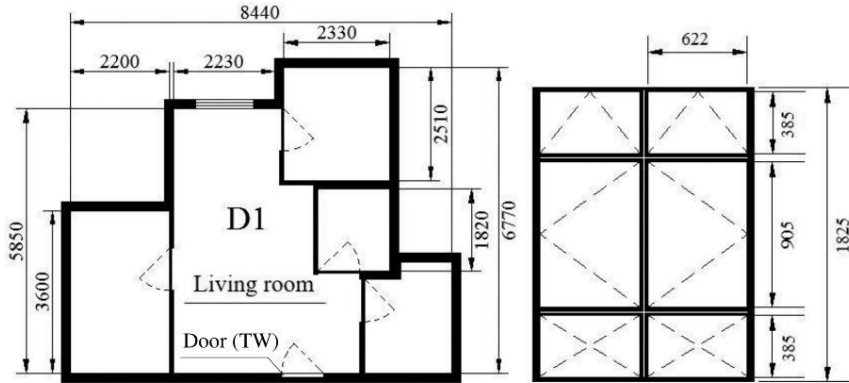


Figure 6.7 Layout of unit D1 with floor dimensions and window details.

In the further investigations, the studied unit's actual architectural characteristics were used, including window dimensions, floor layout, window type (side-hung window), and optimum window opening range (60° by reference to Chapter 5) [132], [147]. Figure 6.7 shows the layout, floor dimensions and window details of unit D1.

6.3 CFD simulations and validations

The nine representative wind data sets as introduced in Chapter 3 were again used to represent wind environments prevailing from the outer zone to the building blocks.

Further investigations were based on CFD simulations, aiming to predict the outdoor and indoor airflow of the buildings for the design parameters summarised in Table 6-1. Based on the presence or absence of TW, two positions of TW relative to window, six TW opening areas,

four TW orientations and nine wind data sets, a total of 468 $((2 \times 6 \times 4 \times 9 \text{ (presence of TW)} + 4 \times 9 \text{ (absence of TW)}) = 468)$ cases were generated for CFD simulations.

According to the Best Practice Guideline for CFD simulation [154], validation should first be conducted to reduce the errors and uncertainties in numerical solutions.

As outdoor wind condition is attributed to characteristics of the urban environment and local wind conditions, experimental results of wind tunnel tests for a location with an urban environment similar to that of Hong Kong were employed for validation. Considering that the validation process shared a certain level of similarities with that presented in Chapter 4, only essential information is given in this Chapter.

Furthermore, due to shear stress, wind speed increases logarithmically with the vertical height from the ground. For identifying the local wind conditions, a representative building height of the studied high-rise building block needs to be determined.

6.3.1 Simulation validations

Urban environment is affected by site layouts and building plans, which can be represented by the street aspect ratio (λ_{st}) (Equation (6.2)) and building area densities (λ_{bd}) (Equation (6.3)) [155]. For the public housing estate in Tseung Kwan O, these two values are 2 and 0.25 respectively [156]. Accordingly, validation of CFD input settings were based on experimental results presented by Hang et al. where the wind tunnel tests were conducted at similar locations λ_{st} and λ_{bd} . [157].

$$\lambda_{st} = \frac{HT_{st}}{WD_{st}} \quad (6.2)$$

Where λ_{st} is the street aspect ratio; HT_{st} is the street height (m); WD_{st} is the street width (m).

$$\lambda_{bd} = \frac{A_p}{A_d} \quad (6.3)$$

Where λ_{bd} is the building area densities; A_p is the planning area of buildings from a top view (m^2); and A_d is the total underlying surface area (m^2).

The Reynolds-averaged Navier-Stokes (RANS) equations and the standard k-epsilon turbulent model were used to simulate the indoor and outdoor airflow [63], [158], [159]. The SIMPLE algorithm (Semi-Implicit Method for Pressure-Linked Equations) was employed to couple pressure and velocity. The transport equations were discretised by the second-order upwind scheme.

Boundary conditions were set according to the laws of mean inlet wind profile, turbulent kinetic energy, and dissipation rate, in the form of $U_z = U_{ref} (HT/HT_{ref})^\alpha$ ($\alpha=0.16$), $k = 1.5(IU_y)^2$ and $\varepsilon = C_\mu^{3/4} k^{3/2} l_t$ (U_y is the initial velocity magnitude (m/s); I is the initial turbulent intensity (%); $C_\mu=0.09$; k is the turbulence kinetic energy (m^2/s^2); ε is the turbulence energy dissipation rate (m^2/s^3) and l_t is the length scales of turbulence (m).

The domain dimensions of the building blocks length (LG), width (WD) and height (HT) were set as $5LG \times 11WD \times 6HT$ (i.e. $5,500m \times 5,500m \times 651m$). They were determined based on trial simulations by gradually shrinking the dimensions to obtain the balance between computing

time and accuracy. The unstructured tetrahedral mesh was used for mesh generation. The grid-independent test was performed by comparing the simulated inlet wind speeds by height for grids generated with a coarse, medium and fine mesh, with stretch factors of 2.5, 2.0 and 1.0 respectively. Results of simulated wind velocities of the three refinements were compared with the wind tunnel experiment results. The testing positions in the experiment (PA, PB, PC, PC' and PD) are shown in Figure 6.8 (b).

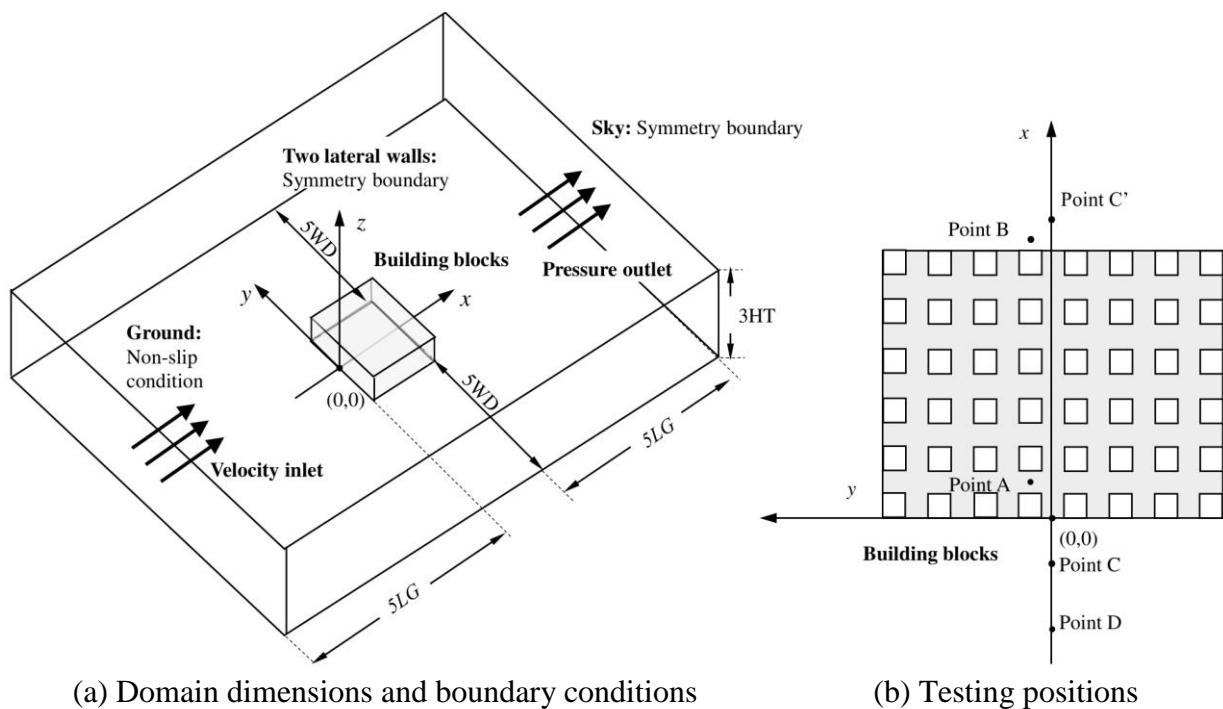


Figure 6.8 CFD settings and testing positions for comparison

Table 6-3 Comparison of three refined meshes

Mesh	Stretch factor	Grid number (million)	RMSE				Average RMSE	y + for first cell
			y=0.1LG		y=0			
			PA: x=0.14LG; z=0-3HT	PB: x=1LG; z=0-3HT	PC-PC': x=-0.3-1.5LG z=0.4HT;	PD: x=-3LG; z=0-3HT		
Fine	1.0	1.29	0.0538	0.0649	0.0910	0.1367	0.0866	35
Medium	2.0	0.36	0.0271	0.0769	0.0906	0.1142	0.0772	71
Coarse	2.5	0.22	0.0192	0.0725	0.1010	0.1031	0.0739	87

The Root-Mean-Square Error (RMSE) and the near the wall y-plus (y^+) values were used to evaluate the mesh quality. RMSE is calculated by Equation (6.4). The results are shown in Table 6-3. It is noted that the coarse mesh returns the smallest error and therefore this meshing method was selected [160]. The y^+ values for the first cell and the average RMSEs for the three refinements are comparable. The y^+ values are within the range 30-300 and confirm a satisfactory mesh quality for standard k-epsilon models [161]. The small difference in the average RMSE confirms a successful grid independent test.

$$RMSE = \left(\frac{1}{n} \sum_{i=1}^n (\phi_m^j - \phi_s^j)^2 \right)^{1/2} \quad (6.4)$$

Where $\phi_s^j = (U / U_0)_s^j$ is the dimensionless simulated mean velocity simulated in position j ; ϕ_m^j is the wind tunnel measured values at the same position j ; and n is the number of values.

6.3.2 Representative building level

To identify the representative building level for determining the local wind conditions for high-rise building blocks, the pressure coefficient (C_p) on the living room windows in steps of five floors (F) (i.e. F5, F10, F15, F20, F25, F30, F35, F40) as shown in Figure 6.9 (a) were simulated [162], [163].

Given that the pressure coefficient (C_p) is affected by the window and TW orientations and the wind directions, accordingly, C_p of the eight pre-determined floors of Block X for different orientations and wind conditions (as showed in Figure 6.9 (b)) were extracted from the

simulation results for further analysis. In Figure 6.9 (b), the two values in brackets (e.g. 5.15; 2.9) correspondingly represent the wind direction in degree from the north (i.e. 5.15°) and wind speed (i.e. 2.9 m/s).

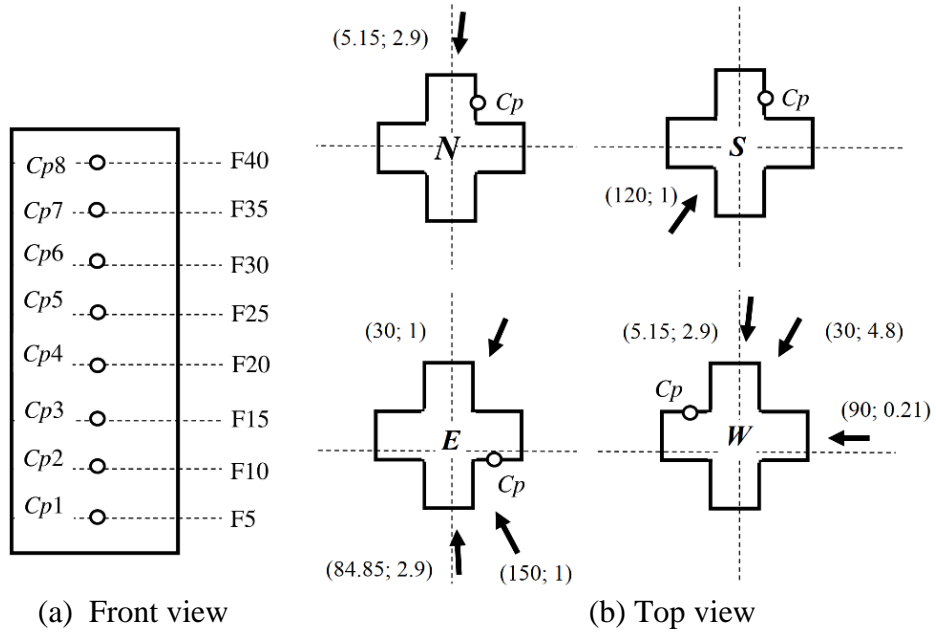


Figure 6.9 Locations of pressure coefficients on the building façade

The representative building level was determined by Pearson correlation coefficients and the Fisher transformation method. Pearson correlation coefficients r (Equation (6.5)) were used to calculate the similarity of pressure coefficients at different building levels [164], [165] and the Fisher transformation method, represented by Equations (6.6) to (6.8), was employed to examine the average Pearson correlation coefficient R of each building level [166], [167]. Results are summarised in Table 6-4.

$$r_{xy} = \frac{\sum_{j=1}^n (x_j - \bar{x})(y_j - \bar{y})}{\sqrt{\sum_{j=1}^n (x_j - \bar{x})^2 \sum_{j=1}^n (y_j - \bar{y})^2}} \quad (6.5)$$

Where r_{xy} is the correlation coefficient between building level x and y ; j is the j^{th} pressure coefficient value; n is the total measured times on a building level (=9); and \bar{x} and \bar{y} are the mean value of pressure coefficient for building level x and y respectively.

$$m_{xy} = \frac{1}{2} \left[\left(\ln(1 + r_{xy}) \right) - \ln(1 - r_{xy}) \right] \quad (6.6)$$

$$\bar{m}_x = \frac{1}{8} \sum_{b=1}^8 m_{xy} \quad (6.7)$$

$$\bar{m}_x = \frac{1}{2} \left[\left(\ln(1 + R_x) \right) - \ln(1 - R_x) \right] \quad (6.8)$$

Where m_{xy} is the transformed correlation coefficient for r_{xy} ; and \bar{m}_x is mean values from m_{x1} to m_{x8} , representing the mean transformed correlation coefficient for building level x ; and R_x is the average Pearson coefficient for building level x .

Table 6-4 Pearson correlation coefficients by building level

Building Level	F5	F10	F15	F20	F25	F30	F35	F40	
Pearson correlation coefficients (r) of x_i and x_j	F5	1.000	0.807	0.956	0.961	0.931	0.942	0.813	0.762
	F10	0.807	1.000	0.907	0.903	0.946	0.862	0.898	0.772
	F15	0.956	0.907	1.000	0.994	0.974	0.912	0.833	0.701
	F20	0.961	0.903	0.994	1.000	0.980	0.934	0.846	0.711
	F25	0.931	0.946	0.974	0.980	1.000	0.957	0.923	0.805
	F30	0.942	0.862	0.912	0.934	0.957	1.000	0.999	0.879
	F35	0.813	0.898	0.833	0.846	0.923	0.999	1.000	0.921
	F40	0.762	0.772	0.701	0.711	0.805	0.879	0.921	1.000
	\bar{x}	-0.236	-0.239	-0.238	-0.253	-0.309	-0.361	-0.398	-0.398
\bar{m}_x	1.443	1.337	1.636	1.685	1.693	1.796	1.630	1.108	
Average Pearson coefficient (R)	0.894	0.871	0.927	0.934	0.935	0.946	0.926	0.803	

It can be seen from Table 6-4 that pressure coefficients at F30 return the highest R (=0.946), indicating that they significantly correlate with the other seven-building levels and is chosen as the representative building level for further investigations.

6.4 ANN model development

An artificial neural network (ANN) was formulated based on simulation results of the 468 cases, to evaluate the relative impact of different design parameters on natural ventilation. ANN was employed because it can tackle ill-defined relationships [168] and can construct a complex nonlinear model for predicting the magnitude of natural ventilation [169]–[171]. ANN has been successfully applied in similar studies [172], [173].

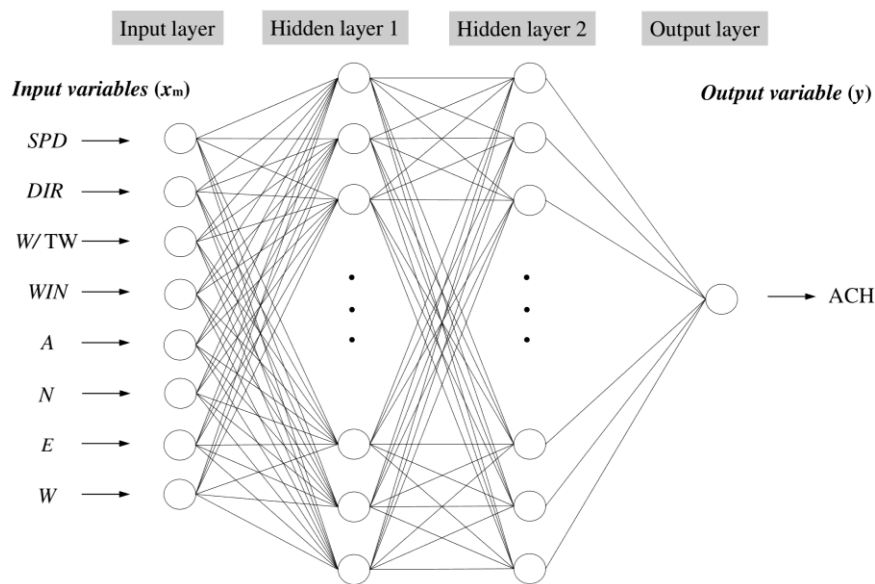


Figure 6.10 Artificial neuron network structure.

Matlab 2017b software was deployed to train ANN models. The back-propagation (BP) neural network algorithm was adopted to associate input values to the output values. It is the most frequently used neural network training method which can improve the performance of the

neural network and minimise error [174], [175]. The transfer function was set as tan-sigmoid for hidden layers and linear for the output layer. The solution was considered converged when the target minimum mean square error (MSE) was achieved.

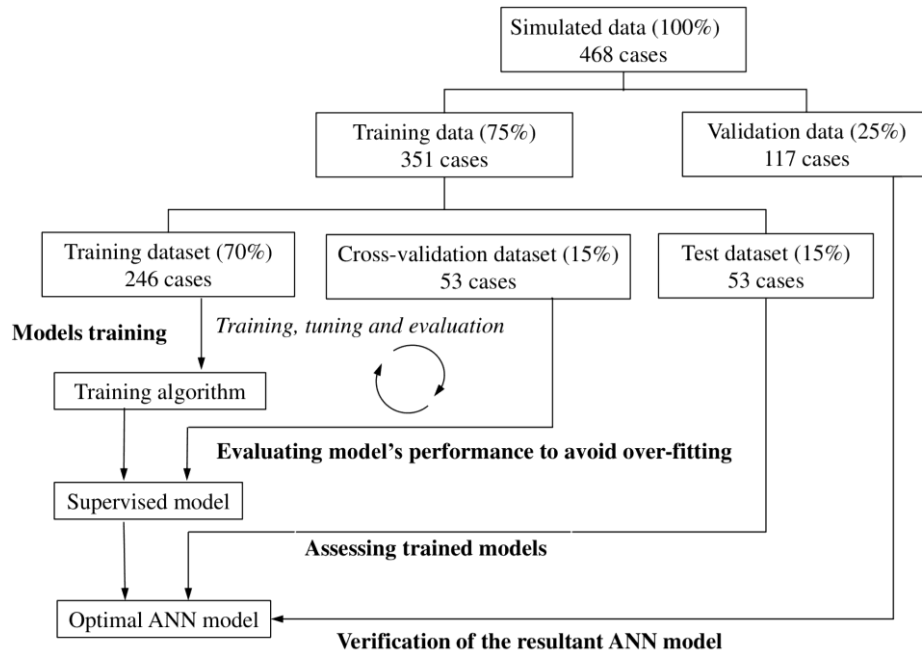


Figure 6.11 ANN models establishment process

Figure 6.11 shows the ANN model establishment process. Simulation results of the 468 cases were divided into two data groups namely training data and validation data in a split of 75% (351 cases) and 25% (117 cases) respectively. The training data were further divided randomly into three sub-groups which are the training dataset (70%), cross-validation dataset (15%) and test dataset (15%) [176]. The training dataset is for training the ANN models, the cross-validation dataset is to evaluate model performance during training to avoid over-training, and the test dataset is for assessing the trained models [177], [178]. The validation dataset that comprises data completely irrelevant to the original network is for verification of the resultant ANN model. A successful verification requires a similar correlation coefficient (r) between the

trained model and the verification model (the difference is less than 0.05) and the MSE is lower than the threshold value (= 0.08) [179].

6.5 Results and discussion

6.5.1 ANN model

After performing the 468 CFD simulation runs and calculation of ACH by Equations (4.3) and (4.5), Matlab 2017b was employed to train ANN models. The resultant ANN model was established by varying the number of hidden neurons for the best model performance. Based on the resultant ANN model, sensitivity analysis was conducted to evaluate the relative impact of different design parameters.

6.5.1.1 The resultant ANN model

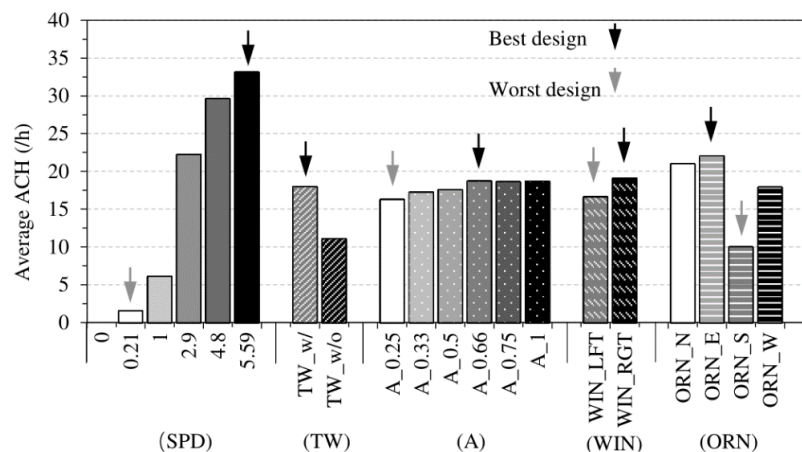


Figure 6.12 Influence of different design parameters on ACH

The dummy variable method was again used in this Chapter for coding the ORN, WIN, TW with the value of 0 and 1 to represent the absence or presence of a particular design option

except for the base group. The average ACH rates obtained from 468 simulation cases were compared (Figure 6.12). It is noted that for each group of design parameters, there are the best and the worst designs, as highlighted. The worst design options were chosen as the base group (i.e. ORN_S; WIN_LFT; TW_w/o). Accordingly, for ORN, only ORN_N, ORN_E, ORN_W were coded, and likewise for the WIN_RGT and those for TW_w/ were coded.

Values for both quantitative and qualitative parameters were normalised to a uniform range. This is a basic procedure for ANN training to prevent overriding of a variable with different dimensions and to avoid premature saturation of hidden neurons [180]. Accordingly, the minimum and maximum values of the input and output variables were scaled to the range of [-1,1] by Equation (6.9)[181].

$$NV = \frac{NV_{\max} - NV_{\min}}{VL_{\max} - VL_{\min}} \cdot (VL - VL_{\min}) + NV_{\min} \quad (6.9)$$

Where NV is normalised vector of an input or output; NV_{\max} and NV_{\min} are scaled values within the range 1 and -1 respectively; VL is value of the input or output variable; and VL_{\max} and VL_{\min} are maximum and minimum value respectively of each parameter.

The numbers of neurons in the hidden layers affect the stability and quality of the ANN model significantly [182]. As such, it is used to determine a model with the lowest error between predicted and actual values. In the ANN model optimisation process, the numbers of hidden neurons for the two hidden layers were varied to have the same values in the range of $NR_h \in [7,17]$ calculated by Equation (6.10), while settings of other variables in the neural network were unchanged.

$$2 \times \sqrt{NR_{ip}} + NR_{op} \leq NR_h \leq 2 \times NR_{ip} + 1 \quad (6.10)$$

Where NR_{ip} is the number of input neurons ($NR_{ip}=9$, with three neurons for quantitative variables and 6 neurons for qualitative variables); NR_{op} is the number of output neurons ($NR_{op}=1$); NR_h is the number of hidden neurons. $NR_h \in [7,17]$.

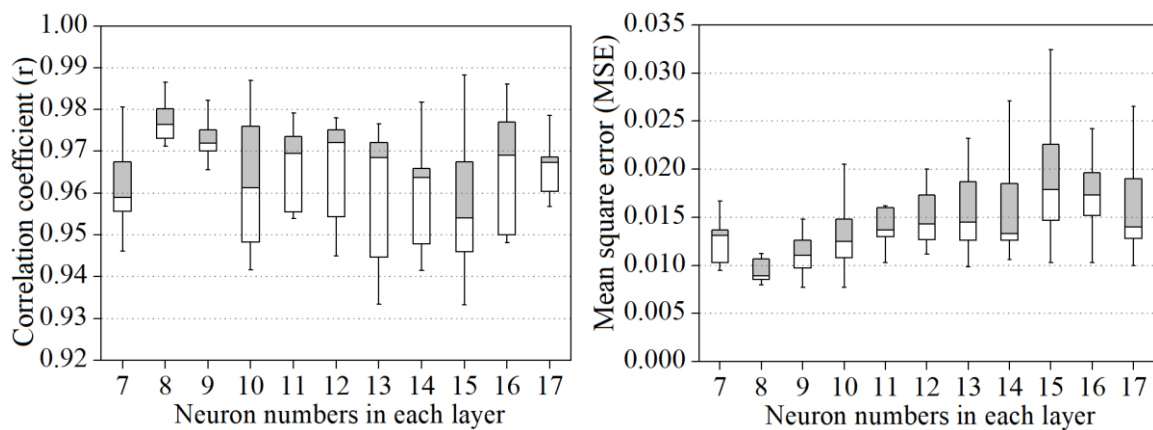


Figure 6.13 r and MSE of models with different neuron numbers

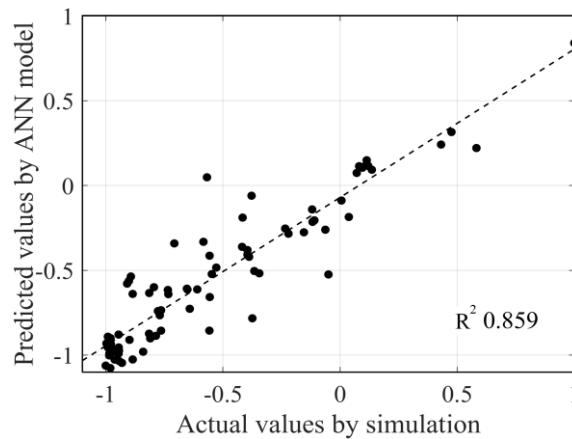


Figure 6.14 Comparison between the actual and predicted ACHs

Models were trained based on different numbers of neurons in the two layers. Each model was trained by ten different training datasets to avoid bias so as to improve model reliability [183].

The minimum mean square error (MSE) and Pearson coefficient (r) of the trained models were recorded. Results are shown in Figure 6.13. The x-axis shows the numbers of neurons in each hidden layer. It can be seen that the model with eight neurons in each hidden layer returns the smallest minimum MSE and the highest r to confirm the best performance.

Based on eight neurons in each hidden layer, the optimal ANN model was selected based upon the difference between correlation coefficients (r) of the trained model and the verification model is lower than 0.05 [179], which are 0.981 and 0.970, and the MSE is the lowest and is lower than the threshold value (≤ 0.08) [179], at 0.008. Adding that the difference between the coefficient of determination (R^2) of actual ACHs and the ACHs predicted by the resultant ANN model is 0.859. Thus, the resultant ANN model is confirmed and passes the verification test. Figure 6.14 compares the predicted and actual results.

6.5.1.2 Sensitivity analysis

Sensitivity analysis was carried out to determine the relative impact of the design parameters on the ACHs. The influence is quantified by the use of a relative impact factor (RIF) which calculates the contribution of each input variable to the output value of the resultant ANN model [184]. RIF for input variable x_m (RIF_m) is defined as:

$$RIF_m = \left| \frac{(y_m)_{+\Delta x_m} - (y_m)_{-\Delta x_m}}{y_{\max} - y_{\min}} \right| 100\% \quad (6.11)$$

Where x_m is the input variable m and y is the value of output variable (ACH) as showed in Figure 6.10; Δx_m is the variance of variable m ; y_{max} and y_{min} are the maximum and the minimum ACH ; and y_m is the calculated ACH based on variance of x_m .

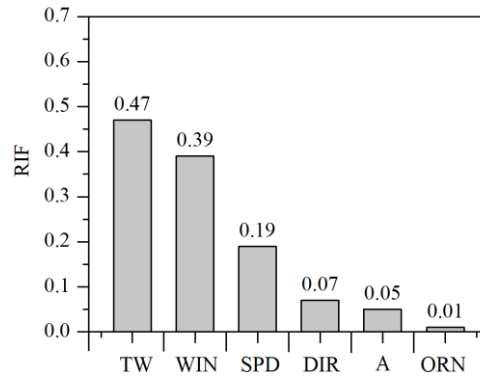


Figure 6.15 RIF by design parameters

For quantitative variables, the variance of variable m is within the range of $\pm 10\%$ and $\pm 20\%$ of the input values, and the change is set as the mean value if they are fixed values. For qualitative variables, the variance is within the upper and lower limits of values, and the change is set as the median value if they are fixed values [185], [186]. For each and every variance of the input variable, the RIF is calculated. Average RIF values for different design parameters are summarised in Figure 6.15 [187], [188].

Amongst the design parameters, TW returns the highest RIF ($=0.47$), followed by (in descending order) WIN ($=0.39$), SPD ($=0.19$), A ($=0.05$), and ORN ($=0.01$). The small influence of DIR (RIF= 0.07) has been explained in Chapter 4.

6.5.2 Influence of different design parameters

6.5.2.1 With or without transom window

It is no surprise (Figure 6.15) that the ACH is most sensitive to the presence of TW (RIF=0.47) because much of the research on natural ventilation has already concluded that cross ventilation is most preferred [37], [38], [189], [190]. This can be explained by the fact that windows and TWs serve separately as air inlets and outlets while those that have only windows have to serve as air inlets and outlets simultaneously.

6.5.2.2 Position of transom window to window

Position of TW to the window is the second most sensitive parameter that affects ACH performance (RIF=0.39). The influence of TW position can be explained by the Coanda effect [191] and the Navier-Stokes equations. The Coanda effect experienced by the WIN_LFT and WIN_RGT air jets are shown in Figure 6.16.

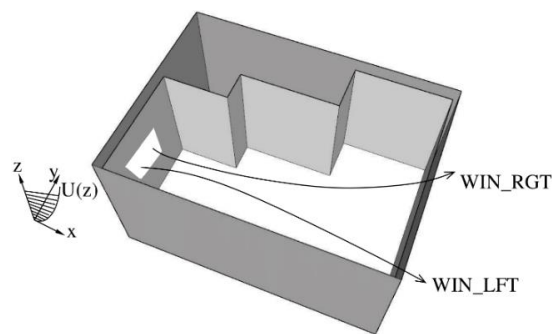
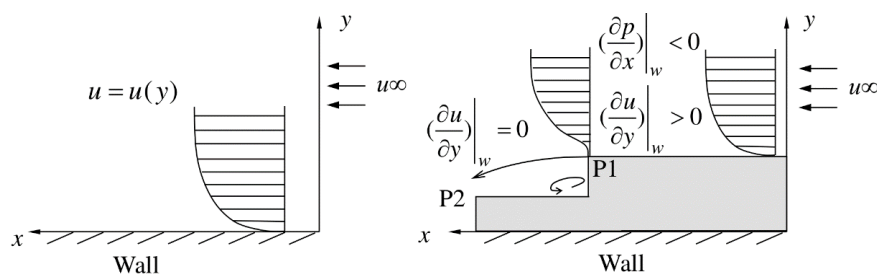


Figure 6.16 Illustration of flow path under two different positions of TW.



(a) WIN_LGT

(b) WIN_RGT

Figure 6.17 Flow development, velocity gradient and pressure gradient for two WINs

Ignoring gravity and assuming the incoming wind is a free-stream flow, WIN_LFT air jet can be simplified as a flow over the wall (Figure 6.17 (a)), while WIN_RGT air jet can be regarded as a flow over backward-facing steps (Figure 6.17 (b)).

The two types of flow can be explained by the Navier-Stokes equations as given below:

Continuity equation:

$$\frac{\partial u}{\partial x} + \frac{\partial v}{\partial y} = 0 \quad (6.12)$$

Momentum equations:

$$\frac{\partial}{\partial x}(\rho u^2) + \frac{\partial}{\partial y}(\rho uv) = -\frac{\partial P}{\partial x} + \mu \left(\frac{\partial^2 u}{\partial x^2} + \frac{\partial^2 u}{\partial y^2} \right) \quad (6.13)$$

$$\frac{\partial}{\partial x}(\rho uv) + \frac{\partial}{\partial y}(\rho v^2) = -\frac{\partial P}{\partial y} + \mu \left(\frac{\partial^2 v}{\partial x^2} + \frac{\partial^2 v}{\partial y^2} \right) \quad (6.14)$$

Where ρ is air density (kg/m^3); μ is dynamic viscosity ($\text{Pa}\cdot\text{s}$); u and v are the velocity component in the x and y direction respectively (m/s); and P is the pressure (Pa).

In the stationary case, the flow velocity component is simplified as $u=u(y)$ [192]. Then the momentum equation can be simplified as:

$$0 = -\frac{\partial P}{\partial x} + \mu \left(\frac{\partial^2 u}{\partial y^2} \right) \quad (6.15)$$

For WIN_LFT, velocity component u develops along with the x -axis of the plate wall with:

$$\frac{u}{u_\infty} = \left(\frac{y}{y_\infty} \right)^\alpha \quad (6.16)$$

For WIN_RGT, the developing flow cannot follow the shape edge of geometry and induces the geometrically-based flow separation at the steps (e.g. P1 in Figure 6.17 (b)) [193]. This gives the relationship:

$$\left. \frac{\partial u}{\partial y} \right|_w = 0 \quad (6.17)$$

$$\left. \frac{\partial p}{\partial x} \right| > 0$$

Then the curvature can be derived from Equation (6.18) with:

$$\frac{\partial^2 u}{\partial^2 y} > 0 \quad (6.18)$$

Before separation, the relationship between velocity gradient, pressure gradient and the curvature of velocity profile are:

$$\frac{\partial u}{\partial y} > 0$$

$$\left. \frac{\partial p}{\partial x} \right| < 0 \tag{6.19}$$

$$\frac{\partial^2 u}{\partial^2 y} < 0$$

Considering velocity u tends to be u_∞ at the boundary layer and the curvature relationships before and on the separation (P1), the wind profile for the WIN_RGT has to involve the extreme increase of the flow first [194], as shown in Figure 6.17 (b). This acceleration of the flow does not reattach to the boundary layer after separation [195], but becomes more intensive in the subsequent step (P2) which results in WIN_RGT with higher indoor air movement than WIN_LFT.

6.5.2.3 Wind conditions

SPD is the third most sensitive design parameter that affects ACH (RIF=0.19). This is reasonable because natural ventilation is mainly wind-driven [196]. Figure 6.18 shows that ACH increases with SPD. The two exhibit a nearly linear relationship, which can be explained in Chapter 4.

However, DIR (RIF=0.07) has only a small influence on ACH. This is due to the angular-linear relationship between SPD and DIR which results in serious collinearity [115], [116]. This relationship happens because DIR is periodic (0° to 360°) while SPD is random and highly variable (0 to $+\infty$). Nevertheless, the collinearity does not affect accuracy of the resultant ANN model trained by the BP method [197].

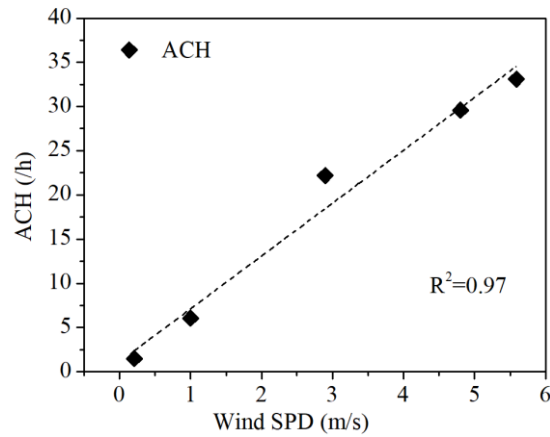


Figure 6.18 Average ACH with wind speed

6.5.2.4 Opening area of transom window

Changing the opening area of TW is the fourth most sensitive parameter that affects ACH (RIF=0.05). The influence of the area of TW on ACH is shown in Figure 6.19, indicating that they exhibit a polynomial relationship ($R^2 = 0.90$). This can be explained by the ventilation rate through openings for CV mode calculated in Equation (4.11) and (5.4). From two equations it is noted that ventilation rate Q , represented by ACH, is affected by C_d which also exhibits a polynomial relationship with A [198]. Similar findings have been reported to explain the polynomial relationship between ACH with A [147].

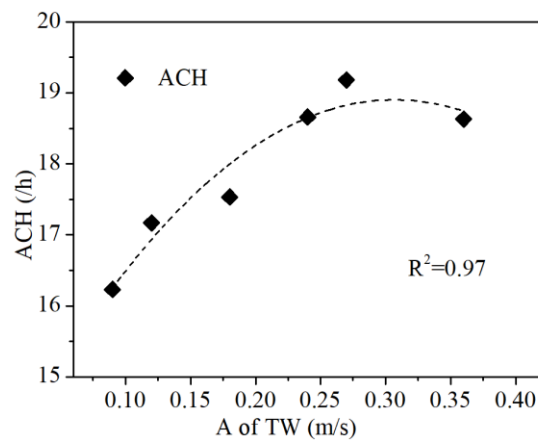


Figure 6.19 Opening area of TW on average ACH

6.5.2.5 Transom window orientation

Among all design parameters, TW orientation exerts the smallest impact on ACH (RIF=0.01). Of the four window orientations, it can be seen from Figure 6.12 that ORN_E returns the highest ACH, followed in descending order by ORN_N, ORN_W, and ORN_S. These results can be explained by the Venturi-effect of the buildings [199].

The amplification factor K (Equation (6.20)) was used to depict the Venturi-effect contributing to the local wind conditions. A higher K means a higher local wind speed to increase the ACH [200], [201].

$$K = \frac{U_{local}}{U_{ref}} \quad (6.20)$$

Where U_{local} is the local wind speed at a particular location on F30 where the window is located (i.e. $Z=80m$) (m/s); and U_{ref} is the free-field mean wind speed at the same location (m/s).

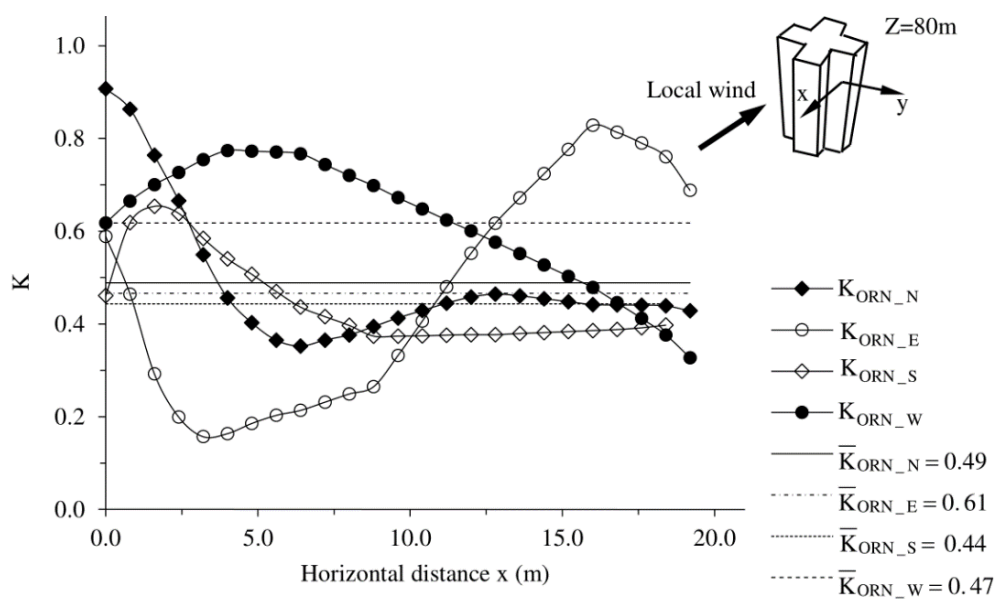


Figure 6.20 Amplification factors K by orientations.

Figure 6.20 shows the change of K with x by orientations, where x is the horizontal distance measured 20 m from block X (m).

It can be seen that the ORN_E returns the highest average K ($\bar{K}_{ORN_E}=0.61$), followed by ORN_N ($\bar{K}_{ORN_N}=0.49$), ORN_W ($\bar{K}_{ORN_W}=0.47$), and the lowest is ORN_S ($\bar{K}_{ORN_S}=0.44$) which confirms the influence of window orientation.

6.5.3 Impact on ACH

With the use of TW of different designs, ACHs that can be achieved in the living room of the studied unit on F30 for the 468 simulation cases were calculated by Equation (4.3) and Equation (4.5). Based on the relative frequency of occurrence (f) of a particular wind dataset, the weighted average \overline{ACH} for different TW designs were also determined by the Equation (6.21). Results are as shown in Table 6-5.

$$\overline{ACH}_{(g,t)} = \sum_{c=1}^t ACH_{(g,c)} \cdot f_c \quad (6.21)$$

Where $\overline{ACH}_{(g,t)}$ is the weighted average ACH for a particular month (t) operating under different TW designs (g= the best, the worst and without TW); f_c is the relative frequency of occurrence of a particular wind condition by month; c is a particular wind condition from wind data sets in Table 3-1.

Table 6-5 ACHs for TW with different designs

TW Designs	TW_w/o		TW_w	
	Worst	Best	Worst	Best
WIN	N/A	N/A	WIN_LFT	WIN_RGT
SPD	0.21	5.59	0.21	5.59
A	0	0	0.05 (A_0.25)	0.27 (A_0.66)
ORN	ORN_S	ORN_E	ORN_S	ORN_E
ACH	0.51	36.4	0.52 (+2.0%)	76.5 (+110.2%)
Weighted average \overline{ACH}	9.8 (—)		21.3 (+117%)	28.5 (+190%)
			24.9 (+153.5%)	

It can be seen in Table 6-5 that as compared to TW_w/o, the incorporation of TW can improve the ACH by 2.0% to 110.2%. Besides, depending on the TW's design, the average improvement in ACH because of its incorporation ranged from 117 % to 190%, with the average increase in ACH is 153.5%. The results confirm the effective use of TW in enhancing natural ventilation in high-rise residential buildings in Hong Kong.

6.6 Summary

The relative impact of different physical characteristics of transom window on natural ventilation in high-rise residential buildings in Hong Kong was investigated by site-measurements, CFD simulations and ANN model analyses. The site measurements were conducted at two carefully selected adjacent units. Through controlled experiments, the influential parameters for TW design were confirmed. Further investigations were based on a representative residential unit selected from a public housing complex in Hong Kong, 9 representative local wind conditions a typical building level identified by the Pearson correlation coefficient and the Fisher transformation method. CFD settings were validated by a previous wind tunnel experiment where the street aspect ratio and the building area densities are similar to Hong Kong. 468 CFD simulations were done to cover different designs for TW.

Based on the simulation results, ANN model was established for evaluating their relative impacts by sensitivity analysis. It was found that natural ventilation performance is most sensitive to the presence of TW, followed in descending order by the position of TW to the window, wind speed, area of TW, orientation of TW, and wind direction. The improvement in ACH for different TW design characteristics were determined. It was found that the incorporation of TW could improve the ACH by 153.5% on average to confirm the effective use of TW to enhance natural ventilation of high-rise residential buildings in Hong Kong. The results found in this study are well-explained and the relative impact of different designs for TW are expected to be useful for decision making by policy makers in search of performance improvement in natural ventilation in Hong Kong and elsewhere in the world.

CHAPTER 7 THE EFFECTIVENESS OF TRANSOM WINDOW IN REDUCING COOLING ENERGY USE

The effectiveness of using transom window in enhancing natural ventilation in high-rise residential buildings in tropical climates in Hong Kong has been confirmed in Chapter 6. However, virtually no work has been done to demonstrate its effectiveness in reducing cooling energy consumption and providing the desired thermal comfort. To fill this gap, the cooling energy usage of a simple air-conditioning system was compared with that of a hybrid system (using enhanced ventilation created by TW supplemented with air-conditioning) for achieving the same thermal comfort in high-rise residential buildings in Hong Kong. A carefully-designed methodology which involves the use of the market survey, statistical analyses, site measurements, and integration of CFD and EnergyPlus simulations was adopted in this study. Market surveys and statistical analyses were used to provide reliable input data for simulations. Site measurements of ventilation were used to assess the uncertainty of CFD simulation results. CFD simulations were employed to provide accurate predictions of ACHs (air change per hour) and air velocities achieved with TWs. EnergyPlus simulations were used to predict the hour-by-hour air temperatures and the cooling energy usage based upon the ACHs obtained from CFD simulations.

7.1 CFD simulations and validations

7.1.1 The representative residential unit

The representative residential unit presented in Chapter 6 was again adopted for CFD

simulations. In the simulations, the studied unit’s actual architectural characteristics were used, including window dimensions, floor layout, window type (side-hung window), optimum window opening range (60° as explained in Chapter 5) [132], [147], and construction details (Table 7-1).

Table 7-1 Construction details

Component		Thickness (m)	Material	Thermal conductivity (W/Mk)	Density (kg/m3)	Solar absorptivity
Wall (Layer)	1	0.005	Mosaic tiles	1.5	2500	0.58
	2	0.01	Cement	0.72	1860	---
	3	0.1	Heavy concrete	2.16	2400	---
	4	0.01	Gypsum plaster	0.38	1120	0.65
Window	1	0.006	Tinted glass	1.05	2500	---

7.1.2 Physical characteristics of TW

Considering that TW should be on the outer door to facilitate cross ventilation, the living room, therefore, becomes the only viable location for its incorporation. TW can be of different designs.

In Chapter 6, the position of TW to the window, wind speed, area of TW, orientation of TW, and wind direction exert substantial influence on natural ventilation performance of a residential unit has been identified. It was found that TW with physical characteristics shown in Figures 7.1 (a) and (b) are the best and worst TW designs. Thus these TW designs were selected for evaluation of the effectiveness of TW in enhancing natural ventilation to achieve thermal comfort and cooling energy saving.

The dimensions of the TW adopted in Chapter 6 was again used in this study.

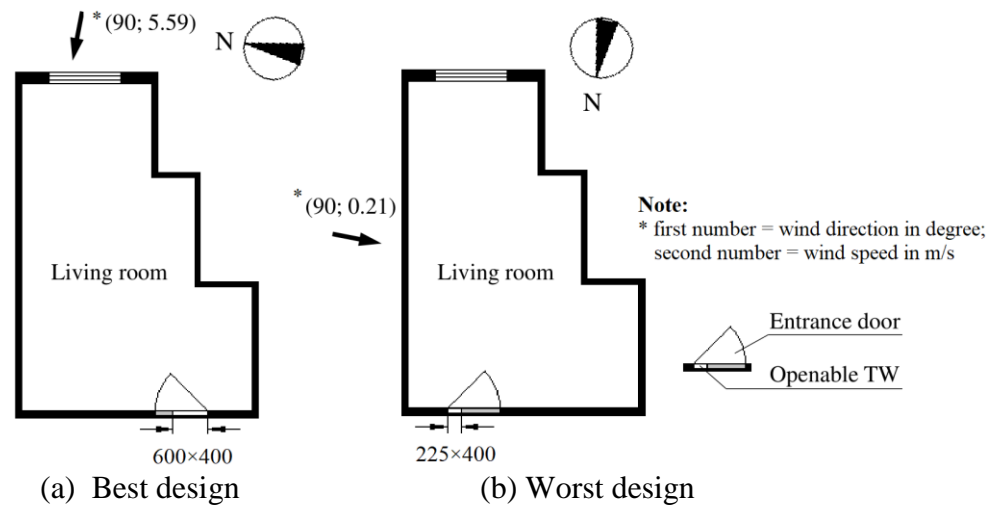


Figure 7.1 Physical characteristics of TW

7.1.3 Local wind environments

The wind environments at the representative building level identified based on the Pearson correlation coefficients and the Fisher transformation method (Chapter 6) was again employed.

7.1.4 Validations and simulations

The validated CFD settings presented in Chapter 6 was again used. For evaluation of the performance of TW integrated with other aperture designs, there were three TW design options (no TW, the best and the worst); four orientations and nine wind data sets to become 108 ($3 \times 4 \times 9 = 108$) simulation cases.

7.1.5 Site verifications

Unlike validation which is to assess the reliability of the modelling [202], site verifications were conducted to assess the uncertainty of the simulation results. Site measurements results presented in Chapter 6 were used for site verifications. However, due to site constraints, the position of TW relative to window cannot be changed to model the best TW design (Figure 7.1 (a)). As a result, site verifications were restricted for cases with the worst TW designs (Figure 7.1 (b)) and those without the use of TW.

7.2 Energy simulations

EnergyPlus was used to simulate energy used by the RAC operating under the AC and the hybrid systems. To predict energy saving, different sets of simulations were conducted.

In EnergyPlus, the built-in model for RACs is called “Window Air Conditioner”. The inputs include the cooling capacity (kW), air volume flow rate (m^3/s), and coefficient of performance (COP). To model the use of the hybrid system, an extra object called “Design Flow Rate” was added to model the natural ventilation mode. Simulations were performed using the “Energy Management System” to enable switching between natural ventilation and air-conditioning modes.

7.2.1 Market survey

To provide realistic equipment characteristics for the simulations, a market survey was conducted to collect performance data of room air-conditioners (RACs). These data were used for the living room of the representative residential unit. The RAC capacity was determined by

cooling load simulations. The associated equipment characteristics were obtained by market survey. The focus was on those with Grade 1 energy label awarded by the government [203].

Table 7-2 Adjusted performance data of RACs

Model	HP	Cooling output (kW)	Input power (kW)	COP	Air volume flow rate (m ³ /s)
1	1.5	1.330	1.243	1.070	0.113
2	2	2.320	2.017	1.150	0.197
3	1.5	1.541	1.270	1.213	0.131
4	2	2.854	2.203	1.296	0.203
5	1.5	1.574	1.230	1.280	0.133
6	2	2.290	1.860	1.231	0.194
Most probable value		2.088	1.729	1.208	0.158

Performance data of 6 models with cooling output (1.33 – 2.85 kW) and input power adjusted for an indoor temperature of 24°C (explained in Section 7.6.2) that matches the studied living room were collected (Table 7-2). The 6 models are 1.5 HP and 2 HP units in layman terms. To avoid mean-bias, Monte Carlo analysis [204][205] was adopted to identify the most probable performance data set for EnergyPlus simulations.

Adjusted performance data were used because standardised performance data obtained from manufacturers' were determined based on the rating condition that assumes outdoor temperature of 35°C and on coil (indoor) temperature at 27°C. The adjustments were done based on the following two models (Equations (7.1) and (7.2)) developed in a previous study [206].

$$j_{MC} = J_{MC}/J_R = 0.7651 - 0.0086T_o + 0.0199T_i \quad (7.1)$$

$$pw_V = PW_V/PW_R = 0.066 + 0.0191T_o + 0.0102T_i \quad (7.2)$$

Where

T_o = the outdoor temperature (°C)

T_i = the indoor temperature (°C)

J_{MC} = the maximum cooling output of the RAC at T_o & T_i (kW)

J_R =the rated cooling capacity of the RAC under the standard rating condition (kW)

j_{MC} =the normalised cooling capacity of the RAC at T_o & T_i

PW_V =the power input to the RAC for J_{MC} at T_o & T_i (kW)

PW_R =the rated power of the RAC under the standard rating condition (kW)

pw_V =the normalised power input to the RAC for J_{MC} at T_o & T_i

7.2.2 The AC and hybrid systems

Cooling period for both only AC and the hybrid systems is when the hourly outdoor air temperature is higher than the balance air temperature of 20.5°C. The balance air temperature is the temperature used for calculation of cooling degree days. It is the average of the maximum and minimum outdoor air temperatures. They are 33°C and 8°C respectively for Hong Kong [207]. Within the cooling period, the AC or the hybrid system was assumed in operation to achieve the design condition according to a pre-determined daily pattern as shown in Table 7-3. The pattern was determined by reference to various sources [206], [208], [209].

For the only AC system, the design condition for the RAC is 24°C dry bulb (DB) temperature and 50% relative humidity (RH), which is commonly used for Hong Kong residential environment for achieving 90% thermal acceptability [208], [210], [211].

For the hybrid system, the design condition for the RAC is the same as the only AC system while natural ventilation is different. For determining the design condition for natural ventilation, reference is made to ASHARE's Standard 55 on users' thermal acceptability [212]. For 90% acceptability, the maximum acceptable indoor operative temperature and the range of acceptable air velocity are determined by Equation (7.3) and (7.4) [213], [214].

$$T_{I, \max 90} = 0.31T_o + 20.3 \quad (7.3)$$

$$TS = 0.1818T_{I, \max 90} - 0.4264V_I + 34.02w - 4.702 \quad (7.4)$$

Where $T_{I, \max 90}$ is the maximum limit of acceptable operative temperature; T_o is the mean outdoor temperature (=23.5°C for Hong Kong) [207]; TS is the overall thermal sensation ($TS = \pm 0.5$ for 90% acceptability[214]); V_I is the acceptable indoor air velocity (m/s); w is the humidity ratio under 50% humidity (kg/kg). Here, the operative temperature is taken as equal to air temperature as a general practice [215], [216].

Based on the calculations by Equations (7.3) and (7.4), the maximum acceptable indoor temperature and the range of acceptable indoor air velocity for the use of natural ventilation are 28°C and 0.70m/s to 3.04m/s.

For estimating cooling energy use for the hybrid system, it is assumed that within the cooling period, priority is given to the use of natural ventilation. On failing to meet the design condition

by natural ventilation, the RAC is put in operation. Once the RAC is in operation, the system will not revert back to the use of natural ventilation until the next day. The control logic is shown in Figure 7.2.

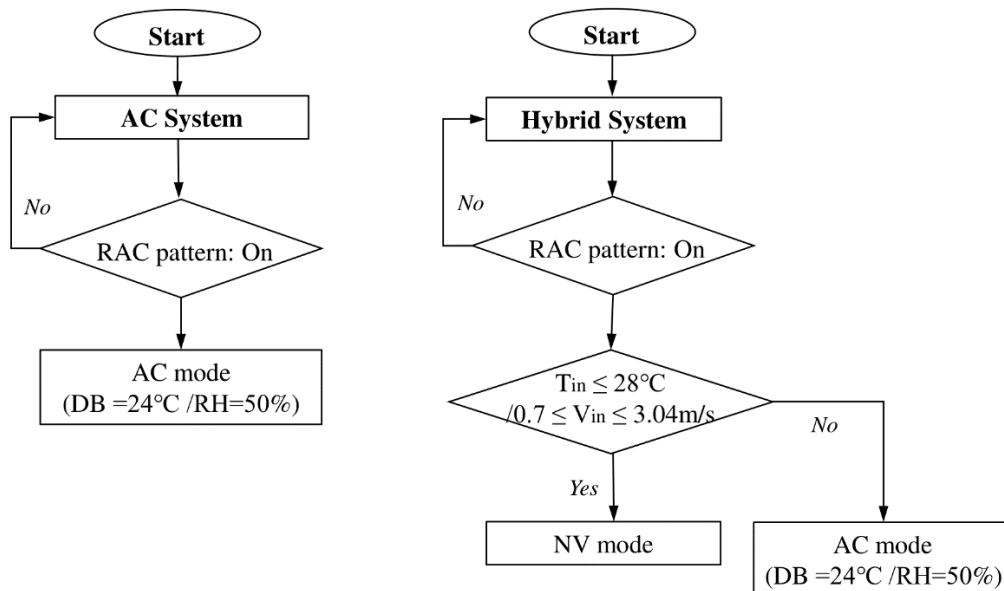


Figure 7.2 Control logic of the two systems

The indoor air temperature is predicted by EnergyPlus simulations and indoor air velocity is by CFD simulations. The RAC operation pattern is given in Table 7-3.

7.2.3 Operating parameters

In the simulations, operating parameters that characterised the buildings' space cooling load were obtained from various sources [206], [208], [209]. These include the lighting power density (W/m^2), small power density (W/m^2), and occupancy (no. of persons) and also their daily patterns (Table 7-3).

Table 7-3 Daily patterns of occupancy, lighting, small power and RAC

Parameter (Peak value)	Occupancy (4 Persons)	Lighting (14 W/m ²)	Small Power (7.33 W/m ²)	RAC	
Daily schedule (Hours)	0-6	0	0	0.19	Off
	6-7	0	0.3	0.37	Off
	7-8	0.25	0.5	0.54	Off
	8-12	0.5	0	0.54	Off
	12-13	0.45	0	0.54	Off
	13-14	0.5	0.5	0.63	On
	14-18	0.5	0	0.43	On
	18-19	0.5	0.5	0.43	On
	19-20	0.75	1	1	On
	20-22	1	1	1	Off
	22-24	0	0.5	1	Off

Note: Occupancy, lighting load and equipment operating patterns are in fractions of their respective peak values.

Outdoor air conditions refer to the hourly weather conditions in Hong Kong in 1995, which according to study, is the typical meteorological year (TMY) for Hong Kong [217]. Ventilation rates for the only AC system and the hybrid system with different TW designs were obtained from CFD simulations. As the ventilation rate is highly fluctuating, weighted average monthly ventilation rates are used in the simulations. Details are explained in Section 7.3.1.

7.3 Results and discussions

7.3.1 Ventilation rates

Based on CFD simulation results for cases with and without the use of TW and further ACH calculations (Equations (4.3) and (4.5)), ACHs that can be achieved in the living room of the studied unit on 30th floor of Block X for different cases under the nine representative wind datasets can be obtained. To convert the simulated ACHs into monthly ACHs, the hourly outdoor wind conditions of the TMY for Hong Kong was first disseminated into bins of the

nine representative wind datasets (Table 3-1) by months. Based on the relative frequency of occurrence (f) of a particular wind dataset, the weighted average monthly ACH (\overline{ACH}) for different TW designs can be calculated. The calculation of (f) and weighted average monthly ACH (\overline{ACH}) are mathematically shown in Equations (7.5) and (7.6).

$$f_c = \frac{O_c}{\sum_{c=1}^{36} O_c} \quad (7.5)$$

Where f_c is the relative frequency of occurrence of a particular wind condition by month; O_c is the frequency of occurrence of a particular wind condition c (from the pre-determined wind database); and 36 is the total number of wind data sets (4 orientations and 9 representative wind data sets).

Based on the monthly f , the monthly average ACH that can be achieved in the living room of the studied unit on F30 under the best and the worst design options can be determined by Equation (7.6).

$$\overline{ACH}_{(g,t)} = \sum_{c=1}^t ACH_{(g,c)} \cdot f_c \quad (7.6)$$

Where $\overline{ACH}_{(g,t)}$ is the weighted average ACH for a particular month (t) operating under different TW designs (g = the best, the worst TW and without TW).

The results for different TW designs are summarised in Table 7-4.

Table 7-4 Weighted average monthly \overline{ACH} (h) by different TW designs

TW Design	Jan	Feb	Mar	Apr	May	Jun	Jul	Aug	Sep	Oct	Nov	Dec	Average
Worst	17.0	21.8	20.8	25.5	20.3	22.0	23.7	22.0	26.4	19.2	19.5	17.9	21.3 (+117%)
Best	27.7	26.9	29.7	28.4	26.9	30.0	28.3	32.0	30.6	26.6	27.0	27.7	28.5 (+190%)
Without	4.6	10.6	8.8	13.3	3.2	13.6	12.2	10.9	19.9	8.2	5.9	6.8	9.8 (--)

7.3.2 Site verifications

For a comparison between the measured and simulated ACHs for cases with the worst TW designs and those without TW, normalisation of the simulated and measured ACHs is needed. As simulations have taken into account a range of external wind conditions (wind speed and wind direction), simulated results based on wind datasets that match well with site conditions were chosen for normalisation. The normalisation process is mathematically shown in Equations (7.7) and (7.8). It aims to identify an ideal ACH (ACH_{Ideal}) for both the simulated and measured ACHs so as to formulate an amplification factor (K) for adjustment of the measured results to account for the difference in operating characteristics.

$$\frac{U_{opening} \cdot A}{U_z \cdot A} \cdot \frac{3600}{V_{eff}} = \frac{ACH}{ACH_{Ideal}} \quad (7.7)$$

$$K = \frac{ACH_{M_Ideal}}{ACH_{S_Ideal}} \quad (7.8)$$

Where $U_{opening}$ is the wind speed through the window openings (m/s); U_z is the external wind speed at the same level as the window opening (m/s); A is the window opening area (m²); V_{eff} is the effective room volume (m³); ACH_{Ideal} is ideal air change per hour (/h); and ACH is the air change per hour in the room (/h).

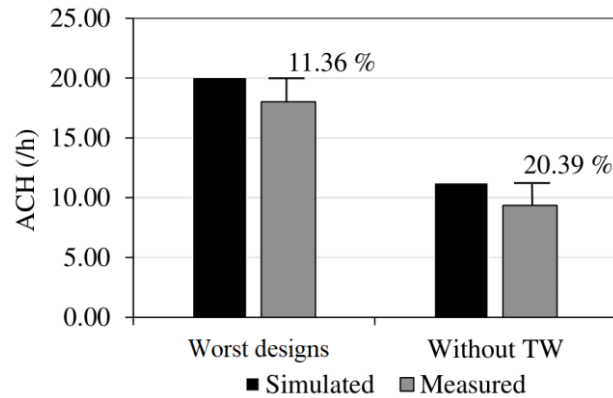


Figure 7.3 Comparison of the measured and simulated results

Based on Equations (7.7) and (7.8), K was found to be 1.11 to adjust the measured results. Figure 7.2 compares the measured and simulated ACHs for cases with the worst TW designs and those without TW. It can be seen that the difference is 11.36% and 20.39% respectively, which is within the generally acceptable value of 25% to confirm a successful site verification [218].

7.3.3 Cooling energy saving

Based on the ACHs in Table 7-4 for different TW designs, the occupancy patterns, installed power and daily patterns of lighting and small power, daily patterns of RAC, construction details of the studied living room, design conditions, and the RAC characteristics, energy simulations for the only AC system and the hybrid system were done (Table 7-5).

It can be seen in Table 7-5 that the cooling energy consumption of the hybrid system is on average 22.5% less than the only AC system. It can be seen that there is no significant difference between savings with TWs of different designs. The result matches with the previous

study saying that even intermittent opening of TW can enhance ventilation [44]. It is also reasonable to see that the cooling energy use of the hybrid system from May to October is slightly higher with the best TW design. This can be explained by the fact that with the best TW design to enhance ventilation in the hot and humid months, cooling energy use increases when switching from natural ventilation to air-conditioning [219].

Table 7-5 Cooling energy use by months

Description	AC system	Hybrid system		
		Best design	Worst design	
Monthly energy consumption (kWh)	Jan	5.6	0.0	0.0
	Feb	10.9	0.0	0.6
	Mar	66.7	24.9	29.0
	Apr	212.0	118.6	130.2
	May	367.9	293.5	293.1
	Jun	433.9	368.2	367.5
	Jul	470.4	405.9	403.0
	Aug	466.8	393.9	389.9
	Sep	416.3	345.5	343.6
	Oct	303.2	236.9	235.7
	Nov	159.6	80.6	87.5
	Dec	26.9	5.3	6.3
Annual energy consumption	2940.4 (---)	2273.3 (-22.7%)	2286.5 (-22.2%)	
Average energy saving (%)	---	-22.5%		

Given the CFD simulation inputs and the results are validated and verified, and the energy simulation results can be well-explained, it can be confirmed that the enhanced ventilation created by TW can achieve thermal comfort and reduce cooling energy use. With regard to the reduction in cooling energy use, given the studied unit D1 has the most unfavourable conditions including the smallest window to floor area ratio, the worst wind environment, and the largest internal heat gains for cooling, it is expected that much bigger savings could be derived in other units with more favourable conditions.

7.4 Summary

In order to investigate the effectiveness of TW in reducing cooling energy use and providing thermal comfort in high-rise residential buildings in Hong Kong, which is of significant interest to building designers in Hong Kong and also in other tropical countries, a rigorous study was conducted. The study adopted market survey, statistical analyses, site measurements, and an integration of CFD and EnergyPlus simulations to compare the cooling energy use of a simple AC system and a hybrid system for achieving the desired thermal comfort in a representative residential unit. The hybrid system makes use of the enhanced ventilation derived from the incorporation of TW of different designs supplemented with air-conditioning. Hour-by-hour air temperatures and velocities were examined to confirm thermal acceptability. It was found that depending on the TW's designs, the average improvement in ACH because of its incorporation ranged from 117 % to 190%, and the associated cooling energy saving, as compared to a simple AC system, ranged from 22.2% to 22.7%. The results confirm the effectiveness of TW in reducing cooling energy use and providing thermal comfort in high-rise residential buildings in Hong Kong. The results found in this study are well-explained which are expected to be useful for decision making by policy makers in search of performance improvement in natural ventilation and building energy use in Hong Kong and elsewhere in the tropics.

CHAPTER 8 CONCLUSIONS AND RECOMMENDATION FOR FUTURE RESEARCH

A review of the relevant literature showed that many researchers dedicated to window design investigations. However, there is virtually no study that has taken into account the interactive effects of the sash of windows, the ventilation modes, the window orientations, the users' window opening habits and the coincident wind conditions to enable designers or policymakers in search of performance improvement in natural ventilation and building energy use. In view of this, comprehensive investigations on window designs to enhance natural ventilation in residential buildings were proposed for this study.

The comprehensive investigations include the identification of the preferred window types, the determination of the most optimum window opening degree, the prediction of natural ventilation enhancement by the incorporation of transom window, and the evaluation of cooling energy saving by the incorporation of TW integrated with other apertures.

The conclusions drawn from this study and the recommendations for future research are detailed below.

8.1 Conclusions

8.1.1 Identification of the preferred windows types

The influence of window types on natural ventilation performance of residential units in Hong Kong, taking into account the interactive effects of the sash of windows, the ventilation modes, window orientations and coincident wind conditions, was investigated for a hypothetical residential unit. The investigation was based on site measurements, CFD simulations and statistical analyses.

The key findings are detailed as follows:

- 1) 9 representative coincident wind data sets were identified by the Central Composite Design method and the Squeeze Theorem.
- 2) A mathematical model for quantifying the interactive influences of different apertures designs on natural ventilation performance was developed by the response surface regression method whereby its adequacy and prediction accuracy were verified.
- 3) Ventilation performance (quantified by ACH) was found most sensitive to wind conditions (mainly wind speed) followed in descending order, by ventilation mode, window type and window orientation.
- 4) There would be a positive effect on ACH when window type is changed together with wind speed and or ventilation mode, or only the window orientation is changed.
- 5) Side hung (SH) window was most preferred, followed in descending order by top hung (TH) and sliding (SLD) windows.

8.1.2 Determination of the most optimum window opening degree

Walk-through surveys indicated that Hong Kong households have limited and inefficient use of natural ventilation. To encourage wider and more efficient use of natural ventilation, the

most optimum window opening degree for residential buildings in Hong Kong was investigated. The investigations involved site measurements, CFD simulations and statistical analyses.

The key findings are detailed as follows:

- 1) Residents in Hong Kong have limited and inefficient use of natural ventilation.
- 2) A mathematical model to enable quick estimation of ACH for different design variables was developed by regression analysis whereby the model's adequacy and prediction accuracy were verified.
- 3) ACH is very much influenced by the window opening degree.
- 4) The optimum window opening degree for three most commonly used window types (side-hung, top-hung and sliding) should be in the range of 0.6 to 0.9 to maximize the use of natural ventilation in residential buildings in Hong Kong.

8.1.3 Prediction of natural ventilation enhancement by the incorporation of transom window

Residential units in Hong Kong are typically limited to single-sided ventilation. To address poor ventilation associated with single-sided ventilation, the use of transom window (TW) was proposed. The effectiveness of TW, and the impact of different physical characteristics of TW on ventilation, particularly in the context of characteristics of high-rise residential buildings was investigated by controlled experiments, CFD simulations and ANN model analyses.

The key findings are detailed as follows:

- 1) The controlled-experiments indicated that the position of TW on the door and the aspect ratios of TW introduce very little influence on ventilation performance.
- 2) Natural ventilation performance was found most sensitive to the presence of TW, followed in descending order by the position of TW to the window, wind speed, area of TW, orientation of TW, and wind direction. The effective roles of TW in facilitating natural ventilation in high-rise residential buildings in Hong Kong TW was confirmed.
- 3) Natural ventilation rate can be improved by 153.5% on average with the incorporation of TW in residential buildings.

8.1.4 Evaluation of cooling energy saving by the incorporation of TW

TW has been demonstrated to be effective in enhancing natural ventilation in high-rise residential buildings in tropical climates such as Hong Kong. However, its effective roles in reducing cooling energy consumption and providing the desired thermal comfort are yet to be confirmed. For this purpose, cooling energy usage of a simple air-conditioning system was compared with that of a hybrid system (using enhanced ventilation created by TW supplemented with air-conditioning) for achieving the same thermal comfort in high-rise residential buildings in Hong Kong. Market survey, statistical analyses, site measurements, and integration of CFD and EnergyPlus simulations were adopted for the investigations.

The key findings are detailed as follows:

- 1) The hybrid system can be used in the high-rise residential buildings in Hong Kong to achieve the same thermal comfort as the only AC system.

- 3) Using of the hybrid system in the extreme hot months (May to October) would increase the cooling energy use and is not recommended.
- 3) Depending on the TW design, the average improvement of ACH for its incorporation ranges from 117%-190%, and the associated cooling energy saving ranges from 22.2% to 22.7% as compared with the only AC system.

8.2 Limitations of the study

The investigations were done based on 9 representative wind conditions and physical characteristics of a hypothetical unit and a representative residential unit including the floor level, the floor area, and the window dimensions, while the influence of surrounding buildings were considered by only the adjustment of air velocity profile. These factors will no doubt affect the local wind environment so as to introduce some restrictions on the use of the mathematical models developed, and some of the findings. However, considering that all window designs will receive a similar extent of influence by these factors, thus the conclusions drawn on the preferred window designs should not be affected. The results of this study therefore provide useful information for designers in selecting window types for residential buildings in Hong Kong.

The decay method [220] was used to determine the airflow rate in the site measurements. However, in further investigations using CFD simulations, given the large volume of simulation cases, the integration method was employed to reduce the time for solving the concentration equations. Despite the use of the two methods have been carefully considered in designing the methodology for this study, it is still worth to evaluate the uncertainty on the airflow rates calculation in the future.

Furthermore, as Hong Kong weather conditions were used in the investigations, the conclusions drawn may not be applicable to other countries or regions having significantly different local climate or living conditions like in Hong Kong.

8.3 Recommendations for Future Research

The present work can be further extended on the followings:

- 1) To include thermal comfort analysis in the study of preferred window types and optimum window opening degree.
- 2) To evaluate ventilation enhancement achieved by other types of transom window because only sliding type was investigated in this study.
- 3) To investigate the risks of the airflow inversion and pollutions dispersion across residential units on the same floor because transom window was assumed facing the corridor in this study.
- 4) To evaluate the uncertainty on the airflow rate calculations for the use of the tracer gas decay method and the integration method in site measurement and in CFD simulations respectively.

REFERENCE

- [1] HKEMSD, “Hong Kong Energy End-use Data 2019,” Electrical & Mechanical Services Department, Kowloon Bay, Hong Kong, 2019.
- [2] C. S. C. Cheung and M. A. Hart, “Climate change and thermal comfort in Hong Kong,” *Int. J. Biometeorol.*, vol. 58, no. 2, pp. 137–148, 2014.
- [3] W. Y. Fung, K. S. Lam, W. T. Hung, S. W. Pang, and Y. L. Lee, “Impact of urban temperature on energy consumption of Hong Kong,” *Energy*, vol. 31, no. 14, pp. 2287–2301, 2006.
- [4] E. Ng and V. Cheng, “Urban human thermal comfort in hot and humid Hong Kong,” *Energy Build.*, vol. 55, pp. 51–65, 2012.
- [5] X. Liu, J. Niu, M. Perino, and P. Heiselberg, “Numerical simulation of inter-flat air cross-contamination under the condition of single-sided natural ventilation,” *J. Build. Perform. Simul.*, vol. 1, no. 2, pp. 133–147, 2008.
- [6] Indoor Air Quality Management Group, “Guidance Notes for the Management of Indoor Air Quality in Offices and Public Places,” 2019. [Online]. Available: https://www.iaq.gov.hk/media/82253/gn_officeandpublicplace_eng-2019.pdf.
- [7] WBDG Cost-Effective Committee, “WBDG Whole Building Design Guide ®,” *National Institute of Building Sciences*, 2016. [Online]. Available: <https://www.wbdg.org/design-objectives/cost-effective>.
- [8] A. Aflaki, N. Mahyuddin, Z. Al-Cheikh Mahmoud, and M. R. Baharum, “A review on natural ventilation applications through building façade components and ventilation openings in tropical climates,” *Energy and Buildings*, vol. 101, pp. 153–162, 2015.
- [9] E. Ng, C. Yuan, L. Chen, C. Ren, and J. C. H. Fung, “Improving the wind environment in high-density cities by understanding urban morphology and surface roughness: A

- study in Hong Kong,” *Landsc. Urban Plan.*, vol. 101, no. 1, pp. 59–74, 2011.
- [10] A. J. Arnfield, “Two decades of urban climate research: a review of turbulence, exchanges of energy and water, and the urban heat island,” *Int. J. Climatol.*, vol. 23, no. 1, pp. 1–26, Jan. 2003.
- [11] E. Gratia, I. Bruyère, and A. De Herde, “How to use natural ventilation to cool narrow office buildings,” *Build. Environ.*, vol. 39, no. 10, pp. 1157–1170, Oct. 2004.
- [12] C. F. Gao and W. L. Lee, “Evaluating the influence of window types on the natural ventilation performance of residential buildings in Hong Kong,” *Int. J. Vent.*, vol. 10, no. 3, pp. 227–238, 2011.
- [13] K. Klemm and M. Jablonski, “Wind speed at pedestrian level in a residential building complex,” in *Plea2004 - The 21th Conference on Passive and Low Energy Architecture*, 2004, no. September, pp. 19–22.
- [14] L. J. Lo, “CFD Simulation of Cross-Ventilation Using Fluctuating Pressure Boundary Conditions,” in *ASHRAE Transactions*, 2011, vol. 117, no. Part 1, pp. 621–628.
- [15] P. Prajongsan and S. Sharples, “Enhancing natural ventilation, thermal comfort and energy savings in high-rise residential buildings in Bangkok through the use of ventilation shafts,” *Build. Environ.*, vol. 50, pp. 104–113, Apr. 2012.
- [16] H. Wang, P. Karava, and Q. Chen, “Development of simple semiempirical models for calculating airflow through hopper, awning, and casement windows for single-sided natural ventilation,” *Energy Build.*, vol. 96, pp. 373–384, Jun. 2015.
- [17] A.-S. Yang, C.-Y. Wen, Y.-C. Wu, Y.-H. Juan, and Y.-M. Su, “Wind Field Analysis for a High-rise Residential Building Layout in Danhai, Taiwan,” *Proc. World Congr. Eng.*, vol. II, pp. 843–848, 2013.
- [18] M. Bilgili, B. Sahin, and A. Yasar, “Application of artificial neural networks for the wind speed prediction of target station using reference stations data,” *Renew. Energy*,

- vol. 32, no. 14, pp. 2350–2360, 2007.
- [19] J. Fu, Q. Zheng, Y. Huang, J. Wu, Y. Pi, and Q. Liu, “Design optimization on high-rise buildings considering occupant comfort reliability and joint distribution of wind speed and direction,” *Eng. Struct.*, vol. 156, pp. 460–471, Feb. 2018.
- [20] J. Clifford Edward Clark, *The American Family Home, 1800-1960*. Chapel Hill: University of North Carolina Press, 1986, 1986.
- [21] Modernize, “Types of windows,” *Modernize, home empowerment*, 2014. [Online]. Available: <https://modernize.com/windows/types>. [Accessed: 25-Nov-2014].
- [22] W. Cheng, J. He, R. Shi, and Z. Chen, “The influence of the width of cantilever plate of bay window on energy consumption in the region of hot summer and cold winter,” in *Proceedings - 6th International Symposium on Heating, Ventilating and Air Conditioning, ISHVAC 2009*, 2009.
- [23] P. Heiselberg and M. Sandberg, “Evaluation of discharge coefficients for window openings in wind driven natural ventilation,” *Int. J. Vent.*, vol. 5, no. 1, pp. 43–52, 2006.
- [24] C. Yang, H. Shi, X. Yang, and B. Zhao, “Research on Flow Resistance Characteristics with Different Window / Door Opening Angles,” *HVAC&R Res.*, vol. 16, no. 6, pp. 813–824, 2011.
- [25] P. Heiselberg, K. Svidt, and P. V Nielsen, “Characteristics of air flow from open windows,” *Build. Environ.*, vol. 36, no. 7, pp. 859–869, 2001.
- [26] A. Roetzel, A. Tsangrassoulis, U. Dietrich, and S. Busching, “A review of occupant control on natural ventilation,” *Renew. Sustain. Energy Rev.*, vol. 14, no. 3, pp. 1001–1013, 2010.
- [27] C. F. Gao and W. L. Lee, “Evaluating the influence of openings configuration on natural ventilation performance of residential units in Hong Kong,” *Build. Environ.*, vol. 46, no. 4, pp. 961–969, 2010.

- [28] C. F. Gao and W. L. Lee, "The influence of surrounding buildings on the natural ventilation performance of residential dwellings in hong kong," *Int. J. Vent.*, vol. 11, no. 3, pp. 297–310, 2012.
- [29] D. M. Gaspar, A. G. Amador, and C. E. del Pozo, "Analysis of three types of window their use for subhumid warm climate," in *PLEA architecture in (R)evolution/bologna 2015*, 2015, no. September.
- [30] E. L. Hult, G. Iaccarino, and M. Fischer, "Using CFD Simulations To Improve Themodeling Of window Discharge Coefficients," in *Proceedings of SimBuild*, 2012, vol. 5, no. 1, pp. 322–328.
- [31] P. Heiselberg, E. Bjørn, and P. V. Nielsen, "Impact of Open Windows on Room Air Flow and Thermal Comfort," *Int. J. Vent.*, vol. 1, no. 2, pp. 91–100, 2002.
- [32] M. Schweiker, F. Haldi, M. Shukuya, and D. Robinson, "Verification of stochastic models of window opening behaviour for residential buildings," *J. Build. Perform. Simul.*, vol. 5, no. 1, pp. 55–74, 2012.
- [33] R. Fritsch, A. Kohler, M. Nygård-Ferguson, and J.-L. Scartezzini, "A stochastic model of user behaviour regarding ventilation," *Build. Environ.*, vol. 25, no. 2, pp. 173–181, Jan. 1990.
- [34] S. Herkel, U. Knapp, and J. Pfafferott, "Towards a model of user behaviour regarding the manual control of windows in office buildings," *Build. Environ.*, vol. 43, no. 4, pp. 588–600, 2008.
- [35] C. Allocca, Q. Chen, and L. R. Glicksman, "Design analysis of single-sided natural ventilation," *Energy Build.*, vol. 35, no. 8, pp. 785–795, 2003.
- [36] P. Karava, T. Stathopoulos, and A. K. Athienitis, "Airflow assessment in cross-ventilated buildings with operable façade elements," *Build. Environ.*, vol. 46, no. 1, pp. 266–279, Jan. 2011.

- [37] Y. Jiang, D. Alexander, H. Jenkins, R. Arthur, and Q. Chen, "Natural ventilation in buildings: Measurement in a wind tunnel and numerical simulation with large-eddy simulation," *J. Wind Eng. Ind. Aerodyn.*, vol. 91, no. 3, pp. 331–353, 2003.
- [38] J. Cho, C. Yoo, and Y. Kim, "Effective Opening Area and Installation Location of Windows for Single Sided Natural Ventilation in High-rise Residences," *J. Asian Archit. Build. Eng.*, vol. 11, no. 2, pp. 391–398, Nov. 2012.
- [39] Z. T. Ai and C. M. Mak, "Determination of single-sided ventilation rates in multistory buildings: Evaluation of methods," *Energy Build.*, vol. 69, pp. 292–300, 2014.
- [40] S. Shi, Z. Gou, and L. H. C. Chen, "How does enclosure influence environmental preferences? A cognitive study on urban public open spaces in Hong Kong," *Sustain. Cities Soc.*, 2014.
- [41] P. A. Favarolo and H. Manz, "Temperature-driven single-sided ventilation through a large rectangular opening," *Build. Environ.*, 2005.
- [42] G. Taylor and B. Vlila, "All You Need to Know About Transom Windows," in *BobVila.com*, 2020.
- [43] D. Snow, "What is a Transom Window?," in *glass.com*, 2018, pp. 1–5.
- [44] C. Howard-Reed, L. A. Wallace, and W. R. Ott, "The effect of opening windows on air change rates in two homes," *J. Air Waste Manag. Assoc.*, vol. 52, no. 2, pp. 147–159, 2002.
- [45] C. M. Chiang, C. M. Lai, P. C. Chou, and Y. Y. Li, "The influence of an architectural design alternative (transoms) on indoor air environment in conventional kitchens in Taiwan," *Build. Environ.*, vol. 35, no. 7, pp. 579–585, 2000.
- [46] N.-T. Chao, W.-A. Wang, and C.-M. Chiang, "A study of a control strategy utilizing outdoor air to reduce the wintertime carbon dioxide levels in a typical Taiwanese bedroom," *Energy Build.*, vol. 29, no. 1, pp. 93–105, 1998.

- [47] A. A. Jamaludin, H. Hussein, A. R. Mohd Ariffin, and N. Keumala, "A study on different natural ventilation approaches at a residential college building with the internal courtyard arrangement," *Energy Build.*, vol. 72, pp. 340–352, 2014.
- [48] K. Ackerly, L. Baker, and P. G. Brager, "Window Use in Mixed-Mode Buildings: A Literature Review," *Cent. Built Environ.*, pp. 1–21, 2011.
- [49] A. Aflaki, K. Hirbodi, N. Mahyuddin, M. Yaghoubi, and M. Esfandiari, "Improving the air change rate in high-rise buildings through a transom ventilation panel: A case study," *Build. Environ.*, vol. 147, pp. 35–49, Jan. 2019.
- [50] N. T. Chen, Y. Y. Li, P. C. Chour, and C. M. Chiang, "The influence on ventilation efficiency in typical dwelling with floor-based displacement ventilation," in *Healthy Building 2003: The 7th International Conference on Healthy Buildings*, 2003, vol. 2, pp. 416–421.
- [51] M. Haase and A. Amato, "An investigation of the potential for natural ventilation and building orientation to achieve thermal comfort in warm and humid climates," *Sol. Energy*, vol. 83, no. 3, pp. 389–399, 2009.
- [52] A. Walker, "WBDG: Whole Building Design Guide," *Natl. Inst. Build. Sci.*, 2016.
- [53] P. Huang, X. Wang, and M. Gu, "Field experiments for wind loads on a low-rise building with adjustable pitch," *Int. J. Distrib. Sens. Networks*, 2012.
- [54] T. Peizhe, L. Liang, Z. Ligu, and Z. Boyuan, "Field Measurement & Research on Natural Ventilation Performance of the New East-main Building of China Academy of Building Research (CABR)," in *Procedia Engineering*, 2016.
- [55] M. Caciolo, P. Stabat, and D. Marchio, "Full scale experimental study of single-sided ventilation: Analysis of stack and wind effects," *Energy Build.*, vol. 43, no. 7, pp. 1765–1773, 2011.
- [56] D. Laussmann and D. Helm, "Air Change Measurements Using Tracer Gases," *Chem.*

- Emiss. Control. Radioact. Pollut. Indoor Air Qual.*, pp. 365–404, 2004.
- [57] P. O’Connell *et al.*, “SF6 in the Electric Industry , Status 2000,” *Cigre*, no. May, pp. 1–7, 2001.
- [58] D. Laussmann and D. Helm, “Air Change Measurements Using Tracer Gases: Methods and Results. Significance of Air Change for Indoor Air Quality,” *InTechOpen, Rijeka, Croatia*, 2011. [Online]. Available: <http://www.intechopen.com/books/chemistry-emission-control-radioactive-pollution-and-indoor-air-quality/air-change-measurements-using-tracer-gases-methods-and-results-significance-of-air-change-for-indoor>.
- [59] Fluent, “ANSYS FLUENT 13.0 User’s Guide,” *Ansys Inc*, 2011.
- [60] Y. Jiang and Q. Chen, “Effect of fluctuating wind direction on cross natural ventilation in buildings from large eddy simulation,” *Build. Environ.*, vol. 37, no. 4, pp. 379–386, 2002.
- [61] a. Terziev, I. Antonov, and R. Velichkova, “Wind Data Analysis and Wind Flow Simulation Over Large Areas,” *Math. Model. Civ. Eng.*, vol. 10, no. 1, pp. 1–8, 2014.
- [62] B. E. Launder and D. B. Spalding, “The numerical computation of turbulent flows,” *Numer. Predict. flow, heat Transf. Turbul. Combust.*, pp. 96–116, 1983.
- [63] Q. Chen, “Comparison of different k- ϵ models for indoor air flow computations,” *Numer. Heat Transf. Part B Fundam.*, vol. 28, no. 3, pp. 353–369, 1995.
- [64] A. Belleri, R. Lollini, and S. M. Dutton, “Natural ventilation design: An analysis of predicted and measured performance,” *Build. Environ.*, vol. 81, pp. 123–138, 2014.
- [65] M. Habibi, F. Aligolzadeh, and A. Hakkaki-Fard, “A techno-economic analysis of geothermal ejector cooling system,” *Energy*, vol. 193, p. 116760, Feb. 2020.
- [66] A. Ahmed and P. Mancarella, “Strategic techno-economic assessment of heat network options for distributed energy systems in the UK,” *Energy*, 2014.

- [67] D. Mazzeo, N. Matera, C. Cornaro, G. Oliveti, P. Romagnoni, and L. De Santoli, “EnergyPlus, IDA ICE and TRNSYS predictive simulation accuracy for building thermal behaviour evaluation by using an experimental campaign in solar test boxes with and without a PCM module,” *Energy Build.*, vol. 212, p. 109812, Apr. 2020.
- [68] Z. Dong, P. Zhu, M. Bobker, and M. Ascazubi, “Simplified characterization of building thermal response rates,” in *6th International Building Physics Conference, IBPC 2015, Energy Procedia*, 2015, vol. 78, pp. 788–793.
- [69] S. Dilmac and N. Kesen, “A comparison of new Turkish thermal insulation standard (TS 825), ISO 9164, EN 832 and German regulation,” *Energy Build.*, vol. 35, no. 2, pp. 161–174, 2003.
- [70] K. A. A. Chandra S, “Heat transfer in naturally ventilated rooms data from full-scale measurements,” *ASHRAE Trans*, vol. 90, p. CONF-840124, 1984.
- [71] G. Carrilho da Graça, Q. Chen, L. R. Glicksman, and L. K. Norford, “Simulation of wind-driven ventilative cooling systems for an apartment building in Beijing and Shanghai,” *Energy Build.*, vol. 34, no. 1, pp. 1–11, 2002.
- [72] Z. T. Ai and C. M. Mak, “Modeling of coupled urban wind flow and indoor air flow on a high-density near-wall mesh: Sensitivity analyses and case study for single-sided ventilation,” *Environ. Model. Softw.*, vol. 60, pp. 57–68, 2014.
- [73] X. Shen, G. Zhang, and B. Bjerg, “Investigation of response surface methodology for modelling ventilation rate of a naturally ventilated building,” *Build. Environ.*, vol. 54, pp. 174–185, Aug. 2012.
- [74] A. I. Khuri, S. Mukhopadhyay, I. Khuri, S. Mukhopadhyay, A. I. Khuri, and S. Mukhopadhyay, “Response surface methodology,” *Response Surf. Methodol.*, vol. 2, no. 2, pp. 1–15, 1996.
- [75] S. L. C. Ferreira, W. N. L. Santos, C. M. Quintella, B. B. Neto, and J. M. Bosque-Sendra,

- “Doehlert matrix : A chemometric tool for analytical chemistry - Review Doehlert matrix : a chemometric tool for analytical chemistry — review,” *Talanta*, vol. 63, no. August, pp. 1061–1067, 2004.
- [76] B. Das and V. Chandra, “Fiber-MZI-based FBG sensor interrogation: comparative study with a CCD spectrometer,” *Appl. Opt.*, vol. 55, no. 29, p. 8287, 2016.
- [77] K. K. Pradhan and S. Chakraverty, “Generalized power-law exponent based shear deformation theory for free vibration of functionally graded beams,” *Appl. Math. Comput.*, vol. 268, pp. 1240–1258, 2015.
- [78] S. Rehman, “Wind energy resources assessment for Yanbo, Saudi Arabia,” *Energy Convers. Manag.*, vol. 45, no. 13–14, pp. 2019–2032, 2004.
- [79] V. Sinha, V. Kumar, and C. Sarkar, “Chemical composition of pre-monsoon air in the Indo-Gangetic Plain measured using a new air quality facility and PTR-MS: High surface ozone and strong influence of biomass burning,” *Atmos. Chem. Phys.*, vol. 14, no. 12, pp. 5921–5941, 2014.
- [80] R. Belu and D. Koracin, “Statistical and Spectral Analysis of Wind Characteristics Relevant to Wind Energy Assessment Using Tower Measurements in Complex Terrain,” *J. Wind Energy*, vol. 2013, pp. 1–12, 2013.
- [81] D. J. Dwyer, *Asian Urbanization A Hong Kong Casebook (Vol.1)*. Hong Kong: Hong Kong University Press, 1971.
- [82] Census and Statistics Department, “Population and Household Statistics Analysed by District Council District,” 2018. .
- [83] US Census Bureau world population estimate, “World Population Review 2019,” *World Population Review*, 2019. [Online]. Available: <http://worldpopulationreview.com/countries/hong-kong-population/>. [Accessed: 20-Sep-2006].

- [84] Census and Statistics Department, “Population and Household Statistics Analysed by District Council District,” 1997. [Online]. Available: https://www.statistics.gov.hk/pub/hist/1991_2000/B11303011997AN97B0100.pdf.
- [85] Census and Statistics Department, “Population and Household Statistics Analysed by District Council District,” 2017. [Online]. Available: <https://www.statistics.gov.hk/pub/B11303012017AN17B0100.pdf>.
- [86] R. Y. C. Tse, “Impact of comprehensive development zoning on real estate development in Hong Kong,” *Land use policy*, vol. 18, no. 4, pp. 321–328, 2001.
- [87] Z. P. Wen, Y. X. Hu, and K. T. Chau, “Site effect on vulnerability of high-rise shear wall buildings under near and far field earthquakes,” *Soil Dyn. Earthq. Eng.*, vol. 22, no. 9–12, pp. 1175–1182, 2002.
- [88] D. W. M. Chan and A. P. C. Chan, “Public housing construction in hong kong: A review of its design and construction innovations,” *Archit. Sci. Rev.*, vol. 45, no. 4, pp. 349–359, 2002.
- [89] K. S. Y. Wan and F. H. W. Yik, “Representative building design and internal load patterns for modelling energy use in residential buildings in Hong Kong,” *Appl. Energy*, vol. 77, no. 1, pp. 69–85, 2004.
- [90] T. Q. Thach *et al.*, “Assessing spatial associations between thermal stress and mortality in Hong Kong: A small-area ecological study,” *Sci. Total Environ.*, vol. 502, pp. 666–672, 2015.
- [91] American Society for Testing and Materials International, “ASTM E741 Standard Test Method for Determining Air Change in a Single Zone by Means of a Tracer Gas Dilution,” *ASTM Int. Stand.*, pp. 1–18, 2017.
- [92] A. Tam, D. Ait-Ali-Yahia, M. P. Robichaud, M. Moore, V. Kozel, and W. G. Habashi, “Anisotropic mesh adaptation for 3D flows on structured and unstructured grids,”

- Comput. Methods Appl. Mech. Eng.*, vol. 189, no. 4, pp. 1205–1230, 2000.
- [93] M. Tomac and D. Eller, “From geometry to CFD grids - An automated approach for conceptual design,” *Prog. Aerosp. Sci.*, vol. 47, no. 8, pp. 589–596, 2011.
- [94] C. L. Archer, “Evaluation of global wind power,” *J. Geophys. Res.*, vol. 110, no. September 2004, pp. 1–20, 2005.
- [95] X. P. Liu, J. L. Niu, K. C. S. Kwok, J. H. Wang, and B. Z. Li, “Investigation of indoor air pollutant dispersion and cross-contamination around a typical high-rise residential building: Wind tunnel tests,” *Build. Environ.*, vol. 45, no. 8, pp. 1769–1778, 2010.
- [96] J. Wang, S. Wang, T. Zhang, and F. Battaglia, “Assessment of single-sided natural ventilation driven by buoyancy forces through variable window configurations,” *Energy Build.*, vol. 139, pp. 762–779, Mar. 2017.
- [97] F. Haghghat, J. Rao, and P. Fazio, “The influence of turbulent wind on air change rates- a modelling approach,” *Build. Environ.*, 1991.
- [98] S. H. Hosseini, E. Shokry, A. J. Ahmadian Hosseini, G. Ahmadi, and J. K. Calautit, “Evaluation of airflow and thermal comfort in buildings ventilated with wind catchers: Simulation of conditions in Yazd City, Iran,” *Energy Sustain. Dev.*, vol. 35, pp. 7–24, 2016.
- [99] Fluent, “ANSYS Fluent User’s guide,” *Ansys Inc*, vol. 15317, no. November, pp. 1–2498, 2009.
- [100] M. Lutz, *Programming python*. United States of America, 2001.
- [101] G. Gan, “Interaction Between Wind and Buoyancy Effects in Natural Ventilation of Buildings,” *Open Constr. Build. Technol. J.*, vol. 4, no. 1, pp. 134–145, 2010.
- [102] L. Moosavi, N. Mahyuddin, N. Ab Ghafar, and M. Azzam Ismail, “Thermal performance of atria: An overview of natural ventilation effective designs,” *Renewable and Sustainable Energy Reviews*. 2014.

- [103] M. A. Bezerra, R. E. Santelli, E. P. Oliveira, L. S. Villar, and L. A. Escaleira, "Response surface methodology (RSM) as a tool for optimization in analytical chemistry," *Talanta*, vol. 76, no. 5, pp. 965–977, 2008.
- [104] D. C. Montgomery, *Design and Analysis of Experiments*, vol. 2. 2012.
- [105] R. Myers, A. Khuri, and W. Carter Jr, "Response Surface Methodology: 1966-1988," *TECHNOMETRICS*, 1989.
- [106] L. C. Haw, O. Saadatian, A. H. Baharuddin, S. Mat, M. Y. Sulaiman, and K. Sopian, "Case study of wind-induced natural ventilation tower in hot and humid climatic conditions," *BEIAC 2012 - 2012 IEEE Business, Eng. Ind. Appl. Colloq.*, vol. 52, pp. 178–183, 2012.
- [107] D. R. Legates and G. J. McCabe, "Evaluating the use of 'goodness-of-fit' measures in hydrologic and hydroclimatic model validation," *Water Resour. Res.*, vol. 35, no. 1, pp. 233–241, 1999.
- [108] Stat-Ease Inc., "Multifactor RSM Tutorial," *Des. 10 User's Guid.*, no. Ccd, pp. 1–56, 2016.
- [109] j. M. Bland and D. G. Altman, "Multiple significance tests: The Bonferroni method," *BMJ*, vol. 310, no. 6973, p. 170, 1995.
- [110] E. W. Steyerberg and F. E. Harrell, "Prediction models need appropriate internal, internal-external, and external validation," *J. Clin. Epidemiol.*, vol. 69, pp. 245–247, 2016.
- [111] M. B. Araújo, R. G. Pearson, W. Thuiller, and M. Erhard, "Validation of species-climate impact models under climate change," *Glob. Chang. Biol.*, vol. 11, no. 9, pp. 1504–1513, 2005.
- [112] C.-R. Chu and Y.-W. Wang, "The loss factors of building openings for wind-driven ventilation," *Build. Environ.*, vol. 45, no. 10, pp. 2273–2279, Oct. 2010.

- [113] C. H. J. Wu, “The impact of customer-to-customer interaction and customer homogeneity on customer satisfaction in tourism service-The service encounter prospective,” *Tour. Manag.*, vol. 28, no. 6, pp. 1518–1528, 2007.
- [114] M. Fernando and R. M. M. I. Chowdhury, “The relationship between spiritual well-being and ethical orientations in decision making: An empirical study with business executives in Australia,” *J. Bus. Ethics*, vol. 95, no. 2, pp. 211–225, 2010.
- [115] R. A. Johnson and T. E. Wehrly, “Some angular-linear distributions and related regression models,” *J. Am. Stat. Assoc.*, 1978.
- [116] M. Denbina and M. J. Collins, “Wind speed estimation using C-band compact polarimetric SAR for wide swath imaging modes,” *ISPRS J. Photogramm. Remote Sens.*, 2016.
- [117] J. A. Carta, P. Ramírez, and C. Bueno, “A joint probability density function of wind speed and direction for wind energy analysis,” *Energy Convers. Manag.*, 2008.
- [118] C. R. Chu, Y. H. Chiu, Y. T. Tsai, and S. L. Wu, “Wind-driven natural ventilation for buildings with two openings on the same external wall,” *Energy Build.*, vol. 108, pp. 365–372, 2015.
- [119] Z. Bu and S. Kato, “Wind-induced ventilation performances and airflow characteristics in an areaway-attached basement with a single-sided opening,” *Build. Environ.*, vol. 46, no. 4, pp. 911–921, Apr. 2011.
- [120] A. Iqbal, A. Afshari, and P. Heiselberg, “The Discharge Coefficient of a Centre- Pivot Roof Window,” *Build. Environ.*, vol. 92, pp. 2–7.
- [121] S. Edition, *RSM simplified Optimizing Process Using Response Surface Mrethods for design of experiment.* .
- [122] L. Vera Candiotti, M. M. De Zan, M. S. Cámara, and H. C. Goicoechea, “Experimental design and multiple response optimization. Using the desirability function in analytical

- methods development,” *Talanta*, vol. 124, pp. 123–138, 2014.
- [123] J. O. P. Cheung and C.-H. Liu, “CFD simulations of natural ventilation behaviour in high-rise buildings in regular and staggered arrangements at various spacings,” *Energy Build.*, vol. 43, no. 5, pp. 1149–1158, May 2011.
- [124] N. P. Gao, J. L. Niu, M. Perino, and P. Heiselberg, “The airborne transmission of infection between flats in high-rise residential buildings: Tracer gas simulation,” *Build. Environ.*, vol. 43, no. 11, pp. 1805–1817, 2008.
- [125] C. A. Glasbey and K. V. Mardia, “A review of image-warping methods,” *J. Appl. Stat.*, vol. 25, no. 2, pp. 155–171, 1998.
- [126] H. Hu, W. Xu, and Q. Huang, “A 2D barcode extraction method based on texture direction analysis,” in *Proceedings of the 5th International Conference on Image and Graphics, ICIG 2009*, 2010.
- [127] E. Murphy-Chutorian and M. M. Trivedi, “Head pose estimation in computer vision: A survey,” *IEEE Trans. Pattern Anal. Mach. Intell.*, vol. 31, no. 4, pp. 607–626, 2009.
- [128] E. Guillou, D. Meneveaux, E. Maisel, and K. Bouatouch, “Using vanishing points for camera calibration and coarse 3D reconstruction from a single image,” *Vis. Comput.*, vol. 16, no. 7, pp. 396–410, 2000.
- [129] L. Li and C. L. Tan, “Recognizing planar symbols with severe perspective deformation,” *IEEE Trans. Pattern Anal. Mach. Intell.*, vol. 32, no. 4, pp. 755–762, 2009.
- [130] J. A. Shufelt, “Performance evaluation and analysis of vanishing point detection techniques,” *IEEE Trans. Pattern Anal. Mach. Intell.*, vol. 21, no. 3, pp. 282–288, 1999.
- [131] T. L. Ooi, B. Wu, and Z. J. He, “Distance determined by the angular declination below the horizon,” *Nature*, vol. 414, no. 6860, p. 197, 2001.
- [132] T. Liu and W. L. Lee, “Using response surface regression method to evaluate the influence of window types on ventilation performance of Hong Kong residential

- buildings,” *Build. Environ.*, vol. 154, no. February, pp. 167–181, 2019.
- [133] S. Landau and H. Crc, *A Handbook of Statistical Analyses using SPSS*, 1st ed. Surrey, United Kingdom, 2004.
- [134] C.-Y. J. Peng and T.-S. H. So, “Modeling strategies in logistic regression with SAS, SPSS, Systat, BMDP, Minitab, and STATA,” *J. Mod. Appl. Stat. Methods*, vol. 1, no. 1, pp. 147–156, 2002.
- [135] M. N. Bagum, M. Konneh, and M. Y. Ali, “Establishing Relationship between Process Parameters and Temperature during High Speed End Milling of Soda Lime Glass,” in *IOP Conference Series: Materials Science and Engineering*, 2018.
- [136] E. W. Steyerberg, S. E. Bleeker, H. A. Moll, D. E. Grobbee, and K. G. M. Moons, “Internal and external validation of predictive models: A simulation study of bias and precision in small samples,” *J. Clin. Epidemiol.*, vol. 56, no. 5, pp. 441–447, 2003.
- [137] T. M. L. Wigley, P. D. Jones, K. R. Briffa, and G. Smith, “Obtaining sub-grid-scale information from coarse-resolution general circulation model output,” *J. Geophys. Res. Atmos.*, vol. 95, no. D2, pp. 1943–1953, 1990.
- [138] M. Ohba, T. Kurabuchi, E. Tomoyuki, Y. Akamine, M. Kamata, and A. Kurahashi, “Local Dynamic Similarity Model of Cross-Ventilation Part 2 - Application of Local Dynamic Similarity Model,” *Int. J. Vent.*, vol. 2, no. 4, pp. 383–394, 2004.
- [139] N. K. Mylaram and S. Idem, “Pressure loss coefficient measurements of two close-coupled HVAC elbows,” *HVAC&R Res.*, vol. 11, no. 1, pp. 133–146, 2005.
- [140] A. Iqbal, A. Afshari, H. Wigö, and P. Heiselberg, “Discharge coefficient of centre-pivot roof windows,” *Build. Environ.*, vol. 92, pp. 635–643, 2015.
- [141] H. Cruz and J. C. Viegas, “On-site assessment of the discharge coefficient of open windows,” *Energy Build.*, vol. 126, pp. 463–476, 2016.
- [142] B. M. Jones, M. J. Cook, S. D. Fitzgerald, and C. R. Iddon, “A review of ventilation

- opening area terminology,” *Energy Build.*, vol. 118, pp. 249–258, 2016.
- [143] P. Karava, T. Stathopoulos, and A. K. Athienitis, “Wind Driven Flow through Openings – A Review of Discharge Coefficients,” *Int. J. Vent.*, vol. 3, no. 3, pp. 255–266, 2004.
- [144] Building Authority Hong Kong, “Code of Practice for Fire Safety in Buildings,” in *Buildings Department*, 2011.
- [145] Business Information Technology Unit, “Building Information Modelling (BIM) Library Components Reference for Development and Construction Division of Hong Kong Housing Authority,” in *Development & Construction Division Housing Department*, 2010, pp. 1–82.
- [146] E-Legislation Hong Kong, “Building (Planning) Regulations,” in *Housing Standards of Domestic Buildings in Hong Kong*, 2012, p. Cap. 123, section 38.
- [147] T. Liu and W. L. Lee, “Influence of window opening degree on natural ventilation performance of residential buildings in Hong Kong,” *Sci. Technol. Built Environ.*, vol. 512, no. 1–2, pp. 1–14, Oct. 2019.
- [148] Z. Tan and X. Deng, “An optimised window control strategy for naturally ventilated residential buildings in warm climates,” *Sustain. Cities Soc.*, vol. 57, p. 102118, Jun. 2020.
- [149] J. Seifert, Y. Li, J. Axley, and M. Rösler, “Calculation of wind-driven cross ventilation in buildings with large openings,” *J. Wind Eng. Ind. Aerodyn.*, vol. 94, no. 12, pp. 925–947, 2006.
- [150] Transport and Housing Bureau, “Housing in Fiugres 2018,” 2018, p. 9.
- [151] J. Jia and W. L. Lee, “Applying storage-enhanced heat recovery room air-conditioner (SEHRAC) for domestic water heating in residential buildings in Hong Kong,” *Energy Build.*, vol. 78, pp. 132–142, 2014.
- [152] P. J. Jones, D. Alexander, and J. Burnett, “Pedestrian wind environment around high-

- rise residential buildings in Hong Kong,” *Indoor Built Environ.*, vol. 13, no. 4, pp. 259–269, 2004.
- [153] Y. Yeun and J. Wang, *Fifty years of public housing in Hong Kong: A golden jubilee review and appraisal*, 1st ed. The Chinese University Press for the Hong Kong, Housing Authority, 2003.
- [154] J. Franke, A. Hellsten, K. H. Schlunzen, and B. Carissimo, “The COST 732 Best Practice Guideline for CFD simulation of flows in the urban environment: a summary,” *Int. J. Environ. Pollut.*, vol. 44, no. 1/2/3/4, p. 419, 2011.
- [155] J. Hang, Y. Li, M. Sandberg, R. Buccolieri, and S. Di Sabatino, “The influence of building height variability on pollutant dispersion and pedestrian ventilation in idealized high-rise urban areas,” *Build. Environ.*, vol. 56, pp. 346–360, 2012.
- [156] Hong Kong Housing Authority, “Standard Block Typical Floor Plans,” in *The Hong Kong Housing Authority*, 2019.
- [157] J. Hang, Y. Li, and M. Sandberg, “Experimental and numerical studies of flows through and within high-rise building arrays and their link to ventilation strategy,” *J. Wind Eng. Ind. Aerodyn.*, vol. 99, no. 10, pp. 1036–1055, 2011.
- [158] J. Liu and J. Niu, “CFD simulation of the wind environment around an isolated high-rise building: An evaluation of SRANS, LES and DES models,” *Build. Environ.*, vol. 96, pp. 91–106, 2016.
- [159] J. Liu, M. Heidarinejad, G. Pitchurov, L. Zhang, and J. Srebric, “An extensive comparison of modified zero-equation, standard k- ϵ , and LES models in predicting urban airflow,” *Sustain. Cities Soc.*, 2018.
- [160] R. M. Susin, G. A. Lindner, V. C. Mariani, and K. C. Mendonça, “Evaluating the influence of the width of inlet slot on the prediction of indoor airflow: Comparison with experimental data,” *Build. Environ.*, vol. 44, no. 5, pp. 971–986, May 2009.

- [161] S. Hussain and P. H. Oosthuizen, "Validation of numerical modeling of conditions in an atrium space with a hybrid ventilation system," *Build. Environ.*, 2012.
- [162] S. Kato, R. Kono, T. Hasama, R. Ooka, and T. Takahashi, "A wind tunnel experimental analysis of the ventilation characteristics of a room with single-sided opening in uniform flow," *Int. J. Vent.*, vol. 5, no. 1, pp. 171–178, 2006.
- [163] F. W. H. Yik and Y. F. Lun, "Energy saving by utilizing natural ventilation in public housing in Hong Kong," *Indoor Built Environ.*, vol. 19, no. 1, pp. 73–87, 2010.
- [164] R. Müller and P. Büttner, "A critical discussion of intraclass correlation coefficients," *Stat. Med.*, vol. 13, no. 23–24, pp. 2465–2476, Dec. 1994.
- [165] P. Filzmoser, K. Hron, and C. Reimann, "The bivariate statistical analysis of environmental (compositional) data," *Sci. Total Environ.*, vol. 408, no. 19, pp. 4230–4238, 2010.
- [166] K. J. BERRY, "A Monte Carlo Investigation of The Fisher Z Transformation for Normal and Nonnormal Distributions," *Psychol. Rep.*, vol. 87, no. 7, p. 1101, 2000.
- [167] N. C. Silver and W. P. Dunlap, "Averaging Correlation Coefficients: Should Fisher's z Transformation Be Used?," *J. Appl. Psychol.*, vol. 72, no. 1, p. 146, 1987.
- [168] S. Kalogirou, M. Eftekhari, and L. Marjanovic, "Predicting the pressure coefficients in a naturally ventilated test room using artificial neural networks," *Build. Environ.*, vol. 38, no. 3, pp. 399–407, 2003.
- [169] H. Wang and Q. Chen, "A new empirical model for predicting single-sided, wind-driven natural ventilation in buildings," *Energy Build.*, vol. 54, pp. 386–394, 2012.
- [170] E. Ng, L. Chen, Y. Wang, and C. Yuan, "A study on the cooling effects of greening in a high-density city: An experience from Hong Kong," *Build. Environ.*, vol. 47, pp. 256–271, 2012.
- [171] C. Ren and S. J. Cao, "Development and application of linear ventilation and

- temperature models for indoor environmental prediction and HVAC systems control,” *Sustain. Cities Soc.*, 2019.
- [172] T. Ayata, E. Arcaklioğlu, and O. Yildiz, “Application of ANN to explore the potential use of natural ventilation in buildings in Turkey,” *Appl. Therm. Eng.*, vol. 27, no. 1, pp. 12–20, 2007.
- [173] C. Ren and S. J. Cao, “Implementation and visualization of artificial intelligent ventilation control system using fast prediction models and limited monitoring data,” *Sustain. Cities Soc.*, 2020.
- [174] Z. Ye and M. K. Kim, “Predicting electricity consumption in a building using an optimized back-propagation and Levenberg–Marquardt back-propagation neural network: Case study of a shopping mall in China,” *Sustain. Cities Soc.*, 2018.
- [175] J. Li, J. H. Cheng, J. Y. Shi, and F. Huang, “Brief introduction of back propagation (BP) neural network algorithm and its improvement,” in *Advances in Intelligent and Soft Computing*, 2012, pp. 553–558.
- [176] J. Yuan, C. Farnham, C. Azuma, and K. Emura, “Predictive artificial neural network models to forecast the seasonal hourly electricity consumption for a University Campus,” *Sustain. Cities Soc.*, 2018.
- [177] F. Costantino, G. Di Gravio, and F. Nonino, “Project selection in project portfolio management: An artificial neural network model based on critical success factors,” *Int. J. Proj. Manag.*, vol. 33, no. 8, pp. 1744–1754, 2015.
- [178] M. Sedighzadeh, A. Mohammadpour, and S. M. M. Alavi, “A daytime optimal stochastic energy management for EV commercial parking lots by using approximate dynamic programming and hybrid big bang big crunch algorithm,” *Sustain. Cities Soc.*, 2019.
- [179] S. Y. Chan and C. K. Chau, “Development of artificial neural network models for

- predicting thermal comfort evaluation in urban parks in summer and winter,” *Build. Environ.*, vol. 164, no. August, p. 106364, 2019.
- [180] G. De Wu and S. L. Lo, “Effects of data normalization and inherent-factor on decision of optimal coagulant dosage in water treatment by artificial neural network,” *Expert Syst. Appl.*, vol. 37, pp. 4974–4983, 2010.
- [181] E. Ogasawara, L. C. Martinez, D. De Oliveira, G. Zimbrão, G. L. Pappa, and M. Mattoso, “Adaptive Normalization: A novel data normalization approach for non-stationary time series,” in *Proceedings of the International Joint Conference on Neural Networks (IJCNN)*, 2010.
- [182] K. G. Sheela and S. N. Deepa, “Review on methods to fix number of hidden neurons in neural networks,” *Math. Probl. Eng.*, vol. 6, 2013.
- [183] H. Li, S. Wang, and R. Tang, “Robust optimal design of zero/low energy buildings considering uncertainties and the impacts of objective functions,” *Appl. Energy*, vol. 254, no. July, p. 113683, 2019.
- [184] T. D. Gedeon, “Data mining of inputs: analysing magnitude and functional measures.,” *Int. J. Neural Syst.*, vol. 8, no. 2, pp. 209–218, 1997.
- [185] D. Delen, R. Sharda, and M. Bessonov, “Identifying significant predictors of injury severity in traffic accidents using a series of artificial neural networks,” *Accid. Anal. Prev.*, vol. 38, no. 3, pp. 434–444, 2006.
- [186] J. N. Fidalgo, “Feature Subset Selection Based on ANN Sensitivity Analysis – A Practical Study,” *Adv. Neural Networks Appl.*, no. 1, pp. 206–211, 2001.
- [187] R. Guo, Y. Hu, M. Liu, and P. Heiselberg, “Influence of design parameters on the night ventilation performance in office buildings based on sensitivity analysis,” *Sustain. Cities Soc.*, 2019.
- [188] S. Duprez, M. Fouquet, Q. Herreros, and T. Jusselme, “Improving life cycle-based

- exploration methods by coupling sensitivity analysis and metamodels,” *Sustain. Cities Soc.*, 2019.
- [189] Z. T. Ai, C. M. Mak, J. L. Niu, Z. R. Li, and Q. Zhou, “The effect of balconies on ventilation performance of low-rise buildings,” *Indoor Built Environ.*, vol. 20, no. 6, pp. 649–660, 2011.
- [190] C. Zhou, Z. Wang, Q. Chen, Y. Jiang, and J. Pei, “Design optimization and field demonstration of natural ventilation for high-rise residential buildings,” *Energy Build.*, vol. 82, pp. 457–465, 2014.
- [191] C. Tao, Y. Zhang, D. G. Hottinger, and J. J. Jiang, “Asymmetric airflow and vibration induced by the Coanda effect in a symmetric model of the vocal folds,” *J. Acoust. Soc. Am.*, vol. 122, no. 2270, 2007.
- [192] H. Sturm, G. Dumstorff, P. Busche, D. Westermann, and W. Lang, “Boundary layer separation and reattachment detection on airfoils by thermal flow sensors,” *Sensors (Switzerland)*, vol. 12, no. 11, pp. 14292–14306, 2012.
- [193] N. Kasagi and A. Matsunaga, “Three-dimensional particle-tracking velocimetry measurement of turbulence statistics and energy budget in a backward-facing step flow,” *Int. J. Heat Fluid Flow*, vol. 16, no. 6, pp. 477–485, Dec. 1995.
- [194] O. Tornblom, “Experimental and computational studies of turbulent separating internal flows (Doctor dissertation),” in *Doctoral thesis from KTH Mechanics*, 2006, pp. 1–81.
- [195] S. Yoshioka, S. Obi, and S. Masuda, “Turbulence statistics of periodically perturbed separated flow over backward-facing step,” *Int. J. Heat Fluid Flow*, vol. 22, no. 4, pp. 393–401, 2001.
- [196] J. S. Touma, “Dependence of the wind profile power law on stability for various locations,” *J. Air Pollut. Control Assoc.*, vol. 27, no. 9, pp. 863–866, 1977.
- [197] S. J. Qin, “Neural Networks for Intelligent Sensors and Control — Practical Issues and

- Some Solutions,” in *Neural Systems for Control*, 1997, pp. 213–234.
- [198] G. Papadakis, M. Mermier, J. F. Meneses, and T. Boulard, “Measurement and Analysis of Air Exchange Rates in a Greenhouse with Continuous Roof and Side Openings,” *J. Agric. Eng. Res.*, vol. 63, no. 3, pp. 219–227, Mar. 1996.
- [199] B. Blocken, J. Carmeliet, and T. Stathopoulos, “CFD evaluation of wind speed conditions in passages between parallel buildings-effect of wall-function roughness modifications for the atmospheric boundary layer flow,” *J. Wind Eng. Ind. Aerodyn.*, vol. 95, pp. 941–962, 2007.
- [200] C. Tantasavasdi, J. Srebric, and Q. Chen, “Natural ventilation design for houses in Thailand,” *Energy Build.*, vol. 33, no. 8, pp. 815–824, Oct. 2001.
- [201] B. Wang, L. D. Cot, L. Adolphe, and S. Geoffroy, “Estimation of wind energy of a building with canopy roof,” *Sustain. Cities Soc.*, 2017.
- [202] Z. Q. Yao, H. C. Shen, and H. Gao, “A new methodology for the CFD uncertainty analysis,” *J. Hydrodyn.*, 2013.
- [203] HK Electric Investments Limited, “Smart Guide for Air Conditioner,” *Electricity at Home*, 2015. [Online]. Available: <https://www.hkelectric.com/en/customer-services/energy-efficiency-safety/electricity-@-home/buying-guide/air-conditioner>. [Accessed: 17-Aug-2015].
- [204] J. Haarhoff and E. H. Mathews, “A Monte Carlo method for thermal building simulation,” *Energy Build.*, 2006.
- [205] E. J. da S. Pereira, J. T. Pinho, M. A. B. Galhardo, and W. N. Macêdo, “Methodology of risk analysis by Monte Carlo Method applied to power generation with renewable energy,” *Renew. Energy*, 2014.
- [206] Y. Bao, T. Liu, and W. L. Lee, “The influence of sleeping habits on cooling energy use in residential sector in Hong Kong,” *Build. Environ.*, vol. 132, no. November 2017, pp.

- 205–213, Mar. 2018.
- [207] Hong Kong Observatory, “Monthly Meteorological Normals for Hong Kong (1981-2010),” *Hong Kong Observatory*, 2020. [Online]. Available: https://www.hko.gov.hk/en/cis/normal/1981_2010/normals.htm. [Accessed: 28-Mar-2020].
- [208] W. L. Lee, “Benchmarking energy use of building environmental assessment schemes,” *Energy Build.*, vol. 45, pp. 326–334, 2012.
- [209] W. L. Lee and H. Chen, “Benchmarking Hong Kong and China energy codes for residential buildings,” *Energy Build.*, vol. 40, pp. 1628–1636, 2008.
- [210] H. Chen, W. L. Lee, and X. Wang, “Energy assessment of office buildings in China using China building energy codes and LEED 2.2,” *Energy Build.*, vol. 86, pp. 514–524, 2015.
- [211] K. W. H. Mui and W. T. D. Chan, “Adaptive comfort temperature model of air-conditioned building in Hong Kong,” *Build. Environ.*, vol. 38, no. 6, pp. 837–852, Jun. 2003.
- [212] X. Chen, H. Yang, and K. Sun, “A holistic passive design approach to optimize indoor environmental quality of a typical residential building in Hong Kong,” *Energy*, vol. 113, pp. 267–281, 2016.
- [213] “ASHRAE STANDARD Thermal Environmental Conditions for Human Occupancy 55-2004,” in *American Society of Heating, Refrigerating and Air-Conditioning Engineers, Inc.*, 2004, no. ANSI/ASHRAE Standard 55-2004, pp. 1–34.
- [214] K. F. Fong, T. T. Chow, and C. Li, “Comfort zone of air speeds and temperatures for air-conditioned environment in the subtropical Hong Kong,” *Indoor Built Environ.*, vol. 19, no. 3, pp. 375–381, 2010.
- [215] M. Kazkaz and M. Pavelek, “OPERATIVE TEMPERATURE AND GLOBE

- TEMPERATURE,” *Eng. Mech.*, vol. 20, no. 3/4, pp. 319–325, 2013.
- [216] T. Chaudhuri, Y. C. Soh, S. Bose, L. Xie, and H. Li, “On assuming Mean Radiant Temperature equal to air temperature during PMV-based thermal comfort study in air-conditioned buildings,” in *IECON Proceedings (Industrial Electronics Conference)*, 2016.
- [217] A. L. S. Chan, T. T. Chow, S. K. F. Fong, and J. Z. Lin, “Generation of a typical meteorological year for Hong Kong,” *Energy Convers. Manag.*, vol. 47, no. 1, pp. 87–96, 2006.
- [218] Z. J. Zhai, W. Zhang, Z. Zhang, and Q. Y. Chen, “Evaluation of Various Turbulence Models in Predicting Airflow and Turbulence in Enclosed Environments by CFD: Part 2—Comparison with Experimental Data from Literature,” *HVAC&R Res.*, vol. 13, no. 6, pp. 853–870, 2007.
- [219] Y. He, M. Liu, T. Kvan, and S. Peng, “An enthalpy-based energy savings estimation method targeting thermal comfort level in naturally ventilated buildings in hot-humid summer zones,” *Appl. Energy*, vol. 187, pp. 717–731, Feb. 2017.